Modulation of TRPV1 Function in Sensory Neuropathy

Sara Pritchard

Supervisors : Dr Chris Benham, Dr Lisa Lione, Dr Areles Molleman

School of Life and Medical Sciences

Submitted to the University of Hertfordshire in partial fulfillment of the requirements of the degree of Doctor of Philosophy

June 2014

Acknowledgements

To the wonderful technical staff and the other PhD students in CP Snow; John, Komal, Yugal, Teeraporn, Ben and Yousef, David, Lena and Carol: you all made me feel at home, helped me with all manner of things from methodology to providing me heat in the labshed of the sky, 3G175, provided me with endless supplies of tubing, numerous gas bottle changes, new laptops so I didn't get neckstrain, somewhere to sit and made me feel part of a team, you showed me how to make the perfect cuppa, told me rubbish jokes and gave me friendship.

To my supervisory team; Chris, Lisa and Areles: you gave me the opportunity to do something completely different with my life, helped me through the process of a PhD in a really relaxed supportive environment and gave me plenty of food for thought along the way.

To my family; Ellie, Annabel, my Mum and my Dad: you gave me the inspiration to start, the motivation to keep going and nagged me to finish so that I could once again get a proper job!

Finally to my beautiful friends; Sarah, Joanne, Kim, Yvie, Colleen and Rory: you sometimes held me up, always pushed me forward (in the nicest possible way) and gave me the occasional kick (which I needed) to get to the finish line.

Thankyou all for giving me so much xx

Abstract

This thesis examined how and why TRPV1 function is being modulated in sensory neuropathy and explored the potential of its rescue in the urinary bladder of STZ-induced diabetic rats. Diabetes induced a rapid decline in TRPV1 function and changes in neurogenically mediated electrically-evoked responses together with a gradual decline in muscarinic function. Diabetic bladder was also deficient in muscarinic and TRPV1 organ bath temperature-induced changes but not in those affecting spontaneous contractile activity. Exposure to a potential neuropathy causative agent, methylglyoxal was studied and its mechanism of action explored through the use of TRPA1 ligands. Methylglyoxal exposure mimicked some of the effects of diabetes on TRPV1, neurogenic electrically evoked responses and muscarinic function. Methylglyoxal effects were seen to be partly through TRPA1 receptor activation but other as yet undefined pathways were also involved. Use of TRPA1 ligands revealed an unexpected complexity of the interaction of the TRPA1 receptor with TRPV1.
Finally the potential of reversing the diminished TRPV1 response was examined through the use of three known sensitising agents, bradykinin, NGF and insulin. Bradykinin was the only agent seen to reverse the TRPV1 diminished response back up to to control equivalent levels and through the use of bradykinin selective ligands, it was seen that the dual activation of BK-1 and BK-2 receptor was necessary to rescue the TRPV1 response. The likely mechanism of action of bradykinin was through prostaglandin production as indomethacin blocked TRPV1 rescue.

In the acute stage of diabetes, TRPV1 function is downregulated and may be caused by exposure to a neuropathy-causing metabolite such as methylglyoxal. The TRPV1 function still retains plasticity at this acute stage because function could be enhanced back to control levels by bradykinin receptor activation : a potential for early therapeutic intervention.

Table of Contents

List of Tables

Table

List of Figures

Figure

Chapter 1 Introduction

Chapter 2

Chapter 3

Chapter 4

Chapter 5

Chapter 6

Chapter 7

Chapter 1 Introduction

Modulation of TRPV1 function in sensory neuropathy

Sensory neuropathy

Neuropathy affects three main types of neurons: autonomic, motor and sensory neurons and the term sensory neuropathy refers to the nerve damage seen specifically to sensory neurons. Sensory neuropathy is a painful complication often associated with diabetes. Commonly sensory neuropathy is associated with a tingling burning pain, and a loss of sensation that has been likened to wearing stockings or gloves. The prevalence of neuropathy is high, estimated to occur in around 66% of people with diabetes (Dyck et al., 1993).

Other medical conditions that are associated with neuropathy include chronic liver disease(Knill-Jones et al., 1972), kidney disease (Maser et al., 1989), HIV infection and AIDS (Keswani et al., 2002), chronic alcohol consumption (Martyn and Hughes, 1997), nutritional deficiencies such as Vitamin B deficiency (Mccombe and Mcleod, 1984), cancer (Roelofs et al., 1984), Lyme disease (Halperin et al., 1987), Charcot-Marie-Tooth (De Jonghe et al., 1997), Guillain-Barre (Brown and Feasby, 1984) and Diphtheria (Mcleod, 1995).

Why is sensory function important?

Sensory nerve function is critical to an organism's survival. Primary afferent sensory nerves act to convey information such as pain, cold and heat from their local environment to the central nervous system. These neurons may also have efferent functions to signal to their local environment by the release of neuropeptides such as Substance P, neurokinins and calcitonin gene-related peptide (CGRP)(Szallasi et al., 2007). Dysfunction in the afferent and efferent systems of peripheral sensory neurons could be detrimental to organ functioning and may be causative to inappropriate sensory signalling and neuronal injury.

Sensory neuropathy in diabetes

Principally diabetic neuropathy affects multiple sensory neurons. This neuropathy appears predominantly in the hands and feet, and manifests as sensory alterations that range from a loss of sensation, an increased sensitivity to sensory stimuli (hyperesthesia) to allodynia, pain due to normally innocuous tactile stimuli. There are also signs of functional changes in the extremities, such as coldness, loss of hair, thinness of skin, and sweating disorders. The sensory loss seen with diabetic neuropathy is thought to be the primary cause of foot problems where minor foot injuries go unnoticed by the patient and can progress to the development of foot ulcers (Boulton et al., 2005). The consequence of a foot ulcer that is non-responsive to treatment can be amputation, and this is 10-30 times more likely to occur in a diabetic (Trautner et al., 1996).

A common characteristic of diabetic sensory neuropathy is hyperalgesia, defined as an increased responsiveness to a noxious stimulus. Hyperalgesia can be caused through sensitisation of the peripheral nerve fibres, so that an increased number of action potentials are generated in response to thermal or mechanical stimuli. Neuropathic pain as a result of neuropathy often also has an element of allodynia, which is defined as pain resulting from a normally innocuous stimulus. Normal tactile sensations are perceived as painful due to changes in the spinal cord driven by nociceptors.

In diabetes some reduction of the neuropathic symptoms can be achieved with long-term glucose homeostasis and insulin replacement. However, some neuropathies remain resistant to resolution and may represent either irreversible neuropathy or a neuropathy with unknown causative factors. Even with good glucose control over a number of years, only around 60% of diabetics achieve a partial resolution of their symptoms.

Existing therapies fail to effectively treat the painful neuropathic symptoms for the majority of patients, for example the gold standard treatment for diabetic

neuropathy, pregabalin, treats only 1 in 4 patients and the relief gained is generally only a 50% reduction in pain (Finnerup et al., 2005, Lesser et al., 2004). Pregabalin does show show some efficacy clinically against neuropathic pain and although its mechanism of action is still not clear, it is believed to act via a selective inhibitory effect on voltage-gated calcium channels containing the α2δ1 subunit (Sills, 2006).

Diabetic sensory neuropathy is resistant to resolution with glucose control and is symptomatically hard to treat. So there is a need for the better understanding of the underlying functional changes seen in sensory neuropathy. This could lead to the development of novel, more effective therapies for diabetic complications.

Diabetes: classification, prevalence and treatment

Diabetes mellitus is a disorder of carbohydrate metabolism caused by deficient action and/or production of insulin, an endocrine hormone produced by the pancreas. As insulin facilitates glucose uptake and utilization, the disease is characterized by a chronic high level of glucose in the blood, hyperglycemia. The disease can be categorized to two main types depending on the form of the insulin deficiency: Type 1 Diabetes (T1D) which accounts for 5-10% of the total diabetic population, and the more prevalent form, Type 2 Diabetes (T2D). The insulin deficit seen in T1D is caused by a profound reduction in the number of functional pancreatic β-cells, commonly as a result of their destruction by autoimmune disease. In T2D the deficiency is in insulin secretion and its subsequent action often termed insulin resistance.

Globally, the diabetic population is already large and numbers are expected to increase: in 2000 the worldwide estimate was a staggering 171 million with this predicted to more than double to 366 million by 2030. Being obese is the main risk factor for development of diabetes and shockingly the majority of sufferers, around 80%, could have avoided this disease simply by maintaining a weight

within the normal range (Bruno and Landi, 2011) .Obesity is increasingly being associated now with poverty and this presents a concerning combination for this vulnerable population due to the minimal access they have to medical assistance.

The initial symptoms of diabetes are excessive thirst and urination, blurred vision, and rapid weight loss. Left untreated diabetes is acutely life threatening and severely disabling. The acute metabolic complications of ketoacidosis or a non-ketotic hyperosmolar state can develop which can lead to coma and prove fatal. Chronically uncontrolled diabetes causes progressive damage to and dysfunction and failure of numerous organs. However, diabetes can be avoided with dietary control to reduce carbohydrate intake and obesity, and treated by restoration of the insulin deficit to facilitate glucose homeostasis. T1D is treated by insulin replacement using recombinant human insulin, whereas T2D is treated by drugs that act to increase insulin secretion and by sensitizing agents that enhance insulin effects. Successful diabetes management is currently seen as maintaining blood glucose levels at levels below 10 mmoles/dl. The better blood glucose control has transformed the prognosis for diabetics as this has markedly reduced the incidence of mortality and extended their life expectancy. However, with disease progression severe diabetic complications continue to develop such as retinopathy, nephropathy, neuropathy and ulceration. Diabetes is also associated with increased risks of cardiovascular, peripheral vascular and cerebrovascular disease (WHO, 1999). These numerous disease-associated complications are often resistant to treatment and cause considerable distress to the patient.

Diabetic complications

Diabetic complications affect multiple organs including the kidneys, eyes, gastro-intestinal system and nervous system. The causative events underlying the pathogenesis of diabetic complications are complex and not fully understood. Chronic hyperglycemia in itself certainly plays a major precipitating and directly causative role but additional factors are likely to contribute. This is because even with good glucose homeostasis in the well-controlled diabetic, complications still occur and are resistant to resolution (Llorente and Malphurs,

2007). Neuropathy is a diabetic complication and may additionally contribute to other diabetic complications because of the role nerves play in the functioning of all organs of the body (Gentile et al., 1998). A deeper understanding of this neuropathy in the context of diabetes would be beneficial, not only for the treatment of neuropathy but for its impact on other complications too.

What causes diabetic neuropathy?

Exactly what causes diabetic neuropathy is unknown. However a number of pathogenic mechanisms for neuronal injury and altered function driven by hyperglycemia have been identified (Aronson, 2008). These include the saturation of glucose metabolic pathways that ultimately lead to the formation of toxic polyols through the polyol pathway, increased advanced glycation end (AGE) products which often have altered properties, nerve hypoxia or ischemia, deficiency of linolenic acid, increased protein kinase C especially the beta isoform and a deficiency in growth factors. All of these pathways converge in producing oxidative stress that seems to be more severe at site of the primary sensory neurons, the dorsal root ganglia (DRG), than at other nerves leading to the hypothesis that a primary target of diabetic neural complications is the sensory neuron (Nickander et al., 1994). In order to treat this serious complication it is important to gain an increased understanding of the molecular mechanisms that drive the onset of sensory neuropathy, and prevent its resolution.

Animal models of diabetes

Diabetes is a complex metabolic disorder and is hard to model *in vitro*. Animal models of diabetes are therefore very important for the study of the disease pathogenesis and can be used for the study of diabetic complications that are seen clinically. Over 130 years ago, the surgical removal of the pancreas in a dog

and the consequent polyuria, polydipsia and diabetes, highlighted the role the pancreas plays in diabetes (Von-Mering, 1889). More recently developed rodent diabetic models use administration of chemicals such as streptozotocin (STZ) and alloxan (ALX) that are selectively toxic to the β-islet pancreatic cells (Lenzen, 2008). Transgenic or highly inbred animal strains have also been developed that spontaneously or conditionally develop diabetes, although the use of these can be restricted by their cost (Rees and Alcolado, 2005). The most commonly used inbred models used in research are the non-obese diabetic mouse (NOD) and the bio breeding rat (Rees and Alcolado, 2005). Both of these models spontaneously develop diabetes but there are drawbacks in that the NOD model demonstrates a large gender difference with females showing an increased propensity of developing diabetes and the BB rat requires administration of exogenous insulin to survive (Rees and Alcolado, 2005). Additionally the TRPV1 receptor has been shown in the NOD model to be functionally mutated (Razavi et al., 2006) which would of no doubt add a confounding issue to the study of this channel in diabetes. There are numerous models of T2D due to the complexity and heterogeneity of the human disease. They include ob/ob and db/db mice, which have been shown to be leptin deficient and leptin resistant respectively (Rees and Alcolado, 2005) and the Zucker rat (also leptin resistant). Transgenic models have been developed for the study of specific elements of the disease but the use of these is very economically restrictive and has other drawbacks especially when wanting to look at a disease from a non-biased viewpoint.

There is no perfect animal model of the human disease however, and all of the models have their limitations and drawbacks as well as their advantages. For many researchers, STZ is the agent of choice due to its more reproducible induction of diabetes through greater stability than ALX at physiological pH (Lenzen, 2008).

STZ is an antimicrobial chemotherapeutic agent (Schein et al., 1974), derived from the earthborn microbe *Streptomyces achromogenes,* and was identified as a diabetogenic agent in 1963. When delivered systemically to rodents as a single large dose (>50 mg/kg) STZ induces a rapid and sustained diabetic state as a

result of direct toxicity on the pancreatic β-cells. It has taken decades of research to uncover how STZ is selectively toxic towards pancreatic β-cells (Weiss, 1982, Szkudelski, 2001, Lenzen, 2008). STZ gains entry with reasonable specificity to rodent pancreatic β-cells via the low affinity glucose transporter GLUT2. Once within the β-cell, STZ is split into glucose and the alkylating moiety, methylnitroso-urea which is cytotoxic through modification of biological macromolecules and DNA fragmentation. STZ evokes pancreatic-β cell destruction and thus induces the diabetic state. Following STZ administration, three distinct phases of blood glucose responses are seen (Lenzen, 2008). The first phase is hyperglycaemia occurring around one hour post STZ administration and lasts for 2-4 hours and is caused by the inhibition of insulin secretion. The second phase is a transient hypoglycaemia, typically occurring between 4- 8 hrs following STZ, and can be so severe that, without glucose administration, it is fatal. The rupture of secretory granules and release of insulin cause this hypoglycaemia during necrosis of the pancreatic β-cells. Within 12-48 hours the STZ-treated animal enters the third permanent diabetic hyperglycaemic phase, so by 48 hours a long lasting diabetic state is induced. Given as a single high dose to adult rats, the STZ model can be described as a model of T1D as STZ administration evokes pancreatic β-cell destruction and a subsequent deficiency in insulin production.

A model of autoimmune T1D can also be established using multiple small doses of STZ (e.g. 40 mg/kg on five consecutive days) which has been used extensively for the study of the immunological pathways that lead to insulitis and pancreatic β-cell death (Rees and Alcolado, 2005). Some investigators also utilize STZ administered neonatally or in combination with a high fat diet to adult animals to induce a T2D model (Islam and Loots, 2009).

The in-house established model of diabetes utilizes a single high dose of STZ (65 mg/kg) delivered to male rats (300-400g), followed by supply of 2% sucrose in drinking water for 48 hours. This is a model of T1D, and has been demonstrated to display a reasonably robust diabetic state together with the appearance of a number of diabetic complications including neuropathy, without the need for administration of insulin to the animals. Although the more prevalent form of

diabetes is T2D and complications such as neuropathy do occur in T2D, the animal models for T2D are economically more expensive and the appearance of complications takes longer and is more variable.

TRPV1 is a candidate for investigation of diabetic neuropathy

A candidate for investigation of diabetic neuropathy is the prototypical Transient Receptor Potential (TRP) family member, TRP Vanilliod 1 (TRPV1) due to its expression, function and changes to its function in diabetes.

Firstly TRPV1 is expressed on the cells affected by sensory neuropathy, the sensory neurons. Secondly TRPV1 is known to play an important role in pain transmission (nociception), the major symptom of neuropathy. Furthermore stimulation of the TRPV1 receptor results in a burning-like pain similar to that described in sensory neuropathy. Finally there is a correlation in TRPV1 function and expression levels with the evolution of sensory neuropathy symptoms: in the early stages of diabetes, the activity of TRPV1 is both attenuated and augmented (pain), whereas in the later stages of diabetes, a loss of TRPV1 activity and expression is seen (sensory loss) (Pabbidi et al., 2008b).

So a strong association between sensory neuropathy symptoms and TRPV1 expression, function and disease-related changes exist and from this, the notion arises that modulation of TRPV1 activity may actually be causative to the onset and maintenance of sensory neuropathy.

TRP channels

Transient receptor potential (TRP) channels are a large family of functionally diverse cation-permeant ion channels. They are present in almost all mammalian cell types. The first member was discovered in the eye of drosophila melanogaster and was called the TRP channel due to a mutation that resulted in

a transient voltage response to light (Minke, 2010). Based on sequence homology, the large superfamily of related ion channels is divided into six main sub-families: canonical (TRPC), vanilloid (TRPV) ,melastatin-related (TRPM), polycystin (TRPP), mucolipin (TRPML) and the ankyrin (TRPA) channels. Common features of these channels include the six transmembrane spanning structure that embeds the channel within the lipid bilayer of cells and for the channels to become functional, the requirement of a tetrameric assembly of homomeric or heteromeric TRP units. Most also share a non-selective permeability to cations and a low sensitivity to membrane voltage. Their functional roles are diverse and range from thermosensation, pheromone recognition, magnesium homeostasis, to regulation of vascular tone.

Members of the TRP family share a basic channel structure that is similar to that of the voltage gated K+ channels. The TRP channel structure is built from four similar or identical subunits, each of which have six transmembrane (TM) domains (TM1-TM6) and cytosolic N- and C-terminal tails. There is a central cation-conducting pore that consists of the TM5, TM6 domains with a connecting loop. Regulatory domains which control how the channel is gated are thought to lie on the regions TM1-TM4 and the tail C-and N-terminals.

TRPV1 channels

TRPV1 is the first member of the TRPV family (TRPV1-TRPV6). TRPV1 is a voltage-dependent cation channel and can be directly activated by numerous stimuli that include noxious heat (>43 ° C), and reduced pH (<6), endogenous lipoxygenase products and fatty acid amides such as anandamide as well as a number of plant derived products such as capsaicin, gingerols, eugenol, resiniferatoxin, piperine and camphor (Pingle et al., 2007). TRPV1 function can also be potentiated by a range of mediators that include endogenous pro-nociceptive mediators such as prostaglandins, bradykinin and ATP (Moriyama et al., 2005), as well as substances such as ethanol and DMSO (Vetter et al., 2008) .

The properties of the TRPV1 channel make it the principal integrator of noxious information in a large number of primary afferent neurons and therefore an interesting target for novel analgesic development (Premkumar and Sikand, 2008).

TRPV1 expression

TRPV1 is expressed in the cell bodies of small to medium sized primary afferents which are located in dorsal root, trigeminal and nodose ganglia, with an intense expression in the dorsal root ganglia, the nociceptive primary afferent sensory neurons. Brain expression of TRPV1 extends to regions of the limbic system such as the hippocampus and the amygdala, striatum, locus ceruleus, cerebellum and the hypothalamus (Menigoz and Boudes, 2011). TRPV1 has been shown to regulate synaptic transmission (glutaminergic and or GABAergic) (Anwar and Derbenev, 2013) and additionally may function to regulate body temperature in the hypothalamus as well as playing a role in reward and appetite. TRPV1 is also found in the peripheral terminals of afferents in many body structures including skin, muscle and viscera. Epithelial cells have also been shown to express TRPV1 receptors and these cells include keratinocytes and urothelial cells, the umbrella-like lining to the bladder (Yamada et al., 2009). In the bladder, TRPV1 appears to be involved in normal bladder function and has been shown to play a role in mechanically (stretch) evoked purinergic signaling in the urothelium (Gevaert et al., 2007). In keratinocytes, TRPV1 and other temperature sensitive TRPV channels such as TRPV3 and TRPV4, are thought to contribute to thermosensation. Mast cells also express TRPV1, here TRPV1 plays a role in regulating the immune response (Ständer et al., 2004).

TRPV1 association with disease

Homozygous and conditional TRPV1 knockout mutant mice demonstrate abnormal nociception, a deficient response to capsaicin and development of thermal hyperalgesia, reduced DRG electrophysiological responses to capsaicin,

heat and acid and a reduced hypersensitivity response during inflammation (Davis et al., 2000, Caterina et al., 2000). Additionally they display abnormal anxiety- and conditioning-related behaviors, increased sensitivity to deoxycorticosterone acetate -salt-induced renal damage, resistance to diet-induced obesity, altered taste sensitivity, and an impaired febrile response (Blake Ja, 2014) . Other evidence gained from the use of TRPV1 transgenic mice models have suggested that the TRPV1 receptor is associated with thermal hyperalgesia, allodynia, functional bowel disease, inflammatory bowel disease, vulvodynia, osteoarthritis, pancreatitis, gastroesophageal reflux disease, bladder disease, cystitis, asthma, migraine, schizophrenia and pain in general (Nilius et al., 2007). Genetics and genetic mapping evidence (OMIM) have identified a potential association of the TRPV1 receptor with breast cancer, myasthenic syndrome and non-insulin dependent diabetes mellitus (Nilius et al., 2007).

TRPV1 on sensory neurons is a noxious molecular integrator that may play a role in neuropathy

The TRPV1 ion channel has particular importance in noiciception and is of interest as a pain therapy target (Roberts and Connor, 2006). The discovery of TRPV1 antagonists (Bevan et al., 1992) and the subsequent proof of their efficacy in models of pain (Culshaw et al., 2006) has fuelled a great deal of interest in this channel both in academia and in industry. TRPV1 is a non-selective cation channel, expressed in around 40% of DRG (Zacharova and Palecek, 2009). The TRPV1 receptor rapidly and directly detects potentially damaging thermal and chemical stimuli, which are then perceived as painful. Additionally TRPV1 activation plays a role in the establishment of persistent peripheral inflammation and central sensitisation.

TRPV1 activation causes the release of pro-inflammatory peptides from peripherally located nerve terminals and evokes action potential driven vesicular release of glutamate and neuropeptides from the central nerve terminals. The glutamate release from primary afferent terminals in the spinal cord is the basic event in pain transmission, while the central release of

neuropeptides acts to two ways: firstly to amplify the glutamate signal and secondly to increase dorsal horn neuronal sensitivity to other incoming signals. Peripheral CGRP and substance P (sP) release contribute to a state of neurogenic inflammation through blood vessel and immune cell effects (Roberts and Connor, 2006)

Genetic deletion of the TRPV1 gene renders mice non-responsive to vanilloids and less sensitive to noxious heat and low pH, confirming the important role TRPV1 contributes to vanilloid, heat and proton sensitivity *in vivo* (Caterina et al., 2000). Functional TRPV1 is thought to exist as tetramers in the plasma membrane (Hong and Wiley, 2005). Following activation of TRPV1, the TRPV1 ion channel undergoes a conformational change and opens allowing cations such as calcium (Ca^{2+}) to enter the cell. This causes an increase in intracellular Ca^{2+} and leads to activation of Ca^{2+}-mediated signal transduction pathways. This can induce exocytosis of neuropeptides such as CGRP, sP, or neurokinin (NK)A from sensory neurons. Following this neuronal exocytosis, the neuropeptides bind to their respective receptors such as CGRP receptor, sP receptor, NK1 or NK2 receptors and thereby elicit tissue specific effects. In the urinary bladder for example, TRPV1 activation by capsaicin leads to detrusor muscle contraction (Saitoh et al., 2007) and because of this provides an amenable model for the study of TRPV1 function *in vitro*.

TRPV1 activation of perivascular nerves causes CGRP and sP release and vasodilation which can result in neurogenic inflammation (Manzini et al., 1991). TRPV1 induced spinal cord CGRP release is associated with nociceptive transmission (Donnerer and Amann, 1992) and elevated blood levels of CGRP have been found during migraines and cluster headaches (Dux et al.) as well as in mycocardial infarction. The role of TRPV1 in pain transmission was clearly demonstrated by Caterina *et al*, who showed a thermal hypoalgesic response of TRPV1 knockout mice (Caterina et al., 2000). Other lines of evidence include numerous expression and pharmacological manipulation studies.

Upregulation of TRPV1 function is associated with somatic allodynia and hyperalgesia and this may be due to changes in TRPV1 trafficking and phosphoryation status (Hong and Wiley, 2005). However, in-house data has

shown a dramatic decrease in TRPV1 function in the urinary bladder from a rat streptozotocin (STZ-diabetic) model. This suggests that TRPV1 modulation is complex and may be site specific.

Changes in TRPV1 functionality are dynamically regulated by receptor phosphorylation and dephosphorylation

TRPV1 activity is modulated by two distinct processes: firstly through alteration of the functional activity of TRPV1 channels already present in the plasma membrane and secondly through translocation of additional TRPV1 channels to the cell membrane (Figure 1.1). Both these processes may be controlled by phosphorylation of the channel at different structural sites (Zhang et al., 2005b).

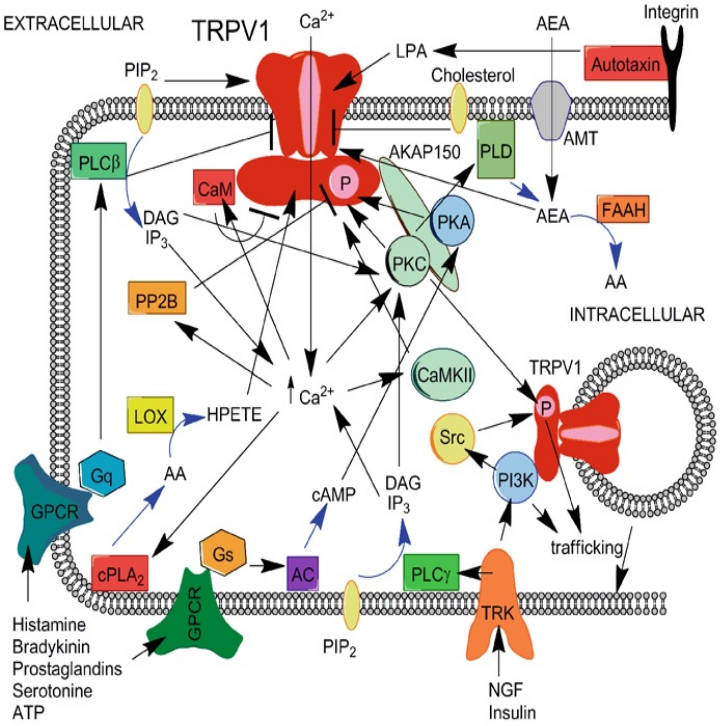

Figure 1.1 Examples of signaling pathways associated with TRPV1 function and modulation (TRPV1 in cell signalling) *Black* arrows denote positive modulation, while an orthogonal line at the end denotes inhibition. *Blue* arrows denote biosynthesis. TRPV1 is schematically depicted in *red*, with both its transmembrane and cytoplasmic domains. PKA, PKC, CaMKII sensitize TRPV1

(Figure 1.1 legend continued) through phosphorylation, denoted as a pink-encircled "*P*" in the channel. Calcineurin (PP2B) desensitizes the channel through dephosphorylation. Both Gq- and Gs-protein coupled receptors (GPCRs) are depicted with some of its agonists. AC denotes Gs-stimulated adenylate cyclase. Phospholipase Cβ and C*γ* catalize the formation of 1,4,5 inositoltriphosphate (IP3) and diacylglycerol (DAG) from PIP2, depicted as a yellow oval, after their activation by a Gq protein or a receptor tyrosine kinase (TRK). Calcium-stimulated phospholipase A2 (PLA2) catalyzes arachidonic acid (AA) formation, which is further converted into TRPV1-activating eicosanoids and leukotrienes such as HPETEs by the lipoxygenase enzymes (LOX). TRPV1 agonist anandamide (AEA) is shuttled into the cell by the anandamide membrane transporter (AMT), and is also synthesized from phospholipids by phospholipase D (PLD). AEA is transformed to AA by the fatty acid amide hydrolase (FAAH). TRK-stimulated phosphoinositide 3-kinase (PI3 K) stimulates TRPV1 trafficking to the membrane and Src-mediated channel phosphorylation, which also stimulates channel trafficking. Membrane cholesterol can directly inhibit channel function and lysophosphatidic acid (LPA), which is synthesized by the integrin-associated enzyme autotaxin, activates the channel after its translocation into the cell. Taken from (Kamkin et al., 2012)

Alteration of the functional activity of TRPV1 channels

The TRPV1 channel has numerous phosphorylation sites within its structure that affect the functionality. Exposure to TRPV1 agonists, interaction with cellular components such as phospholipids and activation of G-protein coupled receptors or other ion channels all can act to affect the functional and state of TRPV1.

TRPV1 agonist exposure causes TRPV1 desensitisation

Repeated application of vanilloid TRPV1 agonists, even briefly, results in Ca^{2+}-dependent desensitization of TRPV1. The Ca^{2+} dependence has been evidenced by the observation that in the absence of extracellular Ca^{2+}, application of capsaicin to urinary bladder does not result in contraction or desensitisation,

whereas application in the presence of Ca^{2+} produces urinary bladder contraction and desensitisation (Santicioli et al., 1987b) This desensitization to agonist exposure is used therapeutically for example to treat neuropathic pain by application of topical capsaicin cream (Mason et al., 2004) or to treat neurogenic overactive bladder by intravesicular application of resiniferatoxin (Lazzeri et al., 1997). This agonist driven desensitisation is dependent on calcium and occurs through activation of calmodulin causing promotion of calcineurin-mediated dephosphorylation of TRPV1. Conversely however, activation of calmodulin- dependent kinase II (CaMKII) phosphorylates TRPV1 and acts to enhance TRPV1 function so inhibition of CaMK11 has been shown to reduce TRPV1 responses (Price et al., 2005).

Cross-desensitisation of TRPV1

TRPV1 is co-expressed with a number of other ion channels and receptors in sensory neurons (Streng et al., 2008). This close association can also impact on TRPV1 receptor function as it has been seen that activation of the TRPA1 ion channel can act to either positively or negatively affect TRPV1 function (N Akopian, 2011). Cross-talk between TRPV1 with the purinergic receptor $P2X_3$ has also been demonstrated resulting in inhibition (Stanchev et al., 2009) whereas sensitisation of TRPV1 by ATP ,a purinergic agonist has been well described in the literature (Tominaga and Moriyama, 2007).

TRPV1 function can be altered through interaction with cell membrane lipids

TRPV1 function may also rely on the presence of intact membrane lipid rafts and has been found to be altered by the manipulation of the raft constituent components such as cholesterol, the phospholipid phosphatidylinositol-4,5-bisphosphate (PIP_2) and ceramide (Liu et al., 2006, Zhang and Nicol, 2004, Prescott and Julius, 2003). Phosphorylation of TRPV1 by PIP_2 is believed by some to hold TRPV1 under an inhibited state and sensitisation of TRPV1 can be

gained by PIP_2 hydrolysis through receptor mediated activation of protein kinase C, A, or phospholipase A (Prescott and Julius, 2003). The receptors that can mediate this activation are numerous but include bradykinin, prostaglandin E2 (PGE2), 5HT and nerve growth factor (NGF). Furthermore, reinstatement of active TRPV1 following desensitisation requires PIP_2 phosphorylation and maintenance of active TRPV1 may depend on a continual basal phosphorylation by the PKC isoform, PKC-epsilon (Srinivasan et al., 2008). So evidence for PIP_2 effect on TRPV1 function in the literature is somewhat conflicting, with evidence for upregulation and downregulation of TRPV1 activity.

Translocation of TRPV1 to the cell membrane

Factors that induce translocation of TRPV1 receptors to the plasma membrane include insulin, insulin growth factor and NGF. Deficiencies in or overexpression of these factors could either impair or sensitise TRPV1 function (Van Buren et al., 2005). Furthermore, phosphorylation of TRPV1 channel can impact on the translocation of the channel to the cell membrane and this may be dependent on the presence of certain scaffolding proteins such as the A-kinase Anchoring Protein 150 which has been shown to mediate PKA and PKC-directed sensitisation of TRPV1 in various nociceptive models (Jeske et al., 2009b). Cyclin-dependent kinase 5 has been shown to increase surface expression of TRPV1 providing a fundamental mechanistic explanation for the heat sensitivity of nociceptors (Xing et al., 2012).

Many of these co-expressed receptors, enzymes, lipids, growth factors and mediators are altered during diabetes.

Basis for this thesis

The basis for this PhD therefore was to examine how and why the TRPV1 receptor is modulated during diabetes. This could gain an understanding of the potential of this receptor in causing and maintaining sensory neuropathy and

perhaps provide a basis for a therapeutic aimed at prevention or resolution of sensory neuropathy.

Chapter 2 Validation of model systems to explore modulation of TRPV1 in sensory neuropathy

Introduction

To enable the reliable examination of TRPV1 modulation in sensory neuropathy, the first studies were based on identifying and validating an appropriate model system. An appropriate model system would:

- express TRPV1 receptors which when activated would result in a functional response that could be easily measured.
- express additional receptors of interest that could be manipulated pharmacologically to investigate modulation of the TRPV1 receptor.
- require minimal dissection/ preparation to avoid phenotypical alteration of the TRPV1 receptor and to aid throughput.
- be able to be studied under diabetic conditions.
- be relevant to sensory neuropathy.
- be able to be normalized to reduce experimental variability and compensate for factors that could change during diabetes.

In terms of choice for the model system, it was considered that a native cellular system or organ would provide various advantages over a recombinant system in that they possess receptors in the native state i.e. expressed at endogenous not amplified levels and may also express other important interacting receptors such as bradykinin, TRPA1 and TrkA1. Another desirable feature of this model system is that the tissue or cells would require minimal dissection and preparation to aid not only assay throughput but more importantly also to reduce or avoid a potential phenotypical alteration of the receptor state from that seen *in vivo*.

Diabetes is a too complex disease to model fully *in vitro* as the metabolic changes that occur go beyond a simple increase in blood glucose levels. Diabetes induces

changes in lipid metabolism, membrane composition, toxic glucose metabolite buildup and oxidative stress. *In vivo* models of Type 1 and Type 2 diabetes are numerous but the Type 1 STZ-induced diabetic model is a very widely used model for study of the complications associated with diabetes. This STZ-induced diabetic model provides a reasonably robust animal model and was the model of choice for the study of diabetes.

The rat urinary bladder as a model system for the study of TRPV1 function in sensory neurons

The first step was to identify a suitable organ model system. Sensory neurons innervate a multitude of easily accessible muscular organs that can be studied in organ bath systems using muscle contraction or relaxation as the 'readout' for activation of the TRPV1 receptor including the bladder, ileum, colon and the fundus. In the bladder TRPV1 function has been quite well defined and the bladder is known to undergo sensory neuropathy during diabetes. TRPV1 provides sensory information for normal bladder function (Birder et al., 2002, Daly et al., 2007) and sensory loss through TRPV1 knockout results in changes in bladder function somewhat similar to that seen in diabetes. Sensory neuropathy of the bladder is known to exist in diabetes and is thought to underlie the very common complication of diabetic cystopathy. The rat urinary bladder is similar to the human bladder in its innervation, basic structure and receptor expression. Functional differences do occur however; the most notable difference is in the voiding frequency as the rat urinates as part of a territorial marking behavior whereas humans urinate much more infrequently. In the daytime, rats have been recorded as urinating every 8 minutes, at night when they are more active, the voiding frequency rises to every 4 minutes highlighting a clear difference between rats and humans in this respect (Herrera and Meredith, 2010). Despite this difference between humans and rats, the primary model of choice was the urinary bladder smooth muscle of STZ-induced diabetic rats.

Human Embryonic Kidney 293 cells stably expressing rat TRPV1 receptor (HEK293-rTRPV1 cells) as a secondary model system

An assessment of a recombinant cellular system was also included, HEK293 cells stably transfected with rat TRPV1 receptor. Here the assay methodology consisted of measurement of intracellular calcium levels through the use of FURA-2AM.

Validation of the suitability of model systems

In terms of the validation process the first step was to examine responses to concentration ranges of standard tool agonists of TRPV1 to ensure that the model system responded robustly to TRPV1 agonist activation. A range of three tool TRPV1 agonist compounds were studied and included capsaicin, the pungent component of *capsicum*, chilli pepper, resiniferatoxin, an analogue of capsaicin that is derived from the latex resin of a cactus *Euphorbia resinifera* and anandamide, an endogenously produced cannabinoid active compound (Figure 2.1)

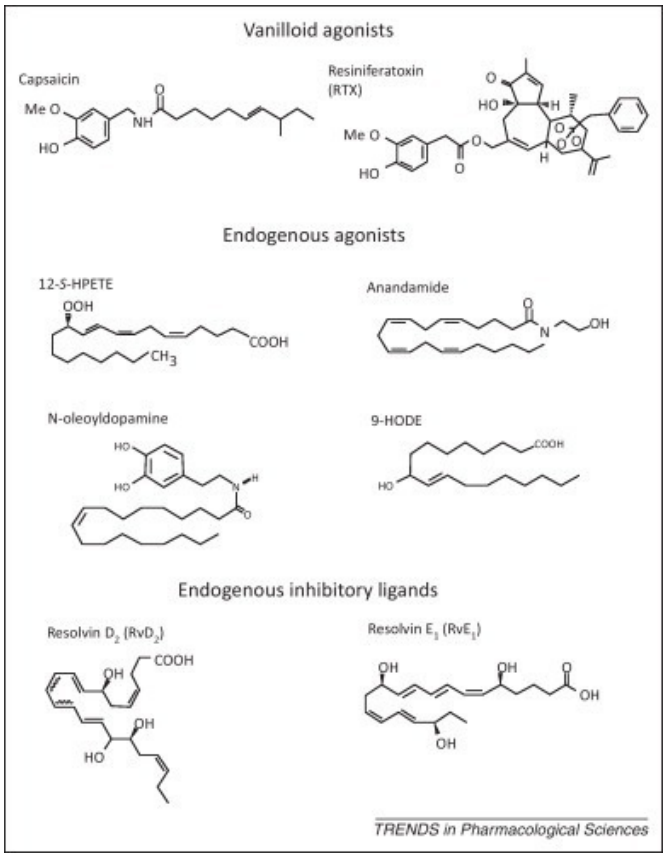

Figure 2.1 Chemical structures of TRPV1 agonists: two vanilloid exogenous agonists, capsaicin and resiniferatoxin (RTX), endogenous agonists anandamide, 12-S-hydroperoxyeicosatetraenoic acid (12-S-HPETE), N-oleoyldopamine, and 9-hydroxyoctadecadienoic acid (9-HODE), and endogenous inhibitory modulators resolvin D2 (RvD2) and resolvin E1 (RvE1). Taken from Szolcsanyi *et al* 2012

Next the effects of a concentration range of a TRPV1 antagonist, SB-366791 versus capsaicin were studied. SB-377791 is a high potency compound with good selectivity (Gunthorpe et al., 2004) (Figure 2.2). SB-366791 has shown activity versus capsaicin induced calcium influx in recombinant systems (Gunthorpe et al., 2004) and in native sensory neuron assays (Varga et al., 2005). Additionally this compound has shown activity in isolated organ assays and *in vivo* (Varga et al., 2005).

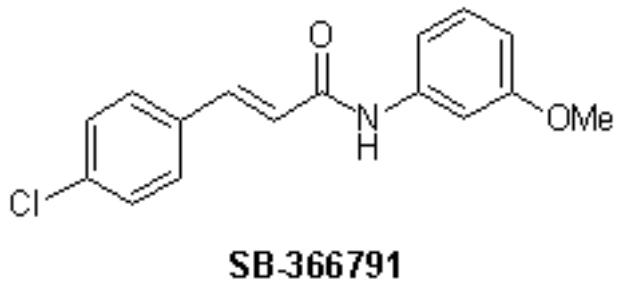

SB-366791

Figure 2.2 Chemical structure of the TRPV1 antagonist SB-366791

Finally as a goal of this thesis was to examine the effects of modulating agents on TRPV1 function and for this it is essential that the system contain appropriate additional receptor expression, the effects of bradykinin agonists were studied.

Methods

Urinary bladder smooth muscle strip studies

Animals

The animal use and welfare were in accordance with the Animals (Scientific Procedures) Act, 1986. Procedures for the STZ model were carried out under Project Licence PPL 70/6788.

Male Wistar rats (Charles River UK) with a bodyweight ranging from 300-500 g were used, where possible coordinating their use with other research and teaching projects. Animals were housed in groups of between two to four rats per cage (Techniplast standard rat housing) with access to a standard rat diet (LabDiet) and water *ad libitum*. The animal facilities (Biological Services Unit, Hatfield) were maintained at 22± 2°C, on a 12 hour light /dark cycle.

Urinary Bladder strip preparation

Rats were euthanized by an approved Schedule 1 methodology, exposure to a rising concentration of CO_2 followed by cervical dislocation. Animal body weights and blood glucose levels from tail vein blood were measured post mortem. Immediately post mortem, the abdominal cavity was opened and the whole bladder removed by an incision behind the bladder below the bladder base. Care was taken not to directly handle the bladder but manipulate it using the attached glandular tissue. Bladders were immediately placed into fridge temperature (4°C) Krebs-Henseleit solution of the composition (in mM): NaCl 118.3, KCl 4.4, $MgSO_4$ 1.2, KH_2PO_4 1.2, $NaHCO_3$ 25, D-glucose 11.1, $CaCl_2$ 2.5, gassed with 95% O_2, 5% CO_2. Placing the bladder on a Krebs-soaked tissue covered cork- board, glandular and fatty tissue was carefully dissected away and discarded. A single incision along the ventral longitudinal axis was made using scissors following insertion of the scissor tip into the bladder neck midway

between the ureters. The bladder tissue was subdivided into 4 strips using a scalpel. Coloured pins were placed through the tissue at the top of each strip to allow identification of ventral and dorsal strips. Strips were placed into fridge temperature Krebs solution gassed with 95% O_2 5% CO_2 during thread placement and individual tissue suspension. A cotton thread loop was tied around the base of each strip and a longer length of thread tied around the top of each strip. Strips were then suspended between tissue holders and isometric force transducers (AD instruments) in 15 mL jacketed organ baths (Harvard), maintained at 37°C with a steady bubble stream of 95% O_2 ,5% CO_2.

Measurement of contractile force of bladder strips

Isometric force transducers were used to determine the change in tension generated (contraction/relaxation) by bladder strips. Transducers were connected to Labchart v5 Software via a bridge amplifier (Powerlab AD instruments). Prior to bladder strip collection and setup, each Bridge amplifier was set to a range of 50 mV with a low pass of 20 Hz and calibrated using a 1 gram weight to allow transformation of measured mV values to grams of tension. Sampling speed was set at 2 per second and recording started before tissue suspension. The initial tension for bladder strips was set to 1 gram. The bladder strips were allowed to equilibrate for 30-45 minutes before any application of drug. Markers were set immediately before drug application. At the end of each experiment, cotton ties were removed from the bladder strips, the bladder strips blotted and mg wet weights measured on a micro-balance. After each experiment, the organ baths were washed with 0.1 M HCl and rinsed with distilled water to prevent salt and drug build-up.

Experimental design

After the initial equilibration period, all strips were exposed to a single concentration of carbachol (10^{-5}M) allowed to contract, washed with three organ bath changes of Krebs and left to equilibrate for 30 minutes. A concentration

range of carbachol was then applied cumulatively (final bath concentration 10^{-8}-3x 10^{-5} M), washed x 3 and left to equilibrate for a minimum of 30 minutes. In general, cumulative applications of drugs were used, diluting serially diluted solutions 1 in 1000 into the organ bath to minimize solvent exposure to the tissue. Pilot studies had revealed a moderate level of strip to strip variability, so studies were performed on duplicate tissue sets (one dorsal, one ventral strip) which would allow one treatment group, one control from each animal.

Data measurement and analysis

Baseline tension values before drug response and tensions generated in response to drug application were measured by the manual positioning of the cursor at an appropriate position on the LabChart software generated traces which reported values in grams tension. In general, the appropriate measurement position for response to drug application was deemed to be at the point of maximal contraction or relaxation, at the base of any spontaneous activity seen. Manual rather than automatic measurement of responses was the preferred method as it allowed for discrimination between spontaneous activity and drug-induced responses. Values in mgs were recorded in Excel and transformed to net mgs tension by subtracting resting tension values. Values were further transformed to mg tension per mg tissue weight by division of the net contraction value by the wet weight of the tissue in mgs. Data were further analysed using Graphpad Prism version 4 with non-linear regression analysis, sigmoidal response curves with variable slope to determine an estimate of potency pEC50 and efficacy Emax.

Statistical analysis was performed in Graphpad Prism using Student's t-test for comparison of two data groups, one-way ANOVA with post-hoc Dunnetts for comparison of more than two groups of data for e.g. for potency and efficacy estimates, and two way ANOVA with post-hoc Bonferroni for comparison of concentration response raw data, p-values of <0.05 were taken as being

significant. As the data was analysed in two ways : by scrutiny of the estimated potency/efficacy values (in tables) and by scrutiny of the actual raw data (in graphs), on occasion statistical significance was only observed in one. It was decided for the sake of transparency to keep both analyses visible as both are valid.

Drug preparation

All drugs were obtained from Sigma-Aldrich unless otherwise stated. Stock solutions of drugs were made as identified in Table 2.1, aliquoted and kept at -20°C or 4 °C before use. Final bath concentrations of solvents were kept to a minimum to avoid potential solvent induced effects. Capsaicin application resulted in <0.2% ETOH final bath concentration, when applied as a full concentration range with cumulative additions.

Table 2.1 :Urinary bladder studies drug information

Drug	Mode of action	Stock (mM)	Solvent	Dilution in	Used to
Carbachol	muscarinic agonist	10	d. H_20	d. H_20	monitor muscarinic response.
capsaicin	TRPV1 agonist	10	ETOH	20% ETOH	examine TRPV1 function
Resiniferatoxin (RTX)(Tocris)	TRPV1 agonist	1 mM	100% ETOH	20% ETOH	examine TRPV1 function
SB-366791	TRPV1 antagonist	10 mM	100% DMSO	100% DMSO	examine antagonism of TRPV1 responses
Allyl isothiocyanate (AITC)	TRPA1 agonist	1 M	100% ETOH	100% ETOH	explore TRPA1 ligand
bradykinin	bradykinin receptor agonist	1	d. H_20	d. H_20	modulate TRPV1 function
[Lys-des-Arg^9]-BK	bradykinin-1 selective agonist	1	d. H_20	d. H_20	modulate TRPV1 function
[Phe^8-y(CH-NH)-Arg^9]-BK	bradykinin-2 selective agonist	1	d. H_20	d. H_20	modulate TRPV1 function
indomethacin	cyclo-oxygenase inhibitor	1	ETOH	-	cyclooxgenase inhibition
nerve growth factor	growth factor	1 mg/ml	1% BSA/ d. H_20	1% BSA/ d. H_20	modulate TRPV1 function
anandamide (Tocris)	TRPV1 agonist	1	ETOH	20% ETOH	

d.H_20 distilled water, ETOH ethanol, BSA bovine serum albumin, HBSS Hanks Balanced Salt Solution

Effects of TRPV1 agonists

To provide a validation of the suitability of the urinary bladder to study TRPV1 responses a study of the responses to three TRPV1 agonists, capsaicin, resiniferatoxin and anandamide was performed. A concentration range of

capsaicin (10^{-9}M- 3x 10^{-6}M), resiniferatoxin (10^{-12}-3x10^{-8}M) or anandamide (10^{-8}- 3 x10^{-5}M) was applied cumulatively to the isolated urinary bladder strip preparation. In a subset of studies the extent of desensitization/ tachyphylaxis to capsaicin following washout and equilibration was examined by applying a second concentration range of capsaicin. To examine how the data could be normalised, to allow a standardization of responses between tissue preparations obtained from the same animal or from different animals on different days, normalisation of responses to tissue weight were performed.

Effects of a selective TRPV1 antagonist SB-366791

To examine the activity of a selective TRPV1 antagonist, SB-366791 on TRPV1 response to capsaicin, a range of concentrations of SB-366791 were applied to the urinary bladder strip 10 minutes prior to application of a concentration range of capsaicin. Individual studies utilized 2 strips as vehicle control (DMSO) and 2 strips received SB-366791. Non-linear regression analysis in GraphPad Prism was performed to obtain pEC50 values and concentration ratios. Schild analysis was performed to provide a pA2 estimate by plotting log(CR-1) values against Log antagonist concentration, using linear regression to obtain the intersect on the x axis which corresponds to the pA2 value for the antagonist.

Recombinant HEK293 rat-TRPV1 studies

Ratiometric intracellular calcium ([Ca]i) measurements in Human embryonic kidney 293 cells stably expressing rat TRPV1 using FURA-2AM

Cell culture

All cell culture procedures described were performed in a cell-culture cabinet to maintain sterile conditions. Human embryonic kidney 293 cells stably expressing rat TRPV1 (HEK293 rat-TRPV1 cells) were cultured in T75 cell culture flasks using Dulbecco's Modified Eagle Medium: Nutrient Mixture F-12 (DMEM/F12 (1:1) Invitrogen 21331), supplemented with 10 % fetal bovine serum (Invitrogen 10500), 1x non-essential amino acid (Sigma M7145), 2 mM L-glutamine (Invitrogen 25030), 100 units/ml penicillin streptomycin (Invitrogen 15140) and 0.8 µg/ml geneticin G418 (Invitrogen 10131). Cell cultures were incubated at 37°C in a 95 % O_2 / 5 % CO_2 humidified cell culture incubator. The rat TRPV1-expressing HEK 293 cells were passaged once a week when confluency was between 80 – 90 % and only cells from passage number 20 or lower were used in the studies reported here. To passage cells or remove cells for use in the FURA-2AM assay, old media was aspirated off, 3 ml of room temperature accutase solution (Sigma A6964) was added and incubated at room temperature for 5 minutes. Accutase was used instead of trypsin EDTA to minimize the proteolytic activation of protease activated receptors. Cells were dislodged from the flask by a swift tap and resuspended in 18 ml of fresh media. For passage, a 1:5 to 1:10 dilution of cells were made into a new T75 flask containing a total volume of 20 ml media and returned to the incubator. For FURA-2AM assay, the cells were transferred into a 50 ml centrifuge tube and topped up with cell culture media; one flask of cells was required per 96-well plate.

FURA-2AM assay of intracellular calcium

Cell loading with fluorescent calcium indicator FURA-2AM

HEK293 rat TRPV1 cells were centrifuged (400g for 5 minutes, room temperature), washed in Hanks Balanced Salt Solution + calcium and magnesium, supplemented with 2.5 mM probenecid and HEPES (HBSS + buffer), gently resuspended in 12 ml HBSS + buffer containing 2 mM Fura-2AM and 25 µL pluronic F-127 (20% solution in DMSO), wrapped in foil and incubated at 37°C for 45 minutes. After this time, cells were pelleted by centrifugation (400g, 5min, room temperature) and washed twice with HBSS + buffer before resuspension in 20 mL of HBSS + buffer / T75 flask. 180 ml (or 160 ml for antagonist studies) per well of cells was pipetted into 96-well clear flat-bottom Greiner plates, wrapped in foil and incubated in a shaker-incubator at 37°C for 20 minutes prior to ratiometric fluorescence measurements and drug additions.

Preparation of drug solutions

For agonist and antagonist studies 10 or 11-point concentration ranges were prepared in a 96-well clear flat bottom Greiner plate at 10 x final concentration required, using the lowest amount of solvent possible and keeping the solvent levels constant throughout the dilution series.(Table 2.2)

Application of agonist and antagonist solutions to cells

20 µls of agonist or antagonist solutions were pipetted into the cell-containing plate immediately before ratiometric fluorescent measurements were made. For antagonist experiments, agonists were applied 10 minutes after antagonist application. Duplicate or triplicate wells were used for each agonist/antagonist concentration.

Ratiometric fluorescent measurement using Flexstation.

Fluorescent measurements (excitation 340, 380 nM, emission 510 nM) were made immediately before and after compound addition. Repeated measurements were made in a subset of agonist studies. The Flexstation internal incubator temperature was set to 37°C.

Data analysis

Ratios of 340/380, representing ratio of free to bound intracellular calcium were calculated using Softmax Pro version 4 software and data was exported as a text file, into excel transformed to delta-ratios and inputted into Graphpad Prism version 4 for visualisation and further analysis. Data is presented as normalised values to capsaicin's maximum response, or percent inhibition of capsaicin's response. Non-linear regression analysis was performed in Graphpad Prism to determine pEC50 and Emax values for agonist responses and pIC50 values for antagonist effects. Statistical analysis was performed in Graphpad Prism using student's t-test for comparison of two groups or one-way ANOVA with post-hoc Dunnetts for comparison of more than two groups of data, p-values of <0.05 were taken as being significant.

Table 2.2 : HEK293 rat TRPV1 intracellular calcium assay drug information

Drug	Mode of action	Stock	Solvent	Dilution in	Used to
FURA-2AM (invitrogen)	fluorescent calcium indicator		100% DMSO		measure i[Ca] responses
pluronic F127	dispersal agent		-		aid loading of FURA-2AM
probenecid		71 mg/ml	50% 1M NaOH, 50% HBSS buffer	HBSS	prevent FURA leakage from cells
capsaicin	TRPV1 agonist	10 mM	ETOH	20% ETOH then 1:10 in HBSS	examine TRPV1 function
resiniferatoxin (RTX)(Tocris)	TRPV1 agonist	1 mM	ETOH	20% ETOH then 1:10 in HBSS	examine TRPV1 function
anandamide (Tocris)	TRPV1 agonist				
SB-366791	TRPV1 antagonist	10 mM	DMSO	HBSS	examine antagonism of TRPV1 responses
ruthenium red (Tocris)	Non-selective antagonist	10 mM	ETOH	d. H_20	examine antagonism of TRPV1 responses
[Lys-des-Arg^9]-BK	BK-1 agonist	10 mM	d. H_20	d. H_20	
[Phe^8-Y-(CH-NH)-des-Arg^9]-BK	BK-2 agonist	10 mM	d. H_20	d. H_20	

DMSO dimethyl suphoxide, HBSS Hanks Balanced Salt Solution, ETOH ethanol

HEK293 rat TRPV1 intracellular calcium study details

TRPV1 agonist and antagonist validation studies

Responses to the TRPV1 agonists capsaicin, RTX, anandamide and met-anandamide were studied. Responses to capsaicin and RTX were additionally studied over a period of time (up to 15 minutes). The effects of a selective TRPV1 antagonist SB-366791 versus 1 μM capsaicin were examined. In addition, the effects of a non-selective antagonist, ruthenium red were studied versus a full concentration range of capsaicin, to examine the nature of this antagonist in this system.

Bradykinin receptor agonist studies

Responses to the bradykinin selective agonists were studied to accertain whether this recombinant cell line expressed bradykinin receptors.

Results

Model system 1: The urinary bladder strip

Effects of the muscarinic agonist carbachol

The initial study of a muscarinic agonist carbachol revealed that this agonist caused a consistent concentration-related contraction of urinary bladder strips from naïve rats. The normalization to response in mgs tension per mg tissue weight did not detrimentally affect the data (Figure 2.3). Non-linear regression analysis obtained pEC50 and Emax values for carbachol (Table 2.3).

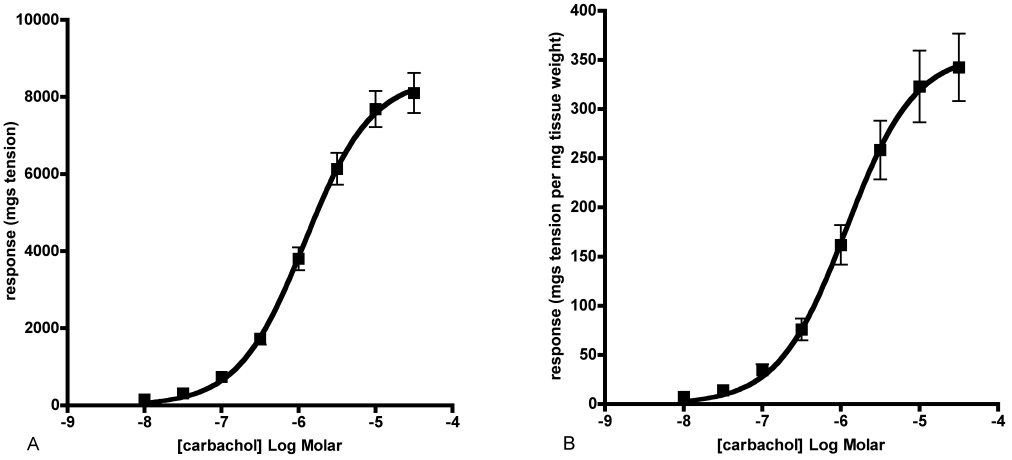

Figure 2.3 Graphs showing raw data (A) and normalized to tissue weight (B) contractile responses to a concentration range of the muscarinic agonist carbachol in urinary bladder from naïve rats. Data represents mean ± s.e.m. for n>6 urinary bladder strips.

Effects of the TRPV1 agonists, capsaicin, resiniferatoxin and anandamide

Next responses to three TRPV1 agonists were examined in urinary bladder. All three agonists caused contractile responses in urinary bladder tissue, with a range of potency and efficacies observed. The responses to resiniferatoxin (RTX) and anandamide (AEA) had a lower maximal efficacy response than to capsaicin. Again normalization of tension responses to tissue weight did not appear to have

a detrimental effect on the dataset (Figure 2.4). Non-linear regression analysis provided estimates of potency and efficacy for all three TRPV1 agonists (Table 2.3). Resiniferatoxin was found to be the most potent TRPV1 agonist with a pEC50 of 11.18, followed by capsaicin at 7.82, with the lowest potency TRPV1 agonist being anandamide with a potency of 5.37. Capsaicin gave the highest maximal efficacy, with resiniferatoxin and anandamide having considerably lower maximal efficacies.

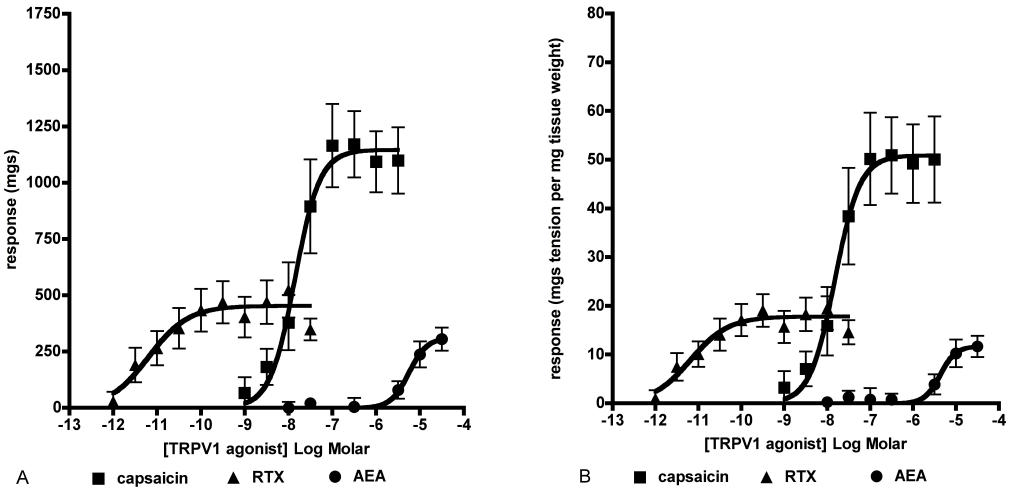

Figure 2.4 Graphs showing raw data (A) and normalized to tissue weight (B)contractile responses to a concentration range of the TRPV1 agonist s capsaicin, resiniferatoxin (RTX) and anandamide (AEA) in urinary bladder from naïve rats. Data represents mean ± s.e.m. for n>6 urinary bladder strips.

Table 2.3 Potency and efficacy estimates for carbachol, capsaicin, resiniferatoxin and anandamide in urinary bladder. Data represent mean ± s.e.m. n>6 urinary bladder strips

	pEC50	Emax
carbachol	5.93 ± 0.10	356.9 ± 18.91
capsaicin	7.82 ± 0.15	50.9 ± 4.26
resiniferatoxin	11.18 ± 0.22	17.8 ± 1.66
anandamide	5.37 ± 0.17	11.7 ± 2.00

Following the application of a concentration range of capsaicin, washout and equilibration, a second application of capsaicin was performed. Here no response to this second application of capsaicin was observed, indicating that a complete desensitisation or tachyphylaxis had occurred.

Effects of a selective TRPV1 antagonist SB-366791

The next part of the validation studies of urinary bladder were to examine the effects of a selective TRPV1 antagonist on capsaicin responses. Here a concentration range of SB-366791 or vehicle control were applied to the urinary bladder, incubated for 10 minutes with no washout and a cumulative concentration range of capsaicin applied. SB-366791 caused a parallel rightward shift in capsaicin potency with no depression of efficacy (Figure 2.5). Schild analysis was performed and a pA2 estimate of 6.32 with a slope of 1.05, close to unity, was obtained.

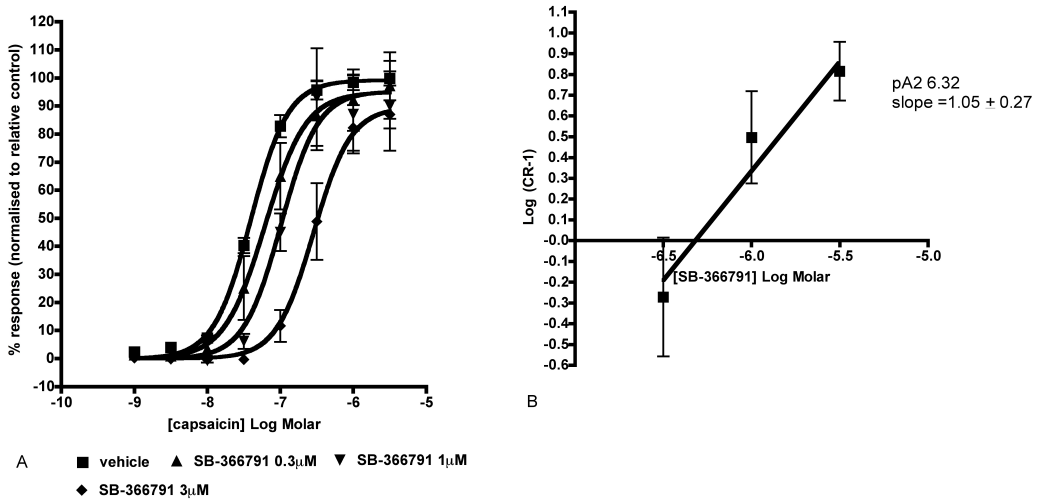

Figure 2.5 Graphs showing the effect of increasing concentration of SB-366791 on capsaicin responses (A) and Schild analysis of this data (B) used to obtain a pA2 estimate for SB-366791. Data represent mean + s.e.m. n>6 urinary bladder strips.

Bradykinin receptor agonist effects

The final validation step for the urinary bladder model system was to examine bradykinin responses. Previous in-house data had shown contractile responses to a bradykinin concentration range (Katisart, 2011)and these studies were to repeat this and extend by the use of bradykinin selective agonists: BK-1 selective agonist, [Lys-des-Arg9]-BK, and the BK-2 selective agonist, [Phe8-y(Ch-NH)-Arg9]-BK. Application of a concentration range of bradykinin elicited a concentration dependent contraction (Figure 2.6). BK-1 and BK-2 agonists also caused a concentration-dependent contraction (Figure 2.6). The BK-2 agonist was seen to be the most potent and efficacious, followed by bradykinin and lastly the BK-1 agonist. From these data, pEC50 and Emax estimates were calculated where the rank order of potency was seen to be BK-2 agonist> bradykinin> BK-1 agonist (Table 2.4)

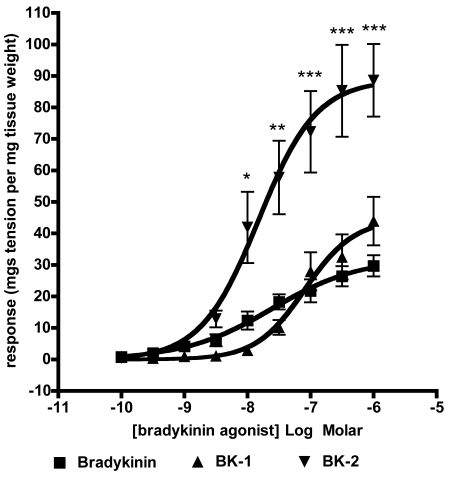

Figure 2.6 Graph showing contractile responses of control urinary bladder strips to bradykinin and bradykinin selective agonists for BK-1 and BK-2. Data represent mean + s.e.m. n>6 urinary bladder strips. Statistical significance was tested by two-way ANOVA with post-hoc Bonferonni, * represents $p<0.05$, ** $p<0.01$, ***$p<0.001$, compared to bradykinin response.

Table 2.4 Direct contractile effects of bradykinin and bradykinin selective agonists: potency and efficacy in urinary bladder strips from control rats. Data represent mean ± s.e.m. of n>6 urinary bladder strips.

	pEC50	Emax
bradykinin	7.62 ± 0.28	32.14 ± 4.40
BK-1	7.08± 0.19^{NS}	44.51± 6.59^{NS}
BK-2	7.82± 0.18^{NS}	88.76± 8.77**

Statistical analysis by one-way ANOVA comparing to bradykinin, NS non-significant, *p<0.05, **p<0.01, ***p<0.001.

Model system 2 : Recombinant HEK293 rat-TRPV1 cells

TRPV1 agonist effects

First the responses to three TRPV1 agonists capsaicin, resiniferatoxin and anandamide were examined in the HEK293-rTRPV1 cellular assay of intracellular calcium. Here resiniferatoxin and capsaicin elicited clear increases in intracellular calcium, whereas anandamide did not produce a notable response. Resiniferatoxin gave equivalent maximal efficacy responses to capsaicin and was seen to be more potent than capsaicin. (Figure 2.7) (Table 2.5)

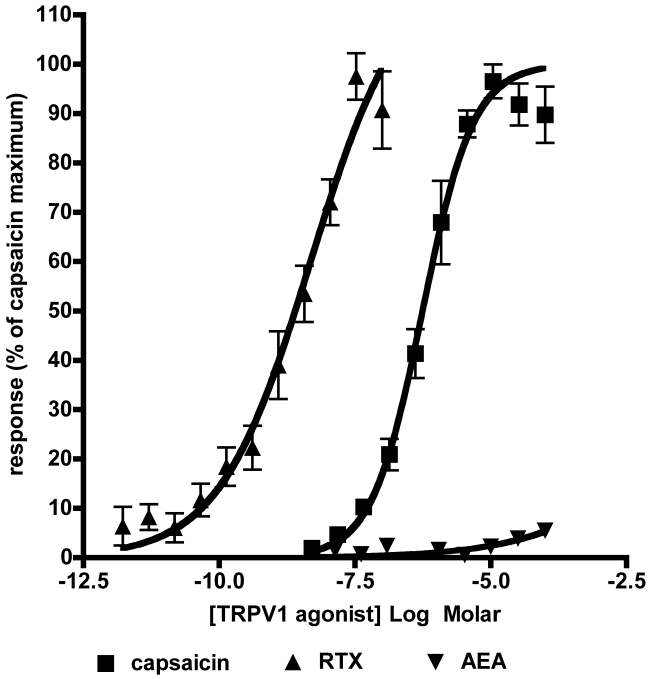

Figure 2.7 Graph showing intracellular calcium responses measured by FURA-2AM ratiometric fluorescence to TRPV1 agonists capsaicin, resiniferatoxin (RTX) and anandamide. Data represents mean $\pm$ s.e.m n of 3 separate experiments

Table 2.5 Potency and efficacy estimates for the TRPV1 agonists in the HEK293-rTRPV1 intracellular calcium model system. Data represent mean + s.e.m. n of 3 experiments.

	pEC50	Emax
capsaicin	6.25 ± 0.05	100
resiniferatoxin	8.32± 0.27	119.5 ± 15.32
anandamide	-	-

TRPV1 antagonist effects

Next the effects of a concentration range of the selective TRPV1 antagonist SB-366791 and the non-selective Ruthenium Red were studied against 1 μM capsaicin response. Both antagonists inhibited capsaicin response in a concentration–related manner (Figure 2.8). pIC50 estimates were calculated using this data , SB-366791 yielded a pIC50 estimate of 5.60 ± 0.68, Ruthenium Red pIC50 6.51 ± 0.07.

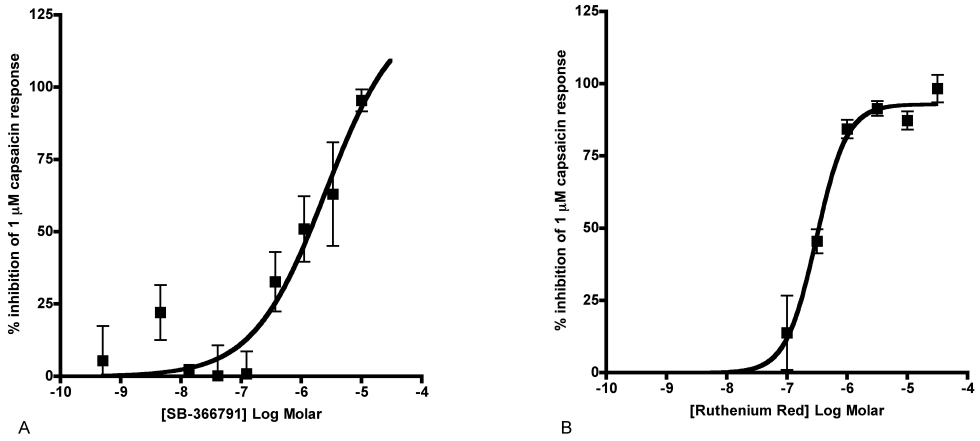

Figure 2.8 Graphs showing inhibition of 1 μM capsaicin intracellular calcium response by selective TRPV1 antagonist SB-366791 (A) and non-selective antagonist Ruthenium Red (B). Data represent mean ± s.e.m. n of 3 separate experiments.

An additional study of Ruthenium Red activity versus a full concentration range of capsaicin was examined. Here increasing Ruthenium Red concentration was seen to cause a depression in efficacy of capsaicin responses (Figure 2.9)

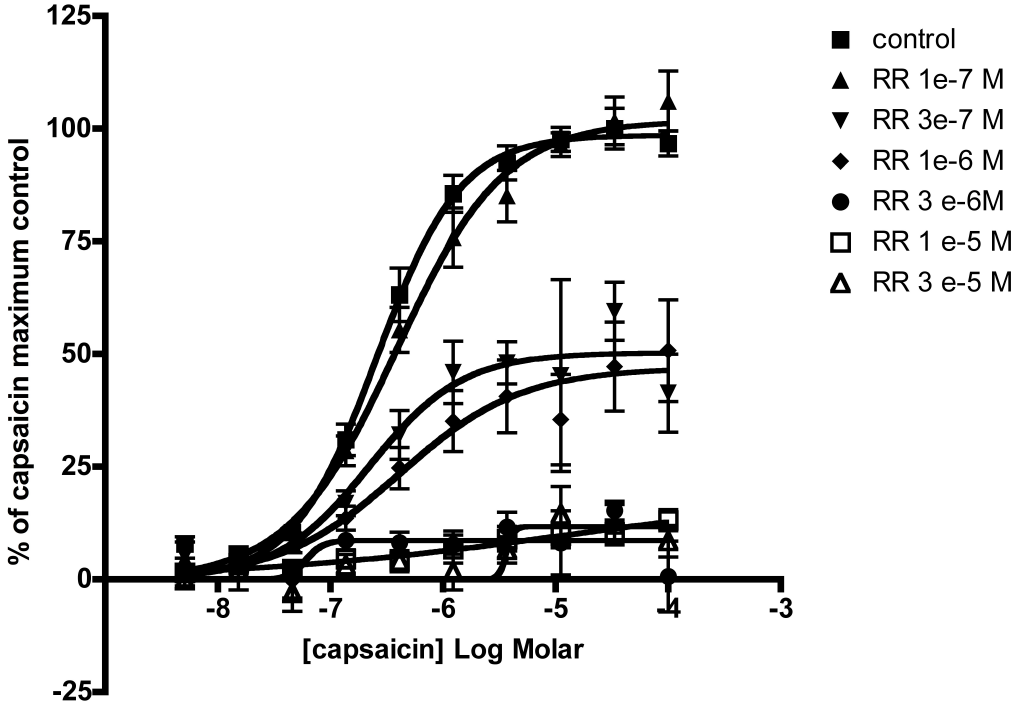

Figure 2.9 Graph showing the effect of a range of Ruthenium Red concentrations on intracellular calcium responses to a concentration range of capsaicin in HEK293-rTRPV1 cells. Data represents mean ± s.e.m. n of 3 separate experiments.

Effects of bradykinin agonists

Finally to examine the utility of this model system on exploration of a modulating agent of TRPV1 function, the effects of bradykinin selective agonists were examined: BK-1 selective agonist, [Lys-des-Arg9]-BK, and the BK-2 selective agonist, [Phe8-y(Ch-NH)-Arg9]-BK. Firstly intracellular calcium responses to the bradykinin selective agonists were monitored. No intracellular calcium response to bradykinin agonists was observed. Secondly, capsaicin responses were monitored following bradykinin agonist application. No potentiation of

capsaicin responses were seen following bradykinin agonist application either separately or in combination (Figure 2.10).

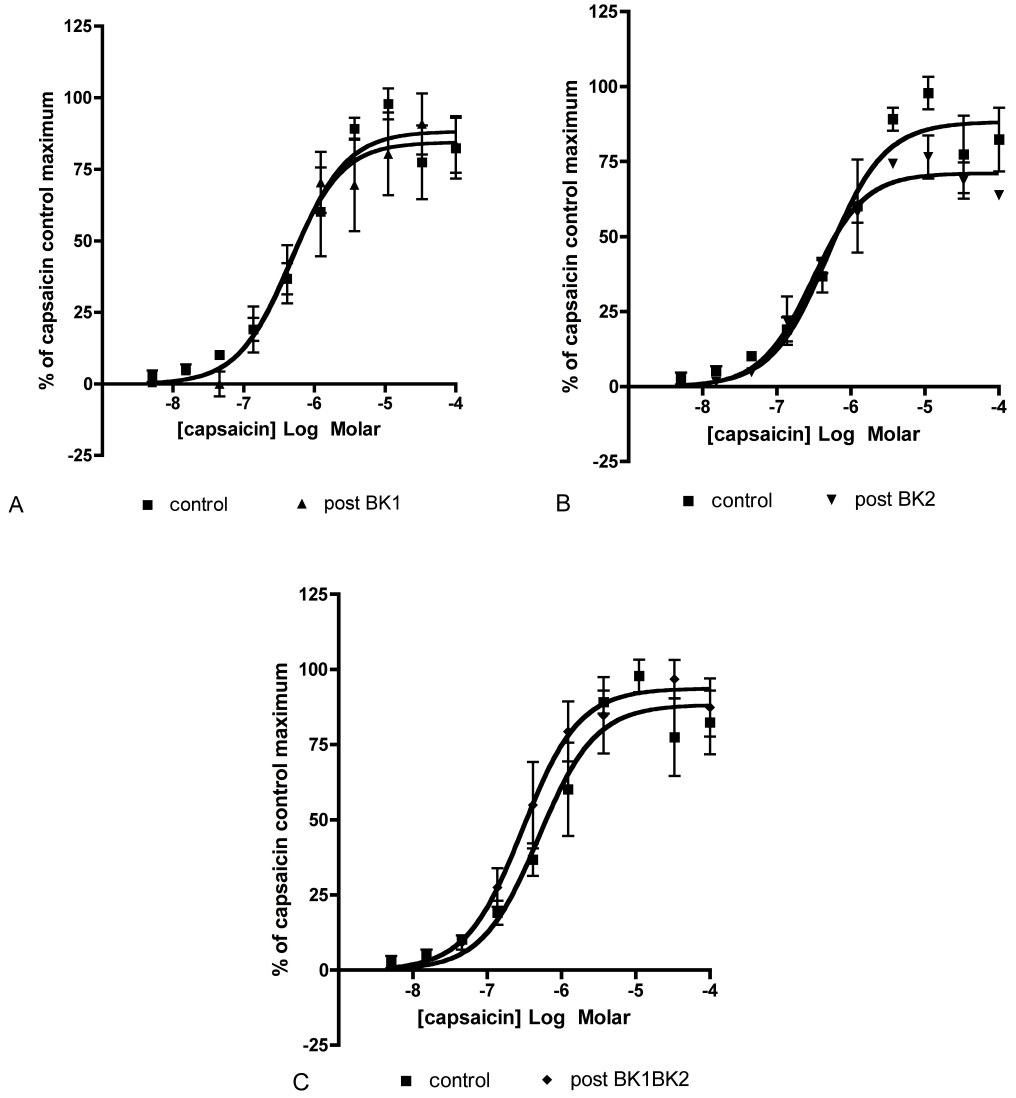

Figure 2.10 Graphs showing intracellular calcium responses to a concentration range of capsaicin following application of control or 1 μM bradykinin-1 selective agonist (A), 1 μM bradykinin-2 selective agonist (B) or a combination of 1 μM bradykinin-1 and 1 μM bradykinin-2 selective agonists (C). Data represent mean ± s.e.m. of n of 3 separate experiments.

Discussion

The urinary bladder model responded robustly to the muscarinic agonist carbachol

Carbachol elicited a very robust contractile response in urinary bladder strips from naïve rats. This response could be used to monitor myogenic responses throughout the diabetic model and following exposure to modulating agents *in vitro*.

The urinary bladder model responded robustly to all three TRPV1 agonists

The urinary bladder model system responded to all three TRPV1 agonists tested. Robust pEC50 and Emax values could be obtained which was seen to be important for the future study of modulation of the TRPV1 response in sensory neuropathy. However no response to a second application of capsaicin was seen indicative of a complete desensitisation to capsaicin. This posed a limitation on the study design. Normalisation to mgs tension per mg tissue weight did not appear to cause a detriment to the dataset. This normalization was thought to be necessary because diabetes is known to cause increases in bladder weight through smooth muscle hypertrophy. Without a normalization to weight or muscle mass, an overestimation of responses would be seen in the STZ-induced diabetic group and a direct comparison to control tissue could not be made.

The TRPV1 selective antagonist SB-366791 inhibited capsaicin responses in urinary bladder

Increasing concentrations of SB-366791, a selective TRPV1 antagonist, caused parallel rightward shifts in capsaicin responses with no depression of efficacy. A pA2 estimate was obtained which was similar to that reported in the literature, although no pA2 value could be found in the literature for a native tissue assay such as the urinary bladder system used here. The competitive inhibitory profile for SB-366791 added confidence that this native tissue assay was a suitable model system for examining TRPV1 modulation on two counts. Firstly it was

seen that the capsaicin response could be shifted within the confines of the concentration range that could be applied and responses obtained. Secondly the use of a selective TRPV1 antagonist further verified the validity of this model system as having TRPV1 receptors present that on activation cause a recordable response.

Previous in-house data had demonstrated that bradykinin application caused a contractile response in urinary bladder tissue and caused a potentiated response to the subsequent application of capsaicin in tissue from STZ-induced diabetic rats (Katisart, 2011)

As a primary model system, initial validation studies on urinary bladder tissue proved to be successful. Additionally the potential utility of a recombinant cellular system, HEK293 rTRPV1 cells was examined.

Two out of three TRPV1 agonists cause a response in HEK293-rTRPV1 cell intracellular calcium assay

Capsaicin and resiniferatoxin but not anandamide caused increases in intracellular calcium in HEK293 cells stably transfected with rat TRPV1. The responses to resiniferatoxin and capsaicin appeared to be of the same magnitude (efficacy) but resiniferatoxin was found to be more potent than capsaicin. This efficacy /potency profile differed from that seen in the native tissue system of urinary bladder where Emax values for resiiferatoxin were clearly lower than that seen for capsaicin. Additionally, although a low response to anandamide in urinary bladder was seen, it was identifiable as a response and able to be measured within the confines of the concentration range that could be applied. This was not the case for the HEK293 rTRPV1 system, where potencies were lower indicating lower receptor expression than that seen in the native tissue urinary bladder. This may appear counter intuitive given that the HEK293 rTRPV1 system is a recombinant system transfected with exogenous receptor and might be expected to contain very high levels of TRPV1 receptor. Ion channel recombinant expression systems tend to have a self-limiting expression

level of receptor as over expression of receptor will lead to cellular toxicity and cell death as will low expression as in this system it is under G418 selection. Therefore the expression levels could well be lower than that seen in a native tissue system.

Resiniferatoxin displayed partial agonism in the urinary bladder system

Low receptor reserve could explain the appearance of partial agonism. In these studies resiniferatoxin (and anandamide) appeared to be partial agonists in the urinary bladder system. However comparing potencies between the two model systems, it could be seen that the urinary bladder system reported higher potency values than the HEK293 rTRPV1 system. This indicates a higher receptor expression in urinary bladder than the HEK293 cells and precluded the low receptor reserve explanation for the partial agonism exhibited by resiniferatoxin and anandamide. An alternate explanation for these data could be that the association rate for resiniferatoxin was slow and may elicit a lower calcium influx in a native system. Indeed this has been identified in the literature as a high potency low pungency agonist (Raisinghani et al., 2005).

This initial validation work was to identify the most suitable model assay system to allow modulation of TRPV1 receptor in sensory neuropathy. Here it was seen that the urinary bladder model proved to be the most suitable assay system as it:

- expressed TRPV1 receptors which when activated by tool agonists resulted in a contractile response that could be easily measured, and was blocked by the use of a selective TRPV1 antagonist SB-366791.
- expressed bradykinin receptors that could be manipulated pharmacologically by bradykinin and selective agonists , causing an initial contractile response which would allow investigation of the modulation of the TRPV1 receptor and quantification of changes to bradykinin receptor by diabetes.
- required minimal dissection and preparation thus hopefully avoiding phenotypical alteration of the TRPV1 receptor.

- able to be studied under diabetic conditions through the use of an animal model of diabetes.
- relevant to sensory neuropathy.
- be able to be normalized through the use of tissue weight to reduce experimental variability and monitored through the use of a muscarinic agonist carbachol to compensate for factors that could change during diabetes.

The HEK-rTRPV1 recombinant system was considered to be less suitable than the urinary bladder system for a number of reasons:

Firstly although this system responded to TRPV1 agonists and antagonists, the potencies seen here were some 10 fold lower than the native tissue system. Secondly the system required a reasonable level of in vitro manipulation which potentially could impact on the phenotypic expression of TRPV1- mainly during passage cells were removed from the plasticware by accutase, although this product is believed to be less harsh than tryptase treatment, it was unknown whether this would activate any protease activated receptors which are known to interact with and sensitise the TRPV1 receptor (Amadesi et al., 2006). Mechanical dissociation, e.g. scraping, is also known to cause ATP release which again could potentially affect TRPV1 function. Using a plated format rather than a suspension method could be utilized however these cells were very easily removed from the 96-well plates and the wash steps used in this format caused a high degree of variability in the assay. Looking at the way in which these cells were grown, it was recognized that the use of G418 as a selection media, could also impact on the phenotype of the TRPV1 receptor. G418 is an analogue of neomycin and neomycin is known to sequester cholesterol and is used in dispersal studies of PIP2, which could release TRPV1 from an inhibited state and cause TRPV1 sensitisation (Thompson et al., 1970). Thirdly it was seen that bradykinin selective agonists had no effects on intracellular calcium or on subsequent capsaicin responses. This would preclude the use of this system to study the effects of potential interacting receptors without the additional

transfection of individual receptors into the cells. Finally diabetes is a complex disease and is hard to model *in vitro*.

Taking everything into consideration it was decided to focus efforts on the urinary bladder system to study the modulation of TRPV1 receptor in sensory neuropathy. The next studies were undertaken to map the onset of dysfunction of TRPV1 in a diabetic rat model: STZ-induced diabetes.

Chapter 3: Mapping the onset of dysfunction in TRPV1 during diabetes

Introduction

To initially gain an understanding of when and how TRPV1 is being modulated during the onset of sensory neuropathy, these studies were undertaken specifically to map the onset of TRPV1 dysfunction following diabetic induction by STZ administration. Previous in-house data had shown a reasonably rapid onset of TRPV1 dysfunction (Katisart, 2011), where a diminished response had been seen by 8 weeks post STZ treatment. The model used here was the bladder muscle in control or STZ-treated rats at 2 day, 2 week, 5-6 week and 7-10 weeks post treatment. The bladder is thought to be a good model for mapping sensory neuropathy as the dysfunction in this organ that develops in diabetes is thought to be directly caused by neuropathy (Burakgazi et al., 2012).

In diabetes, cystopathy is a very common complication. Between 43% and 87% of Type 1 diabetics have cystopathy whereas in Type 2 diabetics the incidence is lower at around 25% (Frimodt-Møller, 1980) . Cystopathy can be defined as bladder dysfunction and this mainly refers to a diminished voiding capacity i.e. incomplete emptying of the bladder. Cystopathy manifests as decreased bladder sensation, increased post-void residual volume, reduced bladder muscle contractility and a diminished urinary flow (Kaplan and Blaivas, 1988). Cystopathy has been seen clinically in patients who have been diagnosed with diabetes for less than 12 months (Ueda et al., 1997) which clearly demonstrates that the onset of bladder dysfunction in diabetes can be rapid. However, even with quite abnormal bladder function, diabetics are often unaware that they have cystopathy until they develop a urinary tract infection, which can result from incomplete bladder emptying (Burakgazi et al., 2012). During a urinary tract infection, the symptoms of cystopathy become much more apparent. In animal models of diabetes, cystopathy has been observed at 8 weeks post diabetic induction using cytometry (Yenilmez et al., 2006), indicating a rapid

onset of bladder dysfunction.

The association of peripheral neuropathy with cystopathy is very high between 75-100% (Frimodt-Møller, 1980), indicating that neuropathy plays a major role in cystopathy. Clinical and animal studies have revealed that cystopathy is a direct result of sensory and autonomic neuropathies (Burakgazi et al., 2012). The symptoms and occurrence of cystopathy have been observed in various animal models of diabetes (Dahlstrand et al., 1992). Here capsaicin responses have been seen to be diminished which is suggestive of a role of TRPV1 for the sensory loss and development of cystopathy (Dahlstrand et al., 1992). In house data has also highlighted that TRPV1 function is diminished in detrusor preparations from STZ-induced diabetes in rats by 8 weeks post diabetic induction(Katisart, 2011). Whether the reduced functionality of TRPV1 is due to reduced neuropeptide content of the sensory nerves or to reduced receptor expression is as yet unclear.

There is also evidence that diabetic cystopathy has a myogenic component (Longhurst and Belis, 1986) and one of the symptoms of cystopathy is reduced muscle contractility. In early stage diabetes, the bladder rapidly increases in size to a) accommodate for the increased volumes of urine that are eliminated, and b) due to bladder stretching which arises from decreased bladder sensation. In TRPV1 knockout mice, an increased bladder size is seen alongside altered micturition thresholds and is indicative of the role TRPV1 plays in bladder sensation (Daly et al., 2007). The expansion of bladder volume is associated with increased bladder mass mainly through detrusor muscle hyperplasia and hypertrophy (Suzuki et al., 2006). This increased muscle mass has a reduced contractility in response to some agonists when corrected to force generated per unit of mass (Du et al., 2000, Longhurst and Belis, 1986), although some investigators report no change in sensitivity(Lincoin et al., 1984) and even increased muscarinic receptor expression (Tong et al., 1999). However, the general consensus is that despite an increased muscular component, the ability of the bladder to contract to elicit effective urinary discharge is impaired. An altered cholinergic enzyme activity has been seen in the bladder of the STZ-

induced diabetic model (Tong et al., 2006, Lincoin et al., 1984) so for this reason carbachol is the muscarinic agonist of choice to examine myogenic function. Carbachol is resistant to degradation by acetylcholine esterase activity and therefore should provide an unbiased measure of muscle contractility. As well as contractile strength, contractile speed has a bearing on the ability of a muscle to contract and has been reported to be impaired in aged rats and humans (Saito et al., 1991, Coolsaet and Blok, 1986). To examine the speed of muscular force generation, an examination of the carbachol response was undertaken, where a single high concentration of carbachol was applied and the time taken to reach 50% of maximum response measured.

To evaluate the total neurogenic component of detrusor muscle contraction, as TRPV1 is not the only receptor present in bladder sensory neurons, an examination of electric field stimulation evoked contraction was undertaken. In TRPV1 knockout mice, an increased spontaneous activity i.e. non-voiding contractions of bladder muscle is present (Birder et al., 2002), therefore an examination of spontaneous activity of the detrusor muscle was undertaken.

Therefore this series of studies were undertaken to map the changes primarily in TRPV1 function that may occur following induction of diabetes by STZ administration. Secondly carbachol responses were monitored to provide information on changes in muscular contractility. Thirdly, where robust changes in TRPV1 function had been seen, some bladder tissue was examined for changes in electrical field stimulation evoked contractility as a measure of total neuronal function. Finally, an examination of spontaneous activity of the detrusor muscle was undertaken. In this series of studies, age-matched, control animals received the same volumetric dose of citrate buffer.

Methods

Induction and monitoring of streptozotocin (STZ) model

Male Wistar rats (initial bodyweights 300-400g) were used for the STZ model as female rats show resistance to STZ-diabetogenic effects and lower/higher bodyweight rats have a higher rate of mortality post STZ administration. Body weights were measured before STZ administration and intermittently throughout the study to allow monitoring of the animals general condition. In order to induce a diabetic state, STZ at 65 mg/kg was administered via a single intraperitoneal (i.p.) injection using a volume of 10 ml/kg. STZ was dissolved in 20 mM citrate buffer, pH 4.5 and allowed to stand at room temperature for 1 hours prior to injection, following the work of de la Garza-Rodea, A. S., et al. (De La Garza-Rodea et al., 2010) who demonstrated that this time period allowed for the more toxic anomer of STZ to equilibrate with the less toxic anomer, thereby standardizing the toxic quality of the preparation. Age matched controls were injected i.p. with 10 ml/kg of 20 mM citrate buffer, pH 4.5. Animals were pair - housed, one control, one STZ, which helps to maintain the STZ-treated animals body temperature. For 48 hours following STZ or control injection, additional 2% sucrose solution was provided in a drinking water bottle, to avoid the initial hypoglycaemia that is seen following STZ. One week following STZ injection, the blood glucose levels from 1 drop of tail vein blood, obtained by a needle prick of conscious rats, were measured using an Accu-check blood glucose monitor. Successful diabetic induction was classed as an approximate three-fold increase in blood glucose level.

Experimental design

Rats were terminated by a schedule 1 approved methodology (exposure to rising CO2 followed by cervical dislocation) at various timepoints following STZ or control solution administration: 2 days, 2 weeks, 5-6 weeks, 7-10 weeks, over a series of studies. Body weights and blood glucose levels from tail vein blood were measured. Bladders were dissected out, weighed and set up in organ baths as described previously.

Effects of STZ on TRPV1-mediated contraction of the urinary bladder

The responses to a concentration range of the TRPV1 agonist capsaicin (1x 10^{-9}- 1 x 10^{-5}M) made in 20% ETOH, applied in a cumulative fashion, were examined. Following the top concentration of capsaicin, tissues were washed x 3 and allowed to equilibrate for 30 minutes.

Recovery after capsaicin contraction

In a subset of studies, following the final top concentration of capsaicin, tissues were not washed but measurements taken every minute until tension had returned to baseline, at which point tissues were washed x 3 and allowed to equilibrate for 30 minutes.

Monitoring of carbachol responses following control or STZ administration

The responses to a concentration range of the muscarinic agonist carbachol (1x 10^{-8}- 3x10^{-5}M) made in distilled water, applied cumulatively were measured. Following the top concentration of carbachol, tissues were washed x 3 and allowed to equilibrate for 30 minutes.

Kinetics of carbachol contraction

To monitor the speed of contraction of the bladder muscle strips to carbachol, a subset of tissues were exposed to 1 x 10^{-5}M carbachol and raw data covering the complete timescale of contraction, sampled every 0.5 sec, were extracted. Data was normalised to % values of maximum contraction to account for the differences between control and STZ-treated animals, and plotted using Graphpad Prism. The time taken to reach 50% of maximum was measured and data was further divided to enable a comparison of the anatomically different bladder strips (dorsal and ventral)

Comparison of changes in capsaicin and carbachol responses

To allow a direct comparison of the changes seen in Emax values for capsaicin and carbachol, Emax values for each timepoint were normalised to their respective control animal values and these ratios plotted together.

Measurement of spontaneous activity

Using cycle variable analysis in Labchart, with the noise threshold set to zero and trigger point at maximum ,frequency and average maximum and minimum values of spontaneous activity were obtained over 5-10 minutes. An example of the triggering pattern is shown in Figure 3.1. Amplitudes were calculated from maximum and minimum values and normalized to mgs response per mg tissue weight to compensate for tissue weight difference between control and STZ-treated tissue.

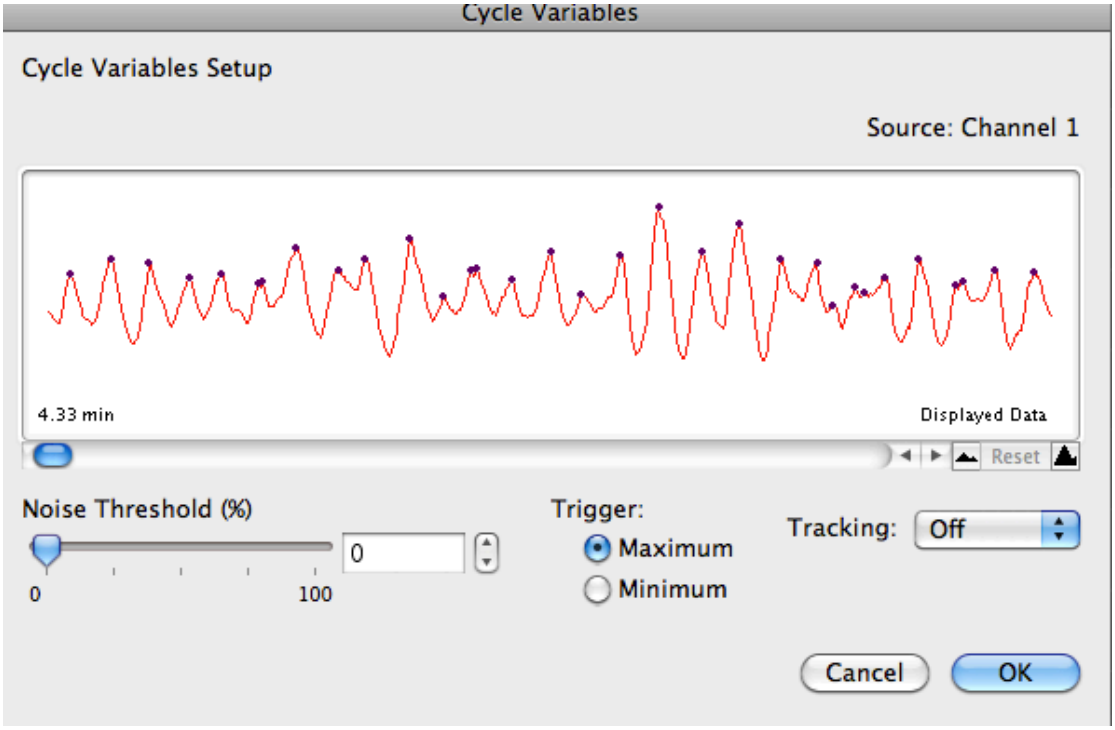

Figure 3.1 Example of triggering pattern used for spontaneous activity analysis of raw data from urinary bladder.

Electrical Field stimulation

Where robust changes in TRPV1 function had been seen a subset of studies in 2-week post control or STZ administration was undertaken to monitor electrical field stimulated contraction. Urinary bladder strips were mounted between platinum electrodes within the organ bath setup. The electrodes were attached to a Harvard electrical stimulator and a Harvard cycle Timer. A train of electrical pulses was applied (0.1 ms pulse width, rate of 50 Hz, 10 sec duration) firstly to a range of voltages (20-100 Volt) to identify the submaximal voltage. Then using this submaximal voltage, to a range of frequencies (0.25 Hz-40 Hz). The frequency range study was then repeated following application of 1 μM tetradotoxin (TTX) to determine whether the electrical field stimulation was evoking contractions neurogenically.

Analysis of data

Data was extracted from Labchart and exported into excel where raw data was transformed into mgs tension per mg tissue weight. Raw data and transformed data were plotted using Graphpad Prism, and non-linear regression analysis performed to obtain pEC50 and Emax values for capsaicin and carbachol.

Results

Monitoring of body weights and blood glucose

Control rats gained weight at a rate of around 10 g per day throughout the study up until the 5-6 week timepoint where weight gain reduced. STZ-treated rats failed to gain weight as quickly as control animals but in general maintained their starting weight. Control rats maintained a blood glucose level within the normal expected range, at all timepoints examined. In the STZ-treated rats, blood glucose increased to three to four fold above control levels by day 2 following STZ administration and remained consistently high upto the last timepoints, 7-10 weeks (Table 3.1).

Table 3.1 Body weight and blood glucose measurements from rats at various timepoints following administration of either control buffer or STZ. Data are mean ± s.e.m for n>3 animals per group

	Control		STZ	
Time after control/STZ administration	body weight (g)	blood glucose (mmol/Litre)	body weight (g)	blood glucose (mmol/litre)
start	314 ± 11	6.9 ± 0.5	315 ±10	6.7 ± 0.6
2 days	320 ± 3^{NS}	7.1 ± 0.4^{NS}	307 ±9^{NS}	26.8 ± 2.4***
2 weeks	497 ± 13***	7.0 ± 0.3^{NS}	346 ±11^{NS}	28.8 ± 0.9***
5-6 weeks	566 ± 19***	6.4 ± 0.2^{NS}	331 ±9^{NS}	28.6 ±1.3***
7-10 weeks	557 ± 20***	7.3 ± 0.3^{NS}	365 ± 11$^{*/\$\$\$}$	29.7 ± 0.6$^{***/\$\$\$}$

Statistical analysis by two-way ANOVA with post-hoc Dunnetts comparing to start control NS no significant difference, * $p<0.05$, $^{**}p<0.01$, $^{***}p<0.001$; comparing to time-matched control $^{\$\$\$}$ $p<0.001$

Bladder weights

Bladder weights were monitored post mortem. Bladders from control and STZ-treated rats both increased with increasing time. The increases seen in the control animals appeared to increase gradually, with an apparent linear relationship of bladder weight over time. At the day 2 timepoint, no difference was seen in bladder weight between the control and STZ-treated rat bladders. By 2 weeks and throughout the remaining time-points to 7-10 weeks, STZ-treated animals had significantly higher weight bladders than control animals. (Figure 3.2).

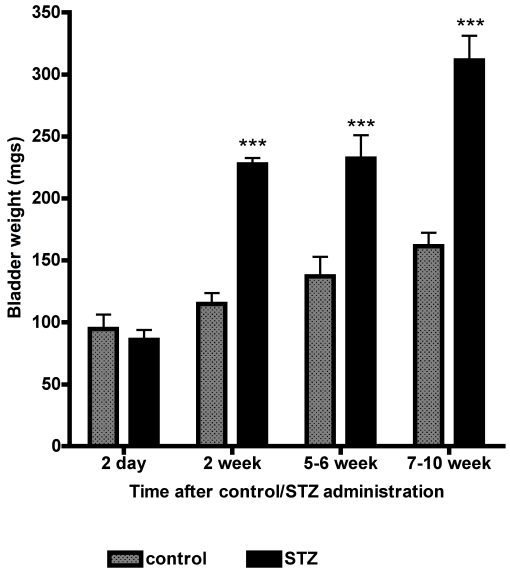

Figure 3.2 Barchart showing bladder weights from control and STZ-treated rats at 2 days, 2 weeks, 5-6 weeks and 7-10 weeks post control or STZ treatment. Data represents mean $\pm$ s.e.m. n>3 bladders. Statistical analysis by two-way ANOVA with post-hoc Bonferroni: * $p<0.05$,** $p<0.01$, ***$p<0.001$ compared to control.

Effects of STZ on TRPV1-mediated contraction of the urinary bladder

Capsaicin produced a concentration-related contractile response in urinary bladder tissue from control and from STZ-treated animals, representative traces from 2 week post-control or STZ-administration are shown (Figure 3.3).

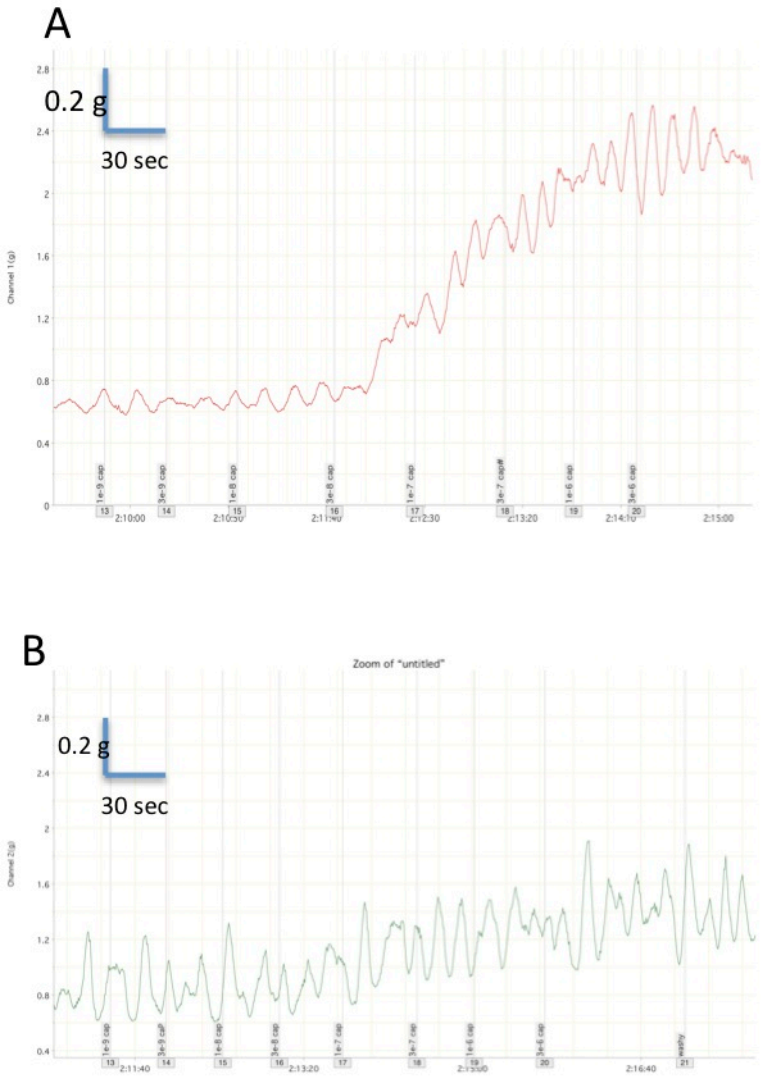

Figure 3.3 Representative raw data traces of responses to a cumulative concentration range of capsaicin in urinary bladder tissue from 2-week post control (A) and STZ-treated (B) rats.

Data indicated that TRPV1 responses in STZ-treated rats was not significantly different from control at the 2 day time-point (Figure 3.4A), but was depressed from 2 weeks (Figure 3.4B) up to 7-10 weeks (Figures 3.4 C,D) post administration of STZ. The difference in response to capsaicin was one of depressed eMax responses as opposed to a difference in pEC50 (Table 3.2).

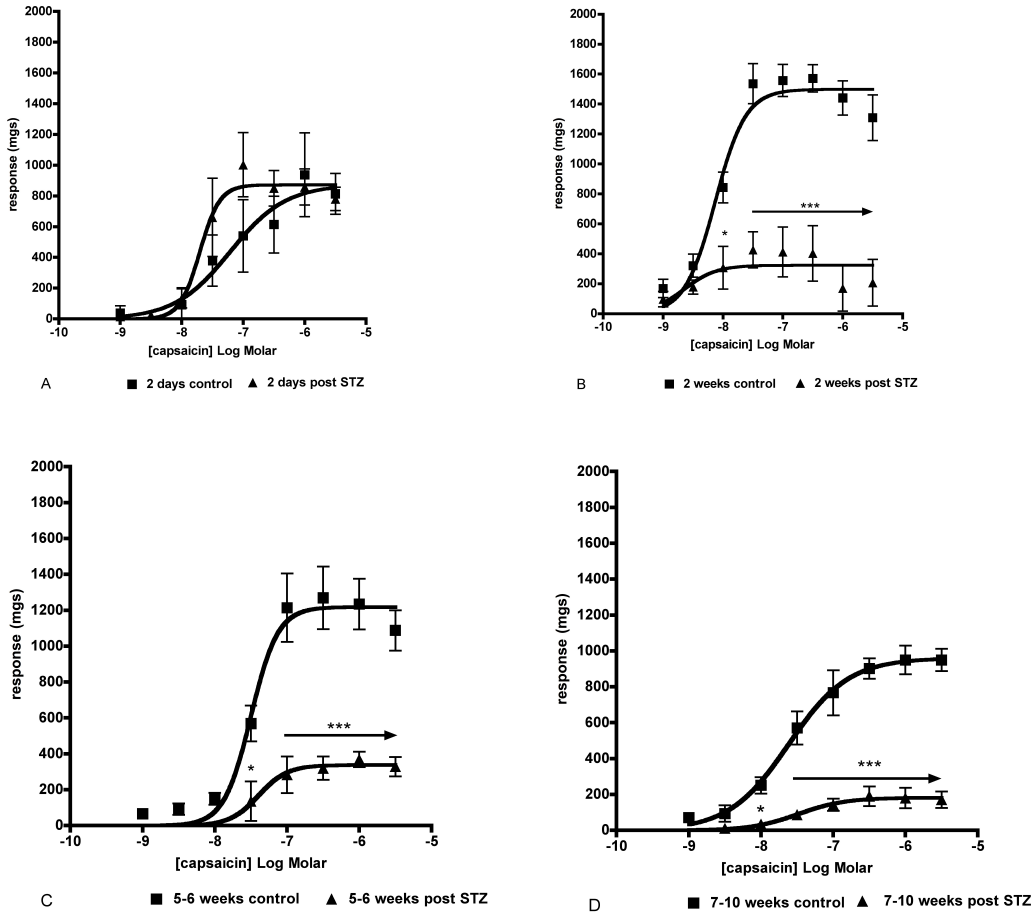

Figure 3.4. Graphs showing responses of urinary bladder from age-matched controls or STZ-treated rats to a concentration range of capsaicin at 2 days (A), 2 weeks (B), 5-6 weeks (C) and 7-10 weeks (D) post administration of STZ or vehicle control. Values represent mean $\pm$ s.e.m n of 6-20 urinary bladder strips. Statistical analysis by two-way ANOVA with post-hoc Bonferroni: * $p<0.05$,** $p<0.01$, ***$p<0.001$ compared to control.

Table 3.2 : Potency and efficacy values for capsaicin responses in urinary bladder strips from control or STZ-treated rats at various times following control or STZ administration. Data represent mean ± s.e.m n>6 urinary bladder strips

Timepoint	pEC50 ± s.e.m.	eMax (mgs) ± s.e.m.
2 days -control	7.23 ± 0.33	873 ± 166
-STZ	7.71 ± 0.12^{NS}	872 ± 67^{NS}
2 weeks - control	8.13 ± 0.07	1499 ± 56
- STZ	8.66 ± 0.41^{NS}	324 ± 62***
5-6 weeks - control	7.50 ± 0.07	1218 ± 67
- STZ	7.39 ± 0.20^{NS}	337 ± 46***
7-10 weeks- control	7.62± 0.11	961± 56
- STZ	7.49 ± 0.23^{NS}	182 ± 24***

Statistical analysis by two-way ANOVA with post-hoc Dunnetts comparing to time-matched control NS no significant difference, * $p<0.05$, $^{**}p<0.01$, $^{***}p<0.001$

TRPV1 responses normalised to tissue weight

When data was expressed as mgs tension per mg tissue weight the same pattern of TRPV1 responses over time following control or STZ administration were seen: no difference in calculated maximum response (eMax) at 2 days (Figure 3.5A), with a depression of eMax from 2 weeks (Figure 3.5B) until the longest timepoint studied, 7-10 weeks (Figure 3.5D). An increased potency of capsaicin was seen at 2 days post STZ, albeit not statistically significant with no apparent alterations in potency seen at later timepoints post STZ. (Figure 3.5).

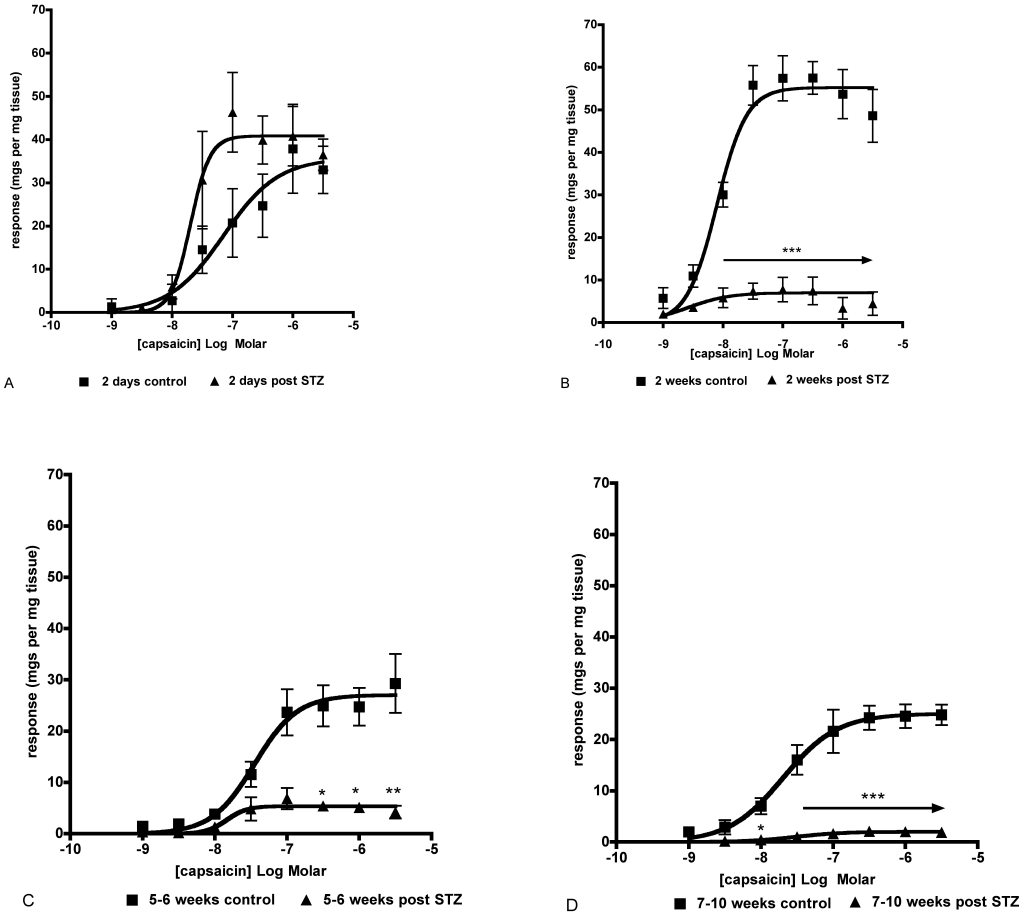

Figure 3.5 Graphs showing responses of urinary bladder from age-matched controls or STZ-treated rats to a concentration range of capsaicin at 2 days (A), 2 weeks (B), 5-6 weeks (C) and 7-10 weeks (D) post administration of control or STZ. Values represent mean $\pm$ s.e.m. n of 6-20 urinary bladder strips. Statistical analysis by two-way ANOVA with post-hoc Bonferroni: * $p<0.05$,** $p<0.01$, ***$p<0.001$ compared to control.

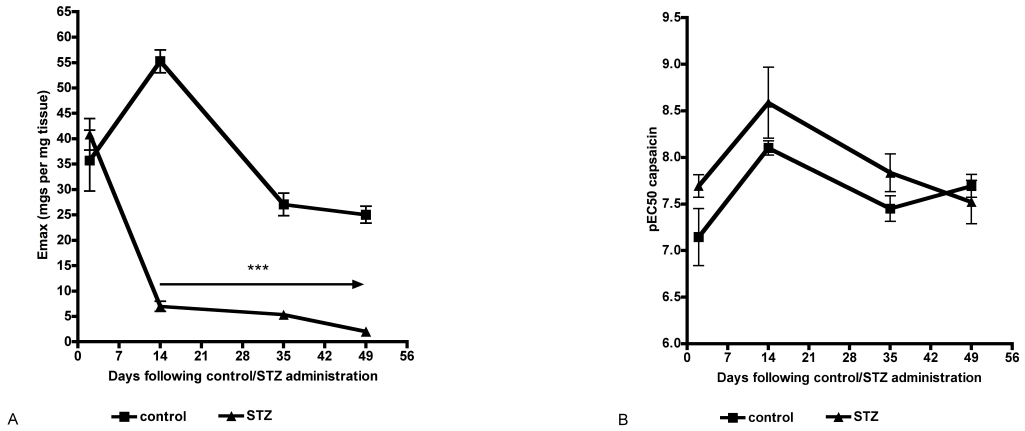

Figure 3.6 Graphs showing calculated maximal responses, eMax(A) and potency estimates, pEC50 (B) of capsaicin in urinary bladder strips over time following control or STZ-administration. Values represent mean± s.e.m. n of 6-20 urinary bladder strips. Statistical analysis by two-way ANOVA with post-hoc Bonferroni: * $p<0.05$,** $p<0.01$, ***$p<0.001$ compared to control.

Recovery after capsaicin contraction

To monitor the rate of tissue recovery back to baseline tension following capsaicin induced contraction, a subset of tissues from 2 week post control or STZ-treated rats were examined. A concentration range of capsaicin was applied and following the application of maximal concentration, measurements of contractile state were taken every minute with no wash out until tissues had relaxed to baseline. When normalised to percent of maximum capsaicin response to accommodate for the differences seen between control and STZ treated tissue, no differences were seen in the rate of relaxation of urinary bladder tissue back to baseline levels between control and STZ treated rats (Figure 3.7). The tissue returned to baseline levels by 15 minutes following maximal capsaicin concentration application, in control and STZ-treated rats.

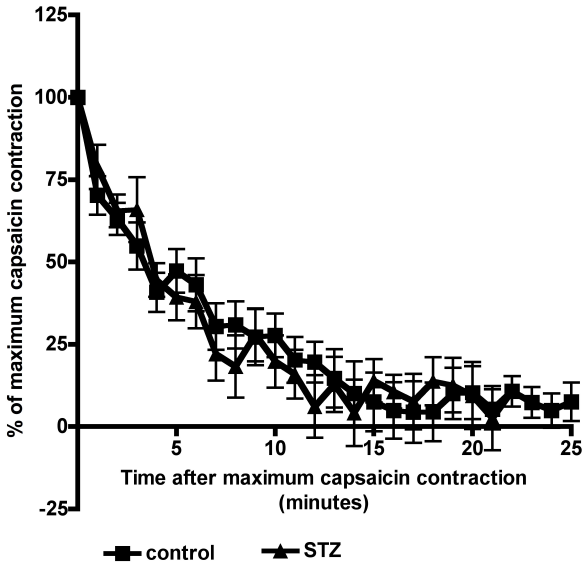

Figure 3.7 Graph showing decline of capsaicin-induced contraction with no washout in bladder tissue from control and STZ-treated rats. Data represents mean ± s.e.m n >6 urinary bladder strips. No significant differences were seen using two-way ANOVA .

Monitoring of Carbachol responses following control or STZ administration

Carbachol responses of urinary bladder strips were monitored following control or STZ administration, representative traces are shown from 2-week post control or STZ-treated rats (Figure 3.8)

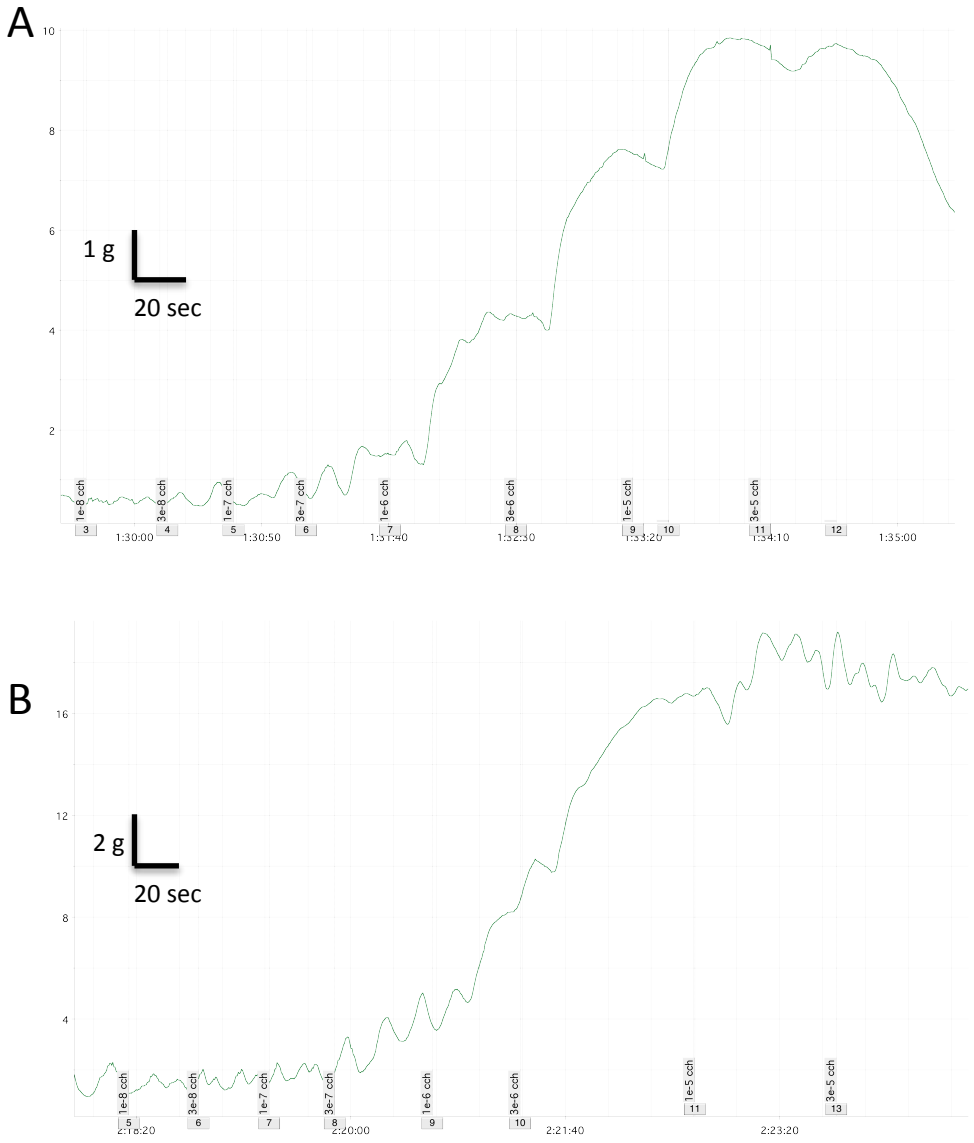

Figure 3.8 Representative raw data traces of responses to a cumulative concentration range of carbachol in urinary bladder tissue from 2- week post control (A) and STZ-treated (B) rats.

Carbachol produced a concentration-related increase in contraction in urinary bladder tissue from control and STZ-treated rats. Responses to a concentration range of carbachol in control tissue were consistent at all timepoints studied. Carbachol responses of bladder tissue from STZ-treated rats were increased significantly in terms of magnitude at 2 days, 2 weeks and 5-6 weeks post STZ administration compared to controls. (Figure 3.9)

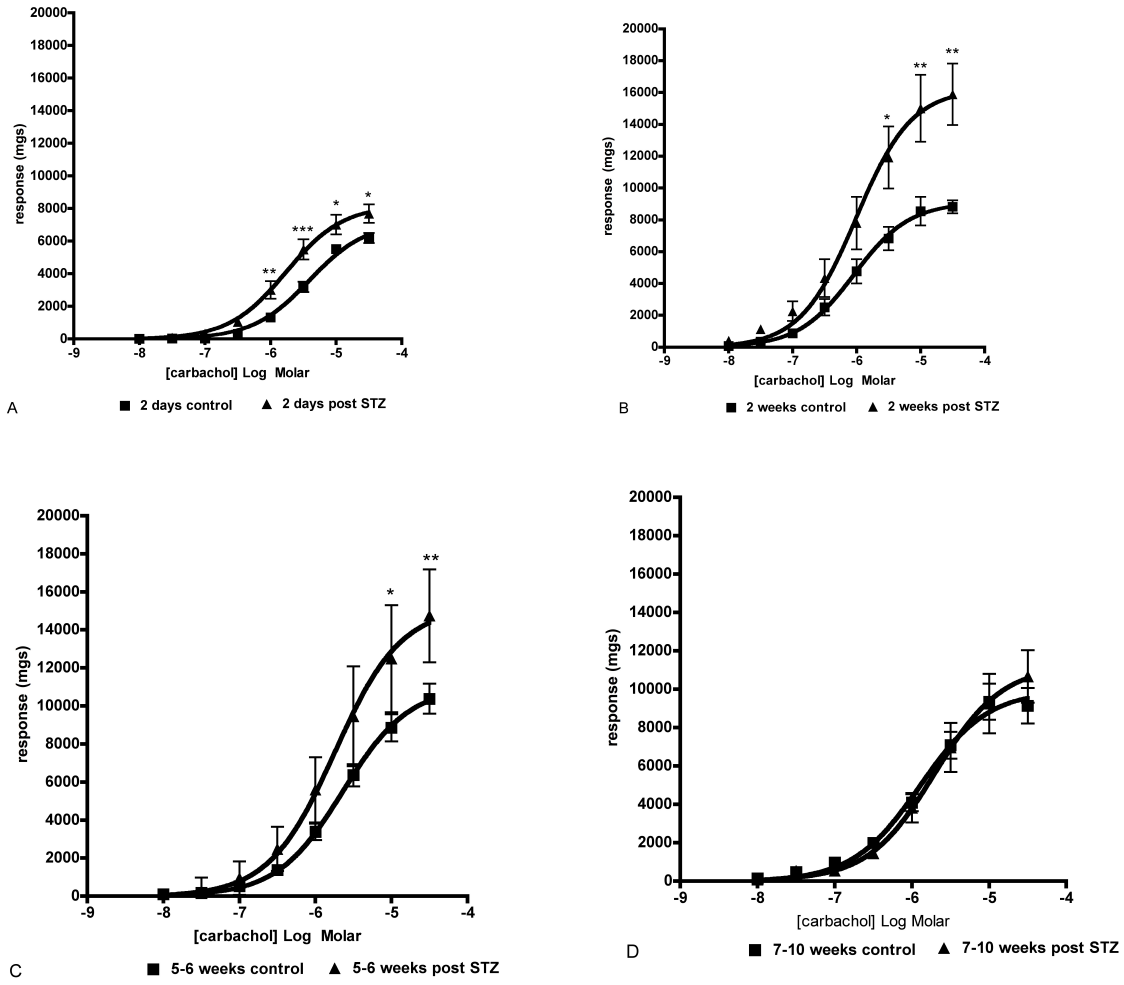

Figure 3.9 Graphs showing responses of urinary bladder from age-matched buffer treated controls or STZ-treated rats to a concentration range of carbachol at 2 days (A), 2 weeks (B), 5-6 weeks (C) and 7-10 weeks (D) post administration of STZ or vehicle control. Values represent mean ± s.e.m. n >12 urinary bladder strips. . Statistical analysis by two-way ANOVA with post-hoc Bonferroni: * $p<0.05$,** $p<0.01$, ***$p<0.001$ compared to control.

Table 3.3 Potency and efficacy values for carbachol responses in urinary bladder strips from control or STZ-treated rats at various times following control or STZ administration. Data represent mean ± s.e.m. n>6 urinary bladder strips.

Timepoint	pEC50 ± s.e.m.	eMax (mgs) ± s.e.m.
2 days -control	5.41 ± 0.05	7191 ± 257
-STZ	5.76 ± 0.08^{NS}	8202 ± 404^{NS}
2 weeks - control	6.04 ± 0.09	9101 ± 423
- STZ	6.01 ± 0.13^{NS}	16225 ± 1160***
5-6 weeks - control	5.64 ± 0.07	11037 ± 492
- STZ	5.74 ± 0.18^{NS}	15206 ± 1631*
7-10 weeks- control	5.89 ± 0.12	9027 ± 619
- STZ	5.70 ± 0.13^{NS}	11244 ± 910^{NS}

Statistical analysis by two-way ANOVA with post-hoc Dunnetts comparing to time-matched control NS no significant difference, * $p<0.05$, $^{**}p<0.01$, $^{***}p<0.001$

Carbachol responses normalised to tissue weight

Carbachol response data expressed as mgs tension per mg tissue weight showed a slight increase in potency and a significant increase in efficacy at 2 days, followed by a significant progressive depression of efficacy, with no effect on potency over time post-STZ administration compared to control animal responses (Figure 3.10, Figure 3.11).

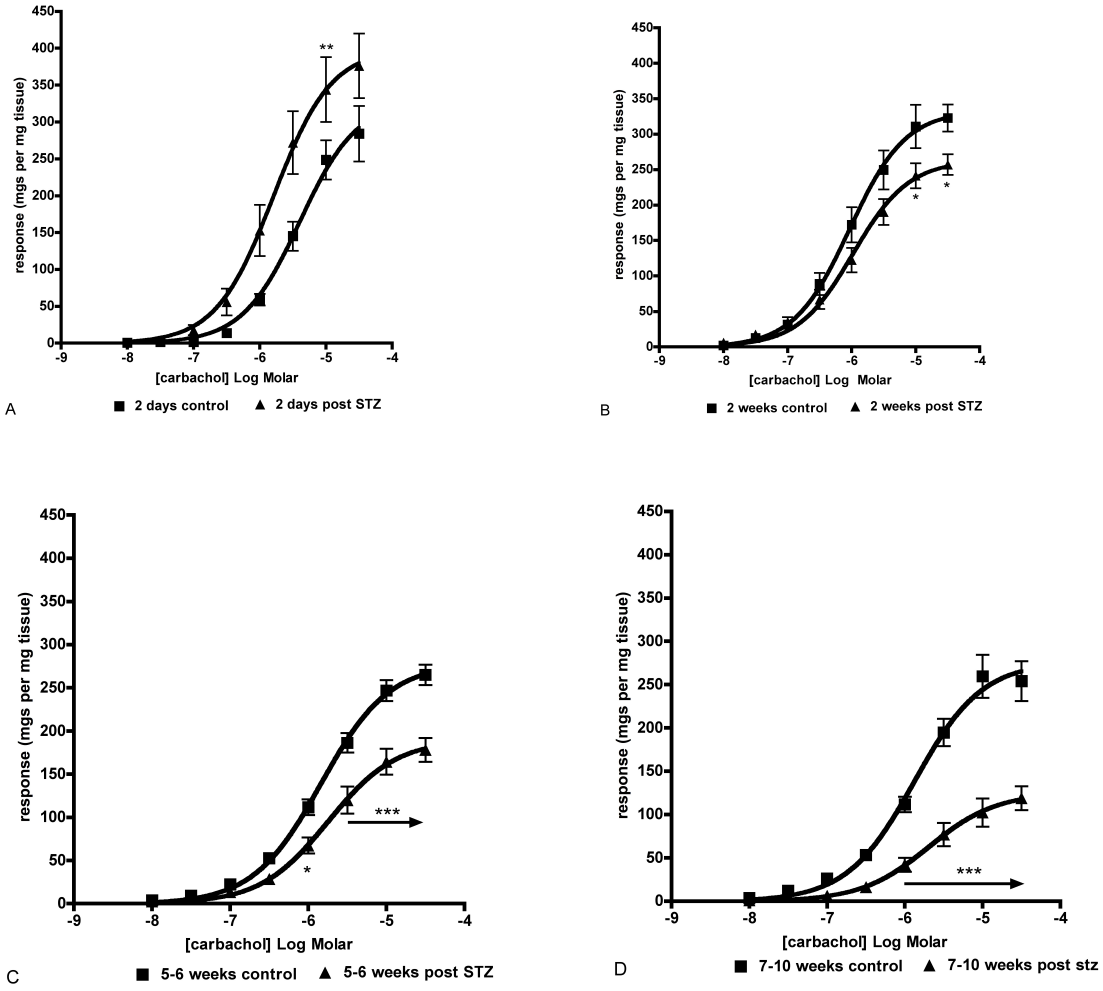

Figure 3.10 Graphs showing responses of urinary bladder to a concentration range of carbachol at 2 days (A), 2 weeks (B), 5-6 weeks (C) and 7-10 weeks (D) post administration of control or STZ. Values represent mean $\pm$ s.e.m. n >12 urinary bladder strips. . Statistical analysis by two-way ANOVA with post-hoc Bonferroni: * $p<0.05$,** $p<0.01$, ***$p<0.001$ compared to control.

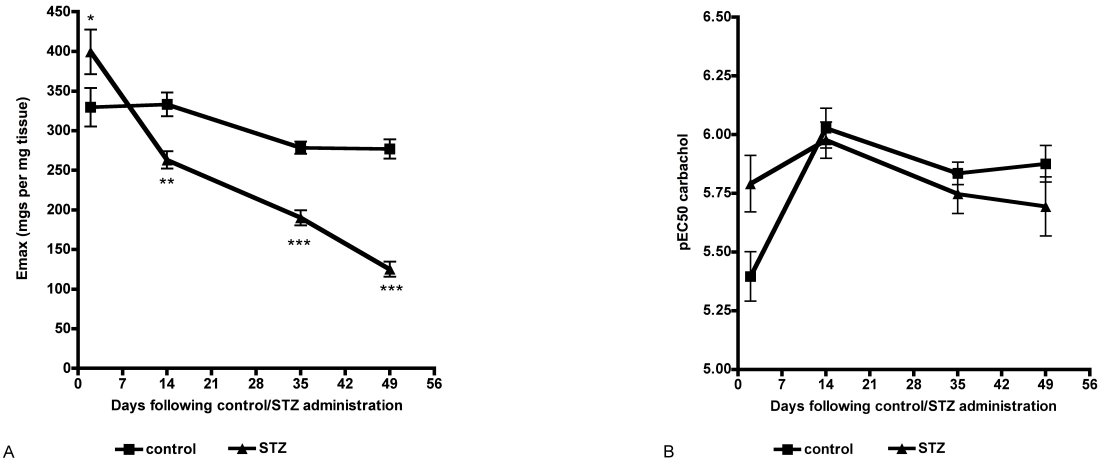

Figure 3.11 Graphs showing calculated maximal responses to carbachol ,Emax (A) and potency estimates ,pEC50 (B) over time following control or STZ administration. Values represent mean ± s.e.m. n > 12 urinary bladder strips. Statistical analysis by two-way ANOVA with post-hoc Bonferroni: * $p<0.05$,** $p<0.01$, ***$p<0.001$ compared to control.

Comparison of changes in capsaicin and carbachol responses

Maximal potency values normalised to respective time-matched controls

To provide a direct comparison between the decline in Emax for capsaicin and carbachol, Emax values for each timepoint studied were normalised to their respective time-matched control animal Emax value and presented as an Emax ratio for capsaicin and carbachol (Figure 3.12). Emax ratio values for capsaicin declined rapidly by 2 weeks and remained low throughout the remaining time period studied. Carbachol Emax ratio declined at a more consistent rate throughout the time-period studied.

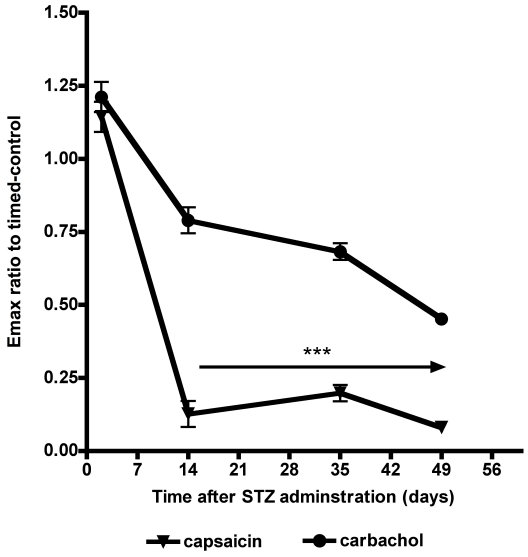

Figure 3.12 Graph showing eMax values normalised to respective time-matched control values for capsaicin and carbachol in STZ-treated rats. Data represent mean ± s.e.m. for n>6 urinary bladder strips. Statistical analysis by two-way ANOVA with post-hoc Bonferroni: * $p<0.05$,** $p<0.01$, ***$p<0.001$ compared to carbachol.

Kinetics of carbachol contraction

A comparison between 2- week post control and STZ responses to a single application of a submaximal concentration of carbachol (1×10^{-5} M) was made. First raw data was extracted to represent the entire muscle contraction following carbachol application dataset, normalised to maximum response seen and finally measurement of the time taken to reach 50% of this response. Mean data was plotted (Figure 3.13). No difference was seen in the kinetics of response between control and STZ animals.

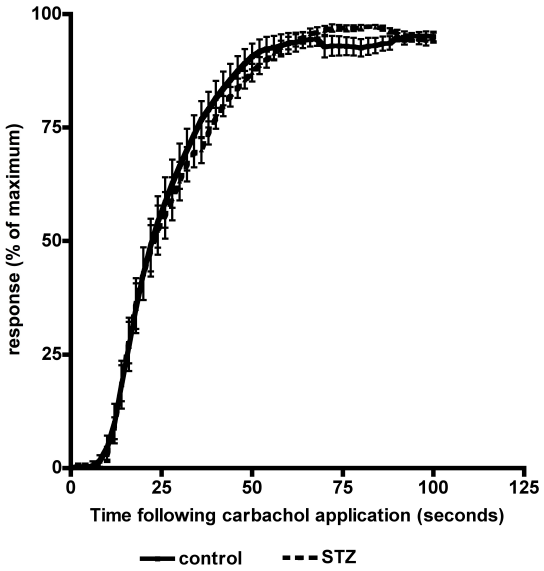

Figure 3.13: Graph showing normalised contraction over time following application of 1 x 10^{-5} M carbachol. Data represent mean ± s.e.m. n of 20 urinary bladder strips. No statistical significant difference was seen using two-way ANOVA.

Data for time taken to reach 50 % contraction was plotted on a scatter plot, and separated into dorsal and ventral bladder muscle tissue, to additionally examine the potential of differences in muscle contractile kinetics between anatomically distinct muscle sections (Figure 3.14). No differences were seen between control and STZ tissue, or between dorsal and ventral located urinary bladder tissue responses to carbachol.

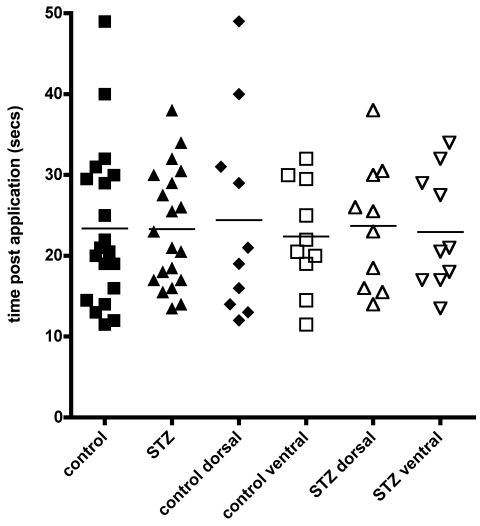

Figure 3.14 Scatter plot showing time taken following application of carbachol to reach 50% contraction. Data represents individual tissue responses and is further divided into the dorsal or ventral anatomical bladder location.

Spontaneous Activity

The frequency and amplitude of spontaneous activity were measured in the urinary bladder from 2 week post control and STZ –treated rats (Figure 3.15).

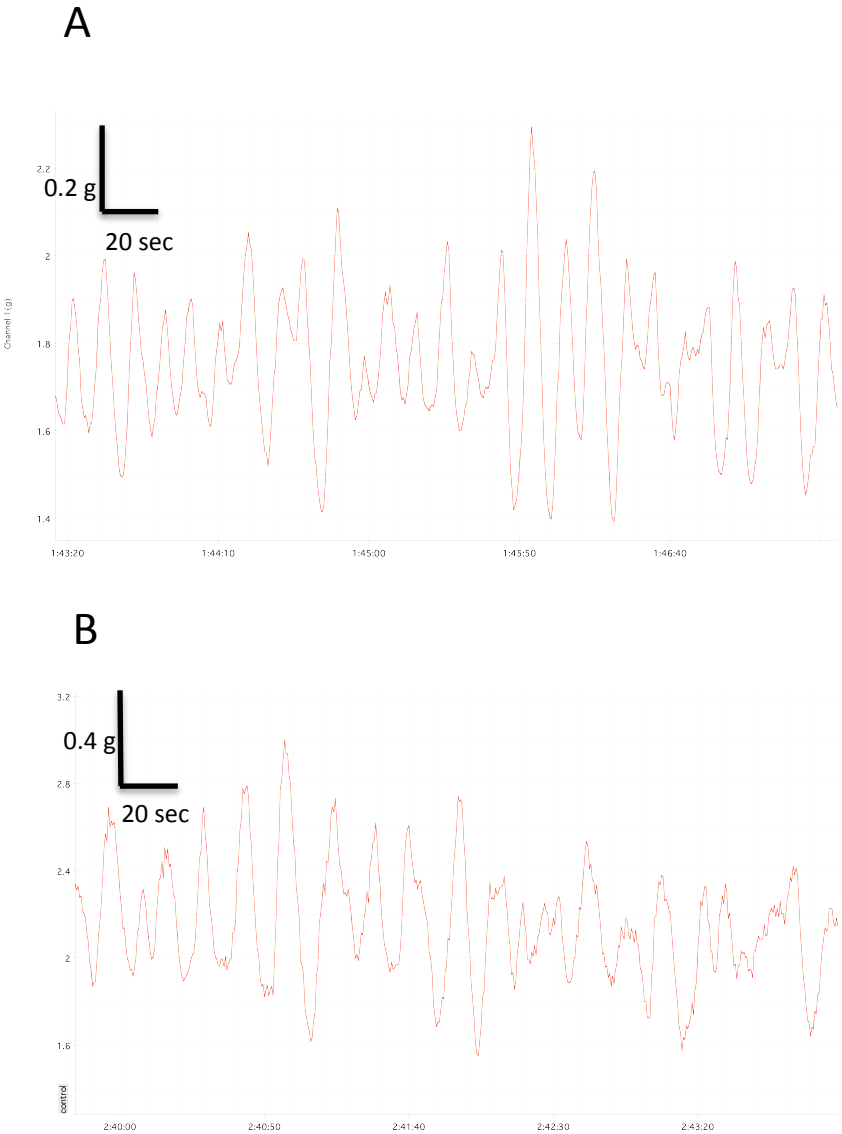

Figure 3.15 Representative trace of spontaneous activity of control (A) or STZ-treated (B) rat urinary bladder tissue.

There was no difference in frequency of spontaneous contractions between control and STZ. There was however a significant reduction in the amplitude of spontaneous contractions in the STZ-treated group (Figure 3.16)

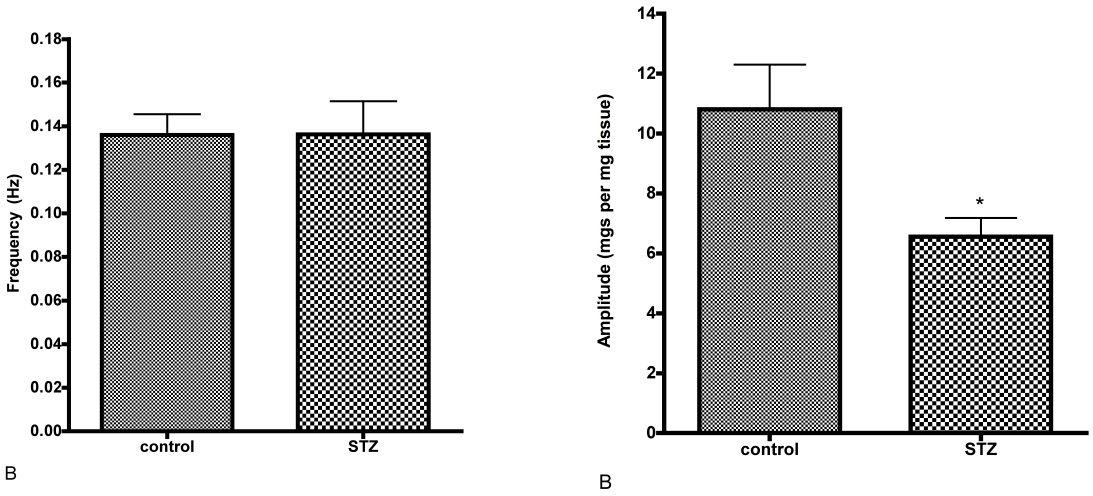

Figure 3.16 Barcharts of frequency (A) and of amplitude (B) of spontaneous contractions seen in 2-week post control or STZ-treated animals. Data represents mean ± s.e.m n of 20 urinary bladder strips. Statistical significance was tested by Student's t-test, * $p<0.05$

Electrical Field Stimulation

Electrical field stimulation was applied to urinary bladder strips from 2 week post control or STZ-treated rats. First a voltage response curve was performed and responses to this range of voltages were measured and normalised to mg responses per mg tissue weight (Figures 3.17, 3.19A). Next using a submaximal voltage, a frequency response curve was constructed and normalised once again to mgs response per mg tissue weight (Figures 3.18, 3.19B). Electrical field stimulation evoked voltage related contraction of urinary bladder tissue from control and STZ-treated rats. Urinary bladder tissue responded at lower voltages in the STZ-treated group as seen by a leftward shift in voltage response curve, with a statistically significant lower maximal efficacy. Electrical field stimulation evoked frequency related contraction of urinary bladder tissue from

control and STZ-treated rats. No differences in frequency responses were observed between control and STZ-treated rats. Following application of 1 μM TTX, no response to the frequency range of electrical field stimulation was observed (data not shown).

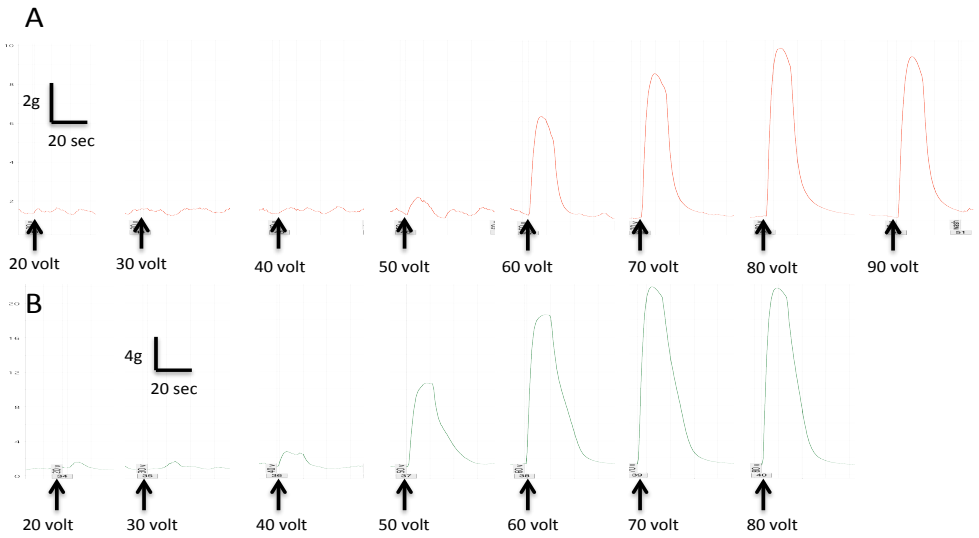

Figure 3.17 : Representative traces of raw data from EFS-evoked contractions to a voltage range in control rat (A) or STZ-treated rat (B) urinary bladder tissue

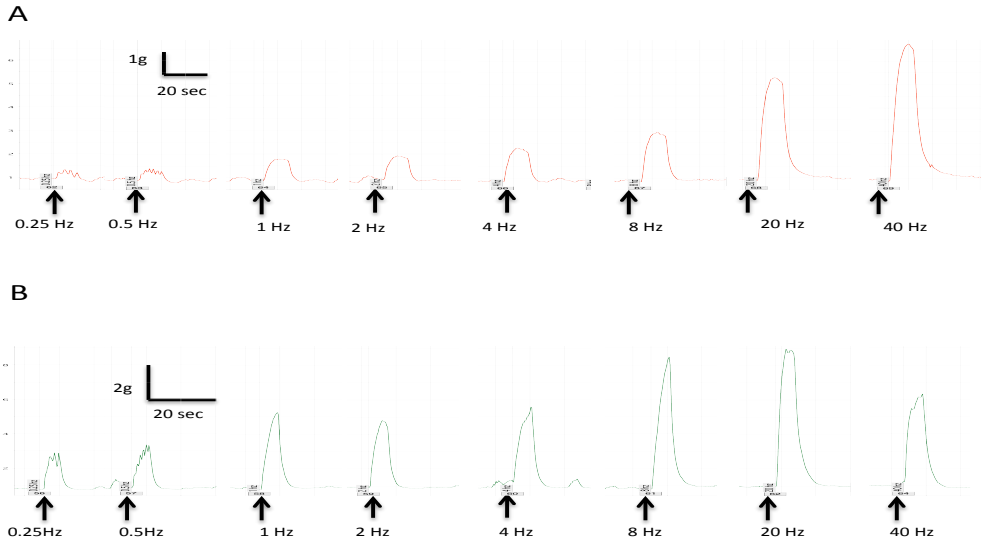

Figure 3.18: Representative traces of raw data from EFS-evoked contractions to a frequency range in control rat (A) or STZ-treated rat (B) urinary bladder tissue

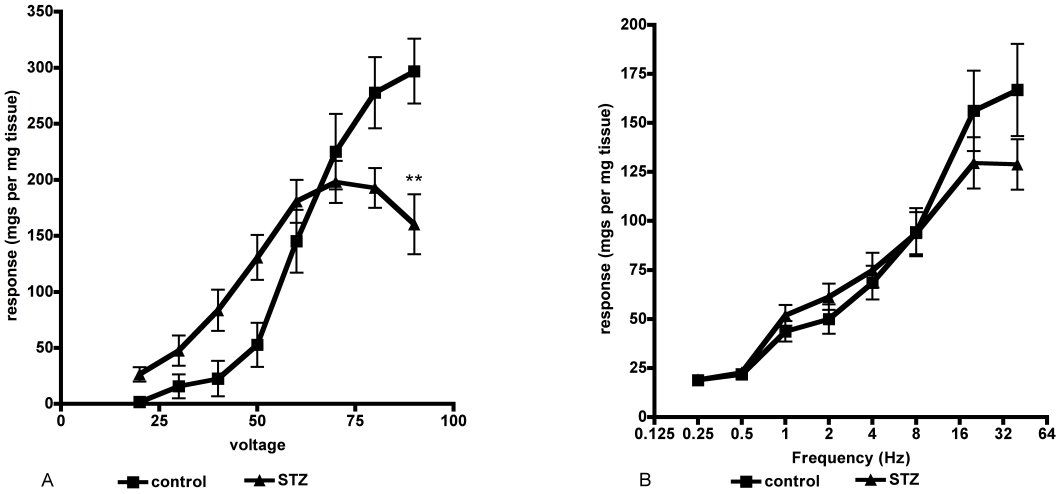

Figure 3.19. Graphs of electrically stimulated responses of urinary bladder strips from 2 week post control or STZ-treated rats to a range of voltages (A) or to a range of frequencies (B) using the submaximal voltage obtained from the voltage response curve. Data represent mean $\pm$ s.e.m. n of 12 urinary bladder strips. Statistical analysis by two-way ANOVA with post-hoc Bonferroni: * $p<0.05$,** $p<0.01$, ***$p<0.001$ comparing to control.

Discussion

Induction of diabetes

STZ-administration was seen to induce a diabetic state by 2 days post treatment where a three-fold increase in blood glucose was seen. This high blood glucose was maintained throughout the studies until the last time points at 7-10 weeks. Animal health was closely monitored and it was noted that although the STZ-treated animals failed to increase body weight they did manage to maintain their starting weights. Many investigators record a loss of body weight (Tammela et al., 1994, Thule and Liu, 2000), however the acute time points together with the administration protocol used in this study appears to be less detrimental to animal health. The STZ-treated rats pattern of activity changed noticeably with increased lethargy coupled with more time taken eating. The insulinopenia evoked by STZ is known to induce hyperphagia through increased neuropeptide Y levels in the hypothalamus (Kalra et al., 1999). A nutrient study with STZ-rats has shown that in the 3 weeks post STZ-administration a rat will choose to increase carbohydrate and protein and reduce fat intake, after this time period however, the rat will choose to increase fat and reduce carbohydrate intake (Kanarek and Ho, 1984). At the later time points of this study (7-10 weeks), animals had noticeably less body fat compared to control treated animals although body composition analysis was not performed. The STZ-mediated destruction of the pancreatic β-cells results in an insulinopaenic state so that carbohydrates can no longer be utilized as an energy source efficiently. This lack of insulin leads to a greater reliance on energy from fat and protein to meet the energy demands of the animal. It is likely that a residual pancreatic function remains following STZ administration although this is not enough to prevent the onset and progression of the diabetic state (Cam et al., 1993). Bladder weights increased gradually in the control treated animal groups, due to these animals still being in the adolescent growth phase. The bladder weights in the STZ-treated group increased markedly by the 2 week time point and continued to increase throughout the remaining time points. This STZ-related enhanced increase in bladder weight and size is likely due to the increased demands on

this organ i.e. increased output of urine, and this was clearly observable in the animal husbandry with an increased need to change animal bedding due to dampness from urine.

Acute onset of TRPV1 dysfunction during diabetes

The responses of control treated animal tissue to capsaicin throughout all the time points studied was reasonably consistent, albeit less consistent than carbachol responses. This reduced consistency highlights the requirement for inclusion of age-matched controls for future STZ studies, as it indicates an increased variability of this neuronally mediated response and may be affected by animal age as well as logistical factors such as room temperature, time taken to dissect tissue etc. With increasing age, a minor depression in capsaicin efficacy in controls was seen again highlighting the need for age-matched controls. There did appear to be a small leftward shift in capsaicin potency at the 2-day post treatment time point, but this was seen to be non-significant on statistical analysis. Capsaicin concentration response curves clearly indicated a reduced responsiveness to capsaicin in the STZ-treated groups from the 2-week post treatment time points. The nature of diminished response was in the efficacy of capsaicin to elicit a response, Emax, rather than in the potency of capsaicin. The patterns of diminished responses to capsaicin were retained when transforming the data to mgs response per mg tissue weight. This is an important finding as the increase in bladder weight alone could account for an apparent diminished responsiveness. When visualizing the data of Emax and EC50 over time, it is clear that by 2 weeks an almost maximal reduced responsiveness in Emax to capsaicin is seen. Additional data on 1-week post treatment was undertaken where a more variable diminished response was seen (data not shown). So robust changes in TRPV1 function are seen by 2 weeks post STZ administration providing an early time point at which modulation of TRPV1 function in sensory neuropathy can be examined. This early onset of a depression in function has been observed in central neurons of the dorsal motor nucleus of the vagus 3-7 days post STZ in mice (Zsombok et al., 2011) and was not due to an alteration in

expression. In the DRG however, early increases in TRPV1 mRNA expression are correlated to thermal hyperalgesia (Pabbidi et al., 2008a)and suggests that there is a location-dependent modulation of TRPV1 during diabetes.

When examining the recovery from capsaicin induced contraction between control and STZ treated animals at this 2-week time point, no differences in the rate of recovery were seen. This measurement was included to compare the longevity of response as a less sustained response might translate into reduced efficacy. Recovery from capsaicin-induced contraction could be governed by neuropeptide breakdown by protease enzymes as it is conceivable that alterations in the neuropeptide breakdown mechanisms i.e. peptidase levels may occur in diabetes. However no such differences were observed at this 2-week time point, which excludes this possible explanation for the difference in capsaicin efficacy. Additionally no reduction in bladder levels of neuropeptides for e.g. substance P have been reported in the early stages of STZ-induced diabetic model (Steers et al., 1994). Conversely some investigators have reported increases in the neuropeptides associated with TRPV1 (substance P, CGRP, neurokinin-A) although no diminishment of capsaicin responses were seen in this study (Santicioli et al., 1987a). However alterations of neuropeptide levels have been reported in the skin (Karanth et al., 1990) which may suggest that the effector mechanisms for TRPV1 activation are differentially altered in diabetes dependent on their anatomical location. An alternate process governing this recovery from contraction is that the receptors causing the contractile response desensitise, and because the rates are similar between control and STZ, this desensitisation process is not responsible for the functional differences seen in this model of diabetes.

Monitoring of carbachol responses revealed a gradual progressive decline

An examination of carbachol responses was also included to monitor myogenic changes following diabetic induction. Throughout all the time points studied, responses to controls were very consistent. 2-days post STZ administration, a small increased response to carbachol was seen, this increased markedly at the 2-week and 5-6 week time points returning back to control levels by 7-10 weeks.

However when data was transformed to accommodate for the increased bladder mass, an increase was still seen at the 2-day time point, but this changed to a decreased efficacy that appeared to progress throughout the remaining time points studied. This decline in muscarinic function is indicative of a progressive myogenic dysfunction caused by the diabetic state. Examining the kinetics of muscular contraction to a single concentration of carbachol revealed no differences in the rate of contraction. This means that in this early stage of diabetes the muscular cell shortening rate is unaffected, at a time where force generation capacity has been diminished. The further examination of dorsal versus ventrally located bladder strips was undertaken as on physical examination of the tissue, morphological changes did appear to be occurring at the 2-week time point. These changes included an expansion of the circular banding clearly identifiable on the ventral strips, round to the dorsal sections. However no differences in contractile speed between dorsal and ventral sections were seen. When directly comparing the changes seen in capsaicin with carbachol, it was apparent that the carbachol changes were more gradually progressive whereas the changes to capsaicin function presented more acutely and were sustained throughout.

Changes in spontaneous activity likely to be due to myogenic changes

Spontaneous contractile activity of bladder smooth muscle is known to occur during the filling stage (Araki, 2011). As it has been reported that a) TRPV1 knockout mice have an higher frequency lower amplitude non-voiding bladder contractions and b) the diabetic state causes increased amplitude and frequency of spontaneous activity due in part to increased prostaglandin production (Tammela et al., 1994), an examination of spontaneous activity was made. It is still unclear what drives spontaneous activity but numerous mechanisms have been identified including the Interstitial Cells of Cajal, prostanoids, gap junctions, and intermural ganglia (Araki, 2011). At the 2 –week post treatment time point, no differences were seen in the frequency of spontaneous activity, whereas a significant reduction in amplitude to transformed data (mgs response to mgs tissue weight). The alteration seen here, a decrease of amplitude of spontaneous

activity, is suggestive of no change to the driving pathways to spontaneous activity, such as prostaglandin production, rather an influence of decreased myogenic activity as seen in the carbachol responses. An explanation for reduced spontaneous activity seen at this early stage could be that the architecture of the bladder wall has changed which in turn has altered the communicative ability of the driver behind spontaneous activity for e.g. the interaction of the interstitial cells with the smooth muscle cells. This is unlikely, as any such change would likely alter not only amplitude of spontaneous activity but frequency as well. These specialised interstitial cells are believed to be important communicator type cells that form associations with neuronal and muscular cells and whose role is thought to be one of coordinating bladder activity (McCloskey, 2010). Later stage changes in spontaneous activity, where a disorganized spontaneous activity is seen may contribute to a loss of coordinated contraction and could underlie in part the dysfunctional voiding of a diabetics bladder.

Electrical field stimulation revealed that other neurogenic alterations occur acutely

Electrical field stimulation was included at the 2-week time point to ascertain whether at this time point where TRPV1 function is clearly diminished whether total neurogenically mediated responses had been affected. A clear leftward shift in voltage responses was observed in the STZ-group. This increased voltage sensitivity has been reported by numerous laboratories at later time points post STZ treatment than used here (Tammela et al., 1994, Longhurst et al., 1991). The reasons for this increased sensitivity have been postulated as an alteration in the membrane lipid composition or other membrane changes or the presence of a partial depolarized state perhaps due to diabetic neuropathy (Tammela et al., 1994) or could additionally be due to changes in inhibitory factor release. However using a submaximal voltage, no differences in frequency responses were seen in these early time point studies. Some investigators have reported increased sensitivity to frequency responses in later stage diabetic animals,

initially described as due to increased cholinergic transmitter release in response to the electrical field stimulation (Luheshi and Zar, 1991). The reasons for this enhanced transmitter release were postulated as either being an early sign of degenerative change in the cholinergic nerve population whereby they lose the normal control over the amount of transmitter release in response to electrical field stimulation or a compensatory mechanism where the cholinergic system attempts to compensate for a progressive failure of the non-cholinergic systems. However other investigators have dissected out pharmacologically the different components of the neurogenic responses into cholinergic, purinergic and residual NANC components albeit in later stage diabetic animals. Here they saw increased sensitivity to electrical field stimulation with a decreased cholinergic proportion and an increased residual component (Liu and Daneshgari, 2005). In the early stage post diabetic studies a clear alteration was only seen in voltage sensitivity to electrical field stimulation. These data suggest that even at this acute stage post diabetic induction, changes in neuronal responses are occurring which are different to those seen at a later stage of diabetes.

Clearly TRPV1 dysfunction has a very rapid onset following induction of diabetes. The dysfunction in TRPV1 is one of reduced efficacy rather than altered potency. This reduced efficacy may transpire to reduced sensitivity in the bladder, which could contribute to bladder volume changes and cystopathy. Changes are also occurring in the myogenic responses. These muscular changes appear more gradual and progressive and could result in the overt reduced contractility seen in later stage cystopathy. The neurogenic TRPV1 changes have a different onset time to the myogenic changes, appearing more acutely, and because of this it is probable that the myogenic changes do not underlie the TRPV1 neurogenic changes. It is conceivable however that the neurogenic changes could underlie and be causative, at least in part to the myogenic changes. At these acute time points, no changes in contractile speed of the muscle was seen, and changes in spontaneous activity were only of amplitude, which could be accounted for by the myogenic alterations seen.

The next phase of work was to investigate whether the diminished response profile of TRPV1 was altered by organ bath temperature.

Chapter 4 : TRPV1 responses at reduced organ bath temperatures

Introduction

All the studies on urinary bladder for this thesis have been run at an organ bath temperature of 37 °C, normal body temperature. However the TRPV1 receptor is well recognized to be a temperature sensitive receptor, responding directly to noxious heat >43 °C. It is thought that the heat sensor on the TRPV1 receptor is a structural component of the receptor (Yao et al., 2011) although there is still controversy over the exact mechanism of temperature sensing. Importantly the temperature threshold for TRPV1 is not fixed at 43 °C and can be altered through potentiation by chemical mediators and the phosphorylation state of TRPV1 (Benham et al., 2003). A number of inflammatory mediators such as prostaglandin E_2 and prostaglandin I_2 can potentiate TRPV1 function and reduce the heat threshold to 35 °C, which means that the TRPV1 receptors can become activated at normal body temperature (Moriyama et al., 2005). Phosphorylation of TRPV1 through activation of protein kinase C also induces a reduced temperature threshold of TRPV1 (Vellani et al., 2001). Thinking about temperature prompted the notion that the profile of a diminished capsaicin response could be altered at lower organ bath temperature. If the thermal threshold for TRPV1 had been reduced in the STZ-diabetic model then this may have driven the subsequent reduction in TRPV1 response.

Core body temperature is reduced and thermoregulatory mechanisms are impaired in diabetes

In animal models of diabetes there is a rapid onset of hypothermia within 3 days of induction of diabetes, although the extent of the reduced body temperature is only around 0.5 °C (Howarth et al., 2005). People with diabetes find it difficult to cope with environmental temperature extremes and also have a reduced body core temperature. Furthermore diabetics with peripheral neuropathy are at a greater risk of developing hypothermia on induction of general anaesthesia and

this is thought to be caused by a delayed thermoregulatory vasoconstriction response (Kitamura et al., 2000).

Smooth muscle contractility is enhanced at reduced organ bath temperature

A few studies in the literature have observed that smooth muscle from airways, vas deferens and bladder has increased contractility at lower temperatures (Ishii and Shimo, 1985, Souilem et al., 1995, Kurihara et al., 1974). The reasons behind this enhancement are thought to be due to altered calcium handling, inhibition of Na+/K+ pump, depolarization of the membrane or increased myosin light chain phosphorylation (Sugaya and De Groat, 2000). Additionally changes in frequency and amplitude of bladder smooth muscle spontaneous activity have been reported with reduced temperature (Sugaya and De Groat, 2000).

To examine the potential effects of reduced organ bath temperature on TRPV1 function studies were undertaken in measure capsaicin responses urinary bladder from control and STZ-treated rats. Carbachol responses were utilized to examine the effects of reduced organ bath temperatures on muscle contractility and the frequency and amplitude of spontaneous contractile activity was monitored.

Methods

Experiments were performed on 3-4 weeks post control or STZ-treated rat urinary bladder strips, set-up as previously described. Organ bath temperatures were initially set to the lowest temperature of study (either 32°C or 34°C), carbachol concentration range applied to all tissues and capsaicin concentration ranges applied to one pair of tissues. After washout, organ bath temperatures were increased to 34°C or 37 °C and resting tensions adjusted to 1 g. After 30 minutes equilibration time, a carbachol concentration range was applied to all tissues, followed by washout and equilibration. Finally a capsaicin concentration range was applied to the capsaicin-untreated tissue pair. In the control tissues three organ bath temperatures were studied; 32°C, 34°C and 37°C. In the STZ-diabetic tissue, two organ bath temperatures were studied; 32°C and 37°C. Spontaneous activity measurements were taken, where frequency and amplitude of spontaneous contractile activity was measured at the different organ bath temperatures studied. Data analysis was performed as previously described.

Results

Carbachol responses at different organ bath temperatures in control rat urinary bladder

First the effects of three different organ bath temperatures, 37°C, 34°C and 32°C on responses to carbachol in urinary bladder tissue from control rats was examined. Increased responses to carbachol were seen at a reduced temperature of 34°C. When the bath temperature was reduced further to 32°C, there was a highly significant enhancement of the response to carbachol (Figure 4.1). pEC50 and Emax estimates were calculated (Table 4.1).

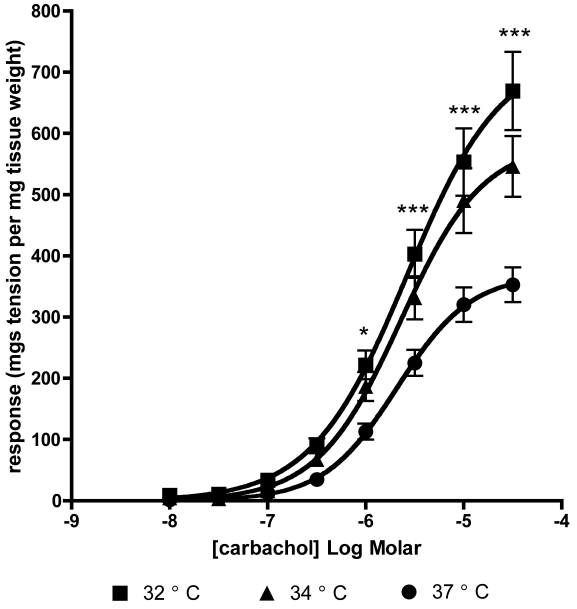

Figure 4.1 Graph showing carbachol responses of urinary bladder tissue from control rats at organ bath temperatures of 37°C, 34°C and 32°C. Data represent mean + s.e.m. of n>6 urinary bladder strips. Statistical significance was tested by two-way ANOVA with post-hoc Bonferonni, * represents $p<0.05$, ** $p<0.01$, ***$p<0.001$, comparing to 37°C responses.

Capsaicin responses at different organ bath temperatures in control rat urinary bladder

Next the responses to capsaicin were examined at the three different organ bath temperatures 37°C, 34°C and 32°C, in urinary bladder tissue from naive rats. Here enhanced responses to capsaicin were only seen at the 32°C organ bath temperature in comparison to responses at 37°C. No enhancement of capsaicin responses was seen at the 34°C organ bath temperature (Figure 4.2). pEC50 and Emax estimates were calculated (Table 4.2).

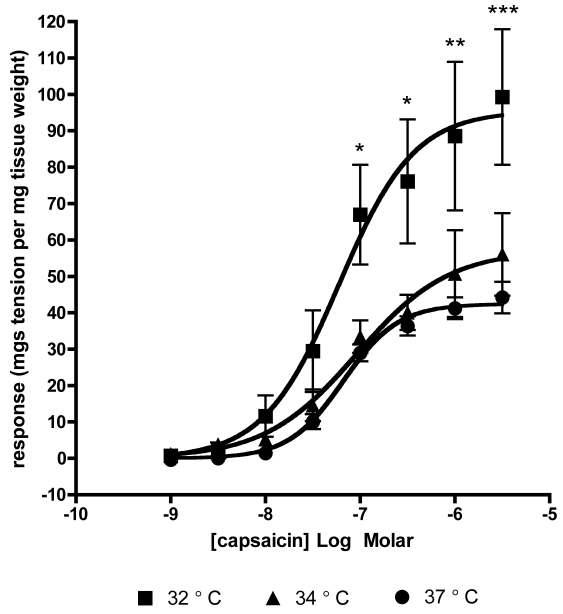

Figure 4.2 Graph showing capsaicin responses of urinary bladder tissue from control rats at organ bath temperatures of 37°C, 34°C and 32°C. Data represent mean + s.e.m. of n>6 urinary bladder strips. Statistical significance was tested by two-way ANOVA with post-hoc Bonferonni, * represents $p<0.05$, ** $p<0.01$, ***$p<0.001$, comparing to 37°C responses.

The effect of organ bath temperature on responses to carbachol in urinary bladder from STZ-diabetic rats

Next the effects of two organ bath temperatures 37°C and 32°C, were examined on carbachol responses in bladder from STZ-diabetic rats. Here no enhancement of carbachol responses were seen with the reduced organ bath temperature of 32°C (Figure 4.3). pEC50 and Emax estimates were calculated (Table 4.1).

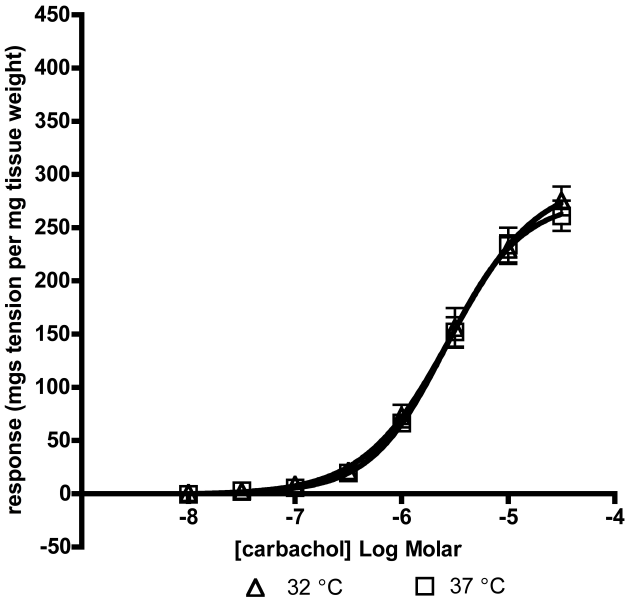

Figure 4.3 Graph showing carbachol responses of urinary bladder tissue from STZ-treated rats at organ bath temperatures of 37°C and 32°C. Data represent mean + s.e.m. of n>6 urinary bladder strips. No statistical significance was seen when tested by two-way ANOVA.

The effect of organ bath temperature on responses to capsaicin urinary bladder from STZ-diabetic rats

The responses to capsaicin in bladder from STZ-diabetic rats were studied at two organ bath temperatures, 37°C and 32°C. Here a classically diminished response to capsaicin was observed at the standard organ bath temperature of 37°C when comparing to control responses (Figure 4.2, Figure 4.4). Reduction of bath

temperature to 32°C had no enhancing effect on this diminished capsaicin response. pEC50 and Emax estimates were calculated (Table 4.2).

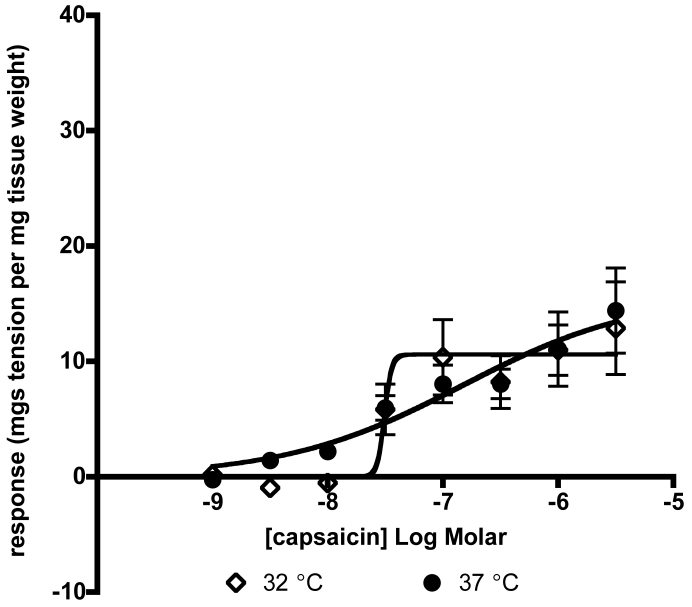

Figure 4.4 Graph showing capsaicin responses of urinary bladder tissue from STZ-treated rats at organ bath temperatures of 37°C and 32°C. Data represent mean + s.e.m. of n>6 urinary bladder strips. No statistical significance was seen when tested by two-way ANOVA.

Table 4.1. Potency and efficacy estimates for urinary bladder responses to carbachol from control and STZ-treated rats at different organ bath temperatures. Data represent mean ± s.e.m. n>6 urinary bladder strips.

	pEC50	Emax
control 32°C	5.58 ± 0.14^{NS}	735.10 ±70.67***
control 34°C	5.65± 0.11^{NS}	586.10 ± 48.26*
control 37°C	5.68 ± 0.08	369.80 ± 22.64
STZ 32°C	5.54 ± 0.08^{NS}	294.90 ± 17.86^{NS}
STZ 37°C	5.59 ± 0.06	275.10 ± 13.65$^{\$\$\$}$

One-way ANOVA with post-hoc Dunnetts ^{NS} non significant , *p<0.05, **p<0.01, ***p<0.001 comparing to same group control, $^{\$}$ p<0.05, $^{\$\$}$p<0.01, $^{\$\$\$}$p<0.001 comparing to control 37°C

Table 4.2. Potency and efficacy estimates for urinary bladder responses to capsaicin from control and STZ-treated rats at different organ bath temperatures. Data represent mean ± s.e.m. n>6 urinary bladder strips

	pEC50	Emax
control 32°C	7.22 ± 0.20^{NS}	95.52 ±11.63***
control 34°C	7.04± 0.24^{NS}	57.23 ± 8.07^{NS}
control 37°C	7.18 ± 0.06	42.44 ± 1.76
STZ 32°C	7.51 ± 0.80^{NS}	10.61 ± 1.16^{NS}
STZ 37°C	6.83 ± 0.62	15.86± 4.86$^{\$\$\$}$

One-way ANOVA with post-hoc Dunnetts ^{NS} non significant , $^{*}p<0.05$, $^{**}p<0.01$, $^{***}p<0.001$ comparing to same group control, $^{\$}$ $p<0.05$, $^{\$\$}p<0.01$, $^{\$\$\$}p<0.001$ comparing to control 37°C

Spontaneous activity at the different organ bath temperatures

To examine the potential effects of organ bath temperature on spontaneous contractile activity of the urinary bladder from control and STZ-treated rats, frequency and amplitude of spontaneous activity was measured. Decreasing organ bath temperature had the effect of decreasing frequency of spontaneous contractile activity in tissue from both control and STZ-treated rats. With decreased organ bath temperature an increase in amplitude of spontaneous contractile activity was seen in tissue from both control and STZ-treated rats (Figure 4.5).

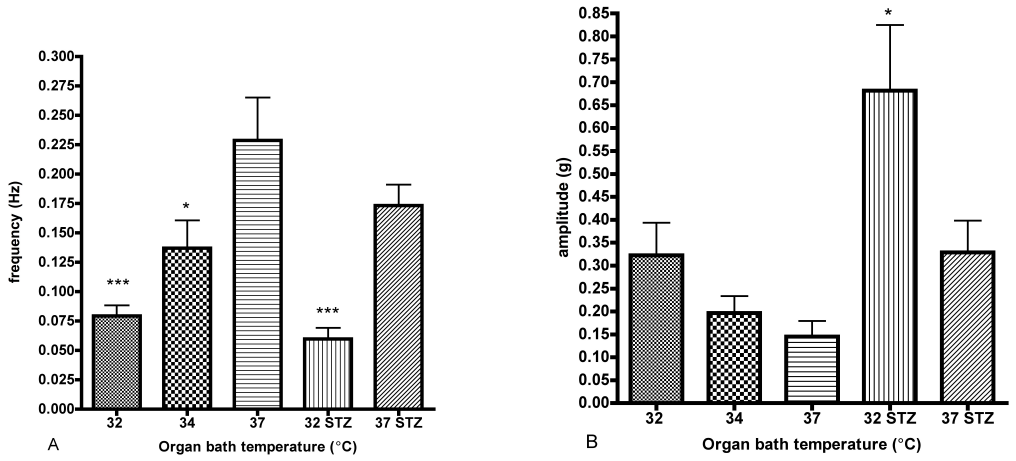

Figure 4.5 Barcharts showing frequency (A) and amplitude (B) of the spontaneous contractile activity of urinary bladder tissue from control and STZ-treated rats at organ bath temperatures of 32°C, 34 °C and 37°C. Data represent mean + s.e.m. of n>6 urinary bladder strips. Statistical significance was tested using one-way ANOVA with post-hoc Dunnett's comparing to respective control, * represents $p<0.05$, ** $p<0.01$, ***$p<0.001$, no significant difference was seen between 37°C control and STZ for frequency or amplitude.

Discussion

Reduction in organ bath temperatures caused marked enhancements in carbachol responses in controls

Carbachol responses were enhanced at the lower organ bath temperatures of 34°C and 32°C. Cooling is known to enhance the contractile ability of smooth muscle in numerous organs. In airway smooth muscle, cooling to 20 °C induces a supersensitivity to electrically evoked and acetylcholine evoked contractions (Ishii and Shimo, 1985) and was seen to reduce resting membrane potential and thereby increase contractility (Souhrada and Souhrada, 1981) . Ishii and Shimo postulated that the cause of this cooling induced supersensitivity was either an accelerated release of calcium from the intracellular stores, an inhibition of calcium extrusion from the cell or an inhibition of calcium reuptake by the intracellular stores. Studies on adrenergic agonist activity in mouse vas deferens also observed enhanced responses at the cooler temperature of 26 °C, and again altered cellular calcium handling was thought to be the mechanism of enhanced responses (Souilem et al., 1992). Another study by Souilem on mouse vas deferens put forward the idea that as well as increased intracellular release of calcium, an inhibition of the Na^+/K^+ pump could be responsible for the hyperreactivity (Souilem et al., 1995). A study on guinea-pig bladder revealed that lowering the temperature caused membrane depolarisation and again the cause for this was thought to be calcium related (Kurihara et al., 1974). So clearly evidence exists in the literature for cooling induced hyperreactivity due to altered calcium handling within the cell or membrane depolarisation. An additional mechanism that has been proposed is an increased phosphorylation of myosin light chain at lower temperatures (Sugaya and De Groat, 2000).

Reduced organ bath temperature caused increased responsiveness to capsaicin in controls

The reduced organ bath temperature induced hyperreactivity was also observed in capsaicin responses in control animal tissue. In terms of the magnitude of

enhancement, similar fold increases in carbachol and capsaicin responses were seen: carbachol increased by approximately 1.58 and 1.98-fold, capsaicin responses were increased 1.35 and 2.3 fold at 34°C and 32 °C organ bath temperatures respectively. It appears that the increases in capsaicin responses at lower temperatures are driven by a myogenic mechanism, rather than any direct effect on the TRPV1 receptor itself.

No temperature induced hyperreactivity was observed for carbachol or capsaicin in STZ-treated rat tissue

Interestingly, no such temperature-enhancement was seen in STZ-diabetic tissue for either carbachol or capsaicin. These data imply that the mechanism driving low temperature enhancement of responses to carbachol and capsaicin is deficient in STZ-diabetic tissue. Furthermore, the deficiency in this temperature sensitive mechanism may be the mechanism by which myogenic function is impaired in diabetes as evidenced by the reduced contractile responses to carbachol. This impairment likely plays a part in the diminished responses seen to capsaicin but because the decreases in capsaicin response are much larger than that seen in carbachol responses, it is unlikely that this myogenic impairment is the total cause of the diminished TRPV1 response. The TRPV1 channel desensitizes to repeated heat activation in much the same way that it desensitizes to acid and chemical agonists (Benham et al., 2003). So these studies do not preclude the notion that a change in the temperature threshold in the diabetic model had occurred and it was heat-induced desensitisation of TRPV1 responses that were causative to the diminished TRPV1 responses seen *in vitro*.

Organ bath temperature causes changes in spontaneous activity

Reduction of the organ bath temperature caused a graded decrease in the frequency and a graded increase in the amplitude of spontaneous contractile activity of tissue from control and STZ-treated rats. Such decreases/increases in response to temperature have been reported in adult rat bladder tissue (Sugaya and De Groat, 2000) where they studied whole bladder *in vitro* and saw that the frequency of spontaneous contractions increased some 1.5 fold from 28°C to 37°C, and amplitudes were two-fold larger at the lower temperature. However the result seen here for the STZ-treated rat group was unexpected. There seems to be a disparity in the effects of temperature on spontaneous activity and muscarinic/TRPV1-driven contractile response. Spontaneous activity and changes to it by temperature are similar in tissue from control and STZ-treated rats, whereas changes to muscarinic/TRPV1 responses appear deficient in STZ-treated tissue. Sugaya summarized three possible mechanisms for the effects of temperature on spontaneous activity: through stretch activated channels, a depolarization of membrane potential, or desynchronization of muscle activity (Sugaya and De Groat, 2000). The mechanism of desynchronization was explained by Sugaya as a 'high level of spontaneous activity renders cells less susceptible to spread of electrical activity from adjacent cells, thereby preventing co-ordinated contractions'. There may well be more than one mechanism underlying the changes seen with temperature and that in itself may provide an explanation for the disparity seen between changes to spontaneous and changes to carbachol/capsaicin evoked contractions.

Chapter 5

Defining the role that acute methylglyoxal exposure may play in TRPV1 modulation

Introduction

Up to this point in my thesis I have examined the consequences of diabetes and the impact of organ bath temperature. The next phase of work was to define the role that a potential causative agent plays in the modulation of TRPV1 function. This could gain a further understanding of the process of neuropathy, and might provide a potential therapeutic avenue to aid neuropathy prevention or regression.

An ideal candidate causative agent would appear early in disease, persist even with good glucose control, be correlated to diabetic neuropathy, cause neuropathy in other disease states and be active at a mechanism of TRPV1 down-regulation. Down-regulation of TRPV1 function is known to occur through four main ways: firstly through direct desensitisation by TRPV1 agonist exposure, secondly through cross-desensitisation for example through TRPA1 activation, thirdly through reduction in receptor number and finally through depletion or down-regulation of effector pathway components.

The candidate I chose to study is methylglyoxal, a highly reactive glucose metabolite recently identified as being a TRPA1 agonist (Eberhardt et al., 2012). Methylglyoxal has been identified as a potential causative factor in many diabetic complications (Mclellan et al., 1994, Thornalley, 1994). Recently high plasma levels have been correlated to the pain severity in diabetics suggestive of a direct correlative role of methylglyoxal to pain and perhaps to induction and maintenance of neuropathy (Eberhardt et al., 2012). This metabolite, I felt, warranted study in the context of how it would affect the TRPV1 receptor, in controls and in diabetic animal tissue.

Methylglyoxal

Methylglyoxal is a glucose metabolite and is a neurotoxic reactive dicarbonyl compound (Fukunaga et al., 2004). High levels of methylglyoxal have been measured in diabetes and this metabolite has been identified as a potential culprit for many of the complications prevalent in diabetes, including neuropathy (Eberhardt et al., 2012). Reactive dicarbonyl compounds such as methylglyoxal are intermediates in the formation of advanced glycation endproducts (AGE), which are glycalated proteins, lipids and nucleic acids. The presence of AGE are considered detrimental in diabetes, Alzheimer's disease, renal failure, aging and atherosclerosis (Ramasamy et al., 2005). In diabetes AGE induces alterations in cellular permeability and activates the receptor for AGE (RAGE) thus driving inflammation and tissue injury and thereby contributes to complications such as nephropathy (Ramasamy et al., 2005)

Methylglyoxal levels are increased early in diabetes before complications develop and have been measured at 842 nmol/l in the plasma of young Type 1 diabetics, compared to the non-diabetic levels of around 439 nmol/l (Han et al., 2007). However given that methylglyoxal is formed within the cell, the intracellular levels may be much higher than the measured extracellular plasma concentrations. Intracellular methylglyoxal levels are complicated to quantify as here it exists as free methylglyoxal and bound in adduct form (Lo et al., 1994). Intracellular levels may be as high as 310 μM (Chaplen et al., 1998), however in red blood cells levels have been measured at 1.66 and 0.80 nmol/ml packed red blood cells from diabetic and non-diabetics respectively (Thornalley, 1988). Methylglyoxal diffuses across the plasma membrane so an extracellular high concentration of methylglyoxal is likely reflective of increased intracellular levels. The levels of methylglyoxal in plasma have been correlated to pain in diabetic patients (Bierhaus et al., 2012). In this study, the plasma level of methylglyoxal in healthy controls was measured at 200 nM, this was shown to be increased in diabetics with no pain symptoms to 500 nM and was increased further to 900 nM in diabetics with pain (Bierhaus et al., 2012). Levels of methylglyoxal have been measured in urine of healthy volunteers at 15 μM

(Espinosa-Mansilla et al., 1998), suggesting that the bladder may be exposed to high levels of methylglyoxal. To cause an effect on TRPA1 channels, the methylglyoxal levels need to increase intracellularly as the site of action is intracellular, and therefore reasonably high concentrations of methylglyoxal are needed for extracellular application. In vitro assays investigating the effects of methylglyoxal on pancreatic cells have shown stimulating effects of 1mM methylglyoxal in the acute setting (Cook et al., 1998), with cytotoxicity by 4-6 hours (Sheader et al., 2001). Studies with DRG showed that an acute extracellular application of 3 mM methylglyoxal rapidly increased intracellular levels of methylglyoxal from 1.5 μM to 2.2 μM (Eberhardt et al., 2012). Additionally this study by Eberhardt also demonstrated that human TRPA1 was activated by the application of 1, 3 and 10 mM methylglyoxal, applied extracellularly. These studies guided the use of mM concentrations of methylglyoxal.

Formation of methylglyoxal

Methylglyoxal is formed inside cells from the triose phosphate intermediates of glycolysis, dihydroxyacetone phosphate and glyceraldehyde 3-phosphate, in a non-enzymatic process known as the Maillard reaction. The Maillard reaction is a complex series of reactions of the carbonyl groups of reducing sugars with the primary amino groups of proteins. From these reactions, the corresponding Schiff bases are produced which then undergo Amadori rearrangements to yield protein-derived aminomethyl- ketones. Reactive oxygen species and reactive nitrogen species are then involved in glycoxidations of these Amadori compounds that are catalysed by transition-metal-ions, yielding 1,2-dicarbonyl compounds such as glyoxal and methylglyoxal. Autoxidation reactions of glucose, Schiff bases or the corresponding Amadori compounds also yield 1,2-dicarbonyl compounds. These dicarbonyl compounds are highly reactive with amino groups on proteins causing further glycoxidation, and resulting in protein cross-linking and modification to produce AGEs. Typically the lysine and the arginine residues are affected. This is important as these residues are commonly located within the active sites on enzymes, and modification here can result in

enzyme deactivation (Reddy and Beyaz, 2006). The hyperglycemia and high levels of ketones present in uncontrolled diabetes thus leads to increased methylglyoxal production (Figure 5.1).

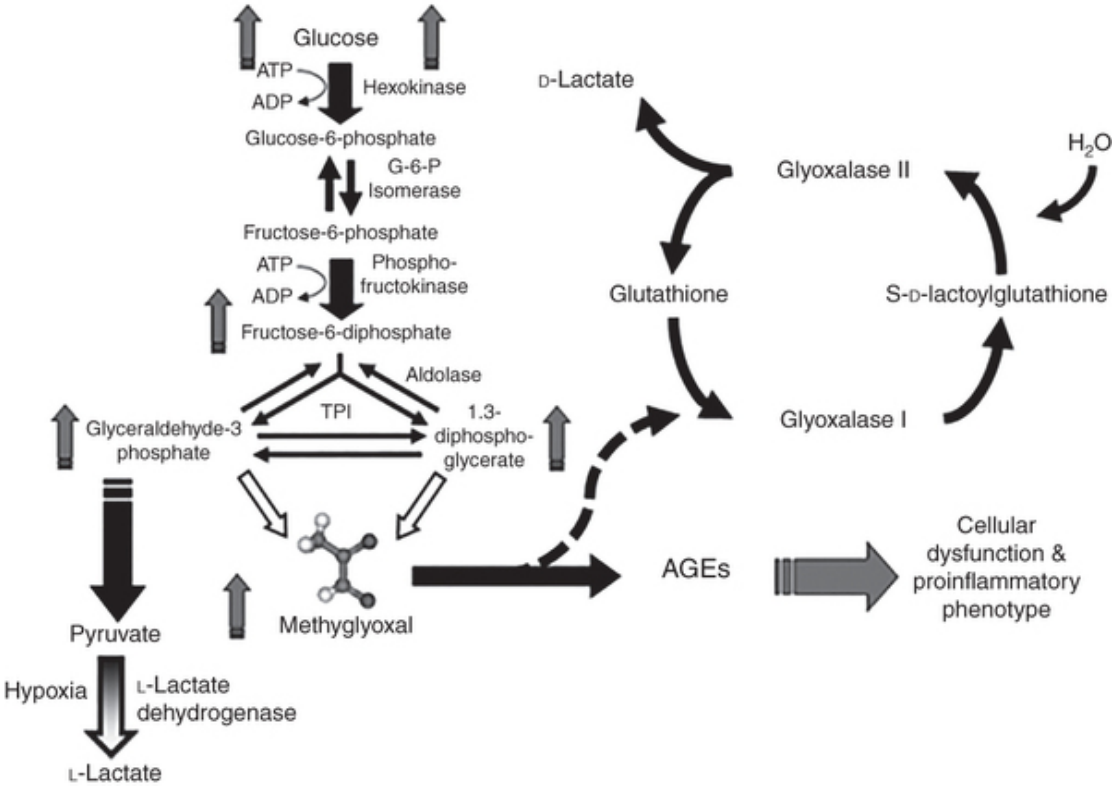

Figure 5.1 Formation and detoxification of methylglyoxal. Taken from (Kiefer et al., 2013)

Detoxification of methylglyoxal

The bodies main defence system against glycation is the glutathione-dependent glyoxalase system consisting of glyoxalase 1 and glyoxalase II that act to detoxify methylglyoxal and other reactive α-oxoaldehydes. In diabetes however, methylglyoxal levels remain high, even with good glucose control, due to an impairment in the glyoxalase system. This is because oxidative stress causes a depletion of glutathione and this suppresses the activity of the enzyme glyoxalases due to their glutathione dependence and can therefore lead to increased levels of methylglyoxal. In diabetes, there is evidence of increased oxidative stress and AGEs themselves may generate reactive oxygen species. RAGE activation by AGEs can additionally activate NADPH oxidase and

mitochondrial pathways also resulting in oxidative stress. Additionally methylglyoxal can modify antioxidant proteins reducing their function, adding to the increased burden of oxidative stress. So without intervention to reduce the oxidative stress or to enhance the detoxification pathways, levels of methylglyoxal and oxidative stress remain high. Lower activity of glyoxalase 1 has been correlated with painful neuropathy in diabetes suggesting that the glyoxalase activity does modulate the diabetic neuropathy phenotype (Skapare et al., 2013) .

AGE generation by methylglyoxal

Methylglyoxal is known to react and bind with arginine, lysine and cysteine residues on proteins, both reversibly and irreversibly. These reactions can rapidly alter protein structure and function, and generate AGEs.

The formation of methylglyoxal- modified proteins involves glyoxidation (Lo et al., 1994). For example methylglyoxal reacts with N- alpha-acetylarginine to first produce glycosylamine and 4,5-dihydroxy-5-methylimidazolidine derivatives, a reversible reaction, which is followed by a slower irreversible production of an imidazolone, N-alpha-acetyl-N delta- (5-methyl-4-imidazolon-2-yl)ornithine. These studies also revealed that methylglyoxal reacts with the arginine residues on BSA to form imidazolone. Methylglyoxal also reacts with and inactivates a major antioxidant enzyme, glutathione thus increasing cellular peroxide levels and contributing to oxidant damage processes (Park et al., 2003). Methylglyoxal interaction with amino acids has also been found to directly produce free radical species: cross-linked radical cations, methylglyoxal radical anions, and in the presence of oxygen, superoxide radical anions (Yim et al., 1995) .

Methylglyoxal may have a directly causative role in induction of Type 2 diabetes

Some studies have shown a causative effect of methylglyoxal in the development of insulin resistance, a hallmark of Type 2 diabetes. Methylglyoxal causes a modification of insulin through attachment to the arginine residue on the alpha-chain of insulin. This methylglyoxal-insulin adduct causes a decrease in insulin-mediated uptake of glucose, reduces insulin secretion and reduces clearance. Methylglyoxal has been shown to impair the signalling of insulin and to play a role in obesity through stimulation of adipogenesis via upregulation of Akt signaling (Jia, 2010)

TRPA1 activation by methylglyoxal

Methylglyoxal applied to the extracellular environment *in vitro* gains access to the cell and stimulates the TRPA1 receptor thus causing the release of neuropeptides. Methylglyoxal is believed to interact with cysteine residues at the N-terminus, a reversible reaction (Andersson et al., 2013) (Figure 5.2) and covalently modify lysine residues (Eberhardt et al., 2012).

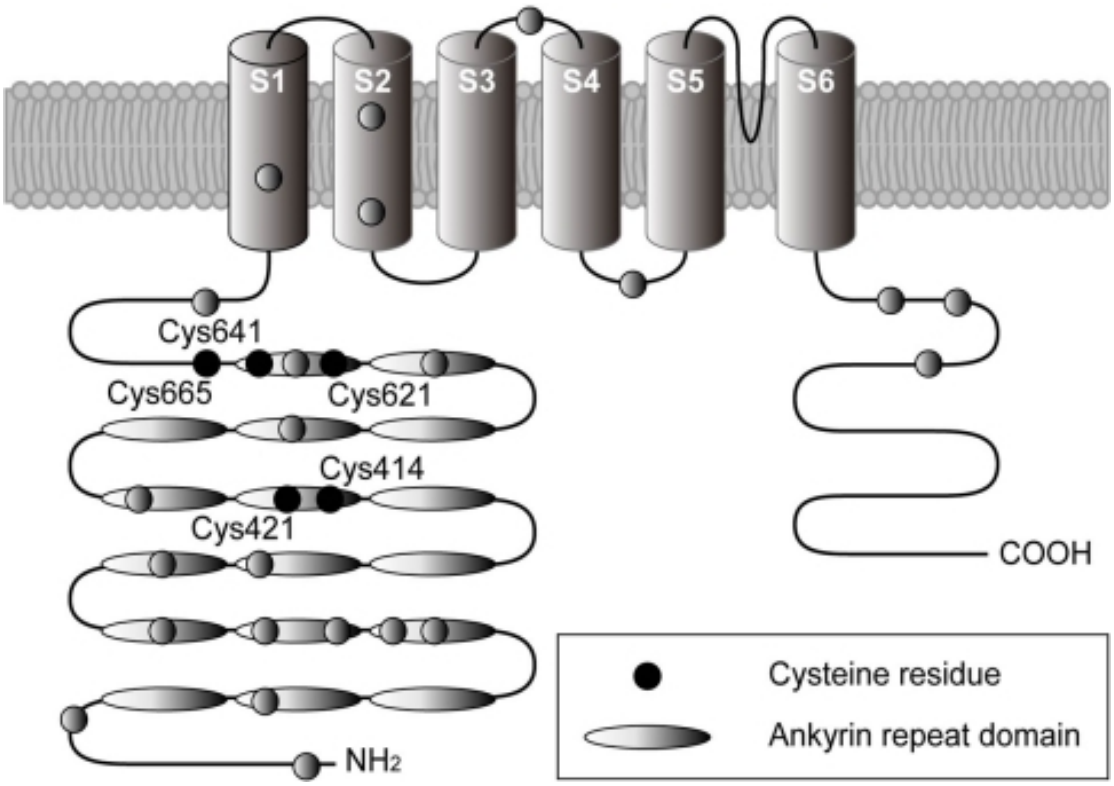

Figure 5.2 Structural model for the TRPA1 receptor. Four TRPA1 subunits are believed to combine to form a functional channel. Each subunit spans the plasma membrane six times (transmembrane domains S1–S6) and has a long cytoplasmic N-terminal domain. The filled circles indicate cysteine residues identified as crucial sites for covalent modification of TRPA1. Taken from (Takahashi and Mori, 2011)

The interaction of methylglyoxal with N-terminal cysteine residues on the TRPA1 receptor triggers a direct TRPA1 activation demonstrated *in vitro* using recombinant cells and DRG (Ohkawara et al., 2012). In a diabetic model, the TRPA1 receptor has been shown to undergo a long-term activation which is thought to underlie the pathogenesis of neuropathy (Koivisto et al., 2012).

Downregulation of TRPV1 receptor function via cross-desensitisation of TRPA1

TRPV1 and another sensory neuron receptor, TRPA1, are co-located on the sensory neuron. This co-localisation is so intricate that a dynamic cross-sensitization and desensitisation can occur between these two receptors. The desensitisation process is likely to involve calcium signaling on shared intracellular components of the receptors. Agonist activation of one receptor leads to self-desensitisation and possibly cross-desensitisation. Similarly, sensitization processes on one receptor may lead to cross-sensitisation. In addition to direct receptor cross- sensitization/ desensitisation, alterations in common effector mechanisms; sensory neuropeptide release, receptor activation and peptide deactivation processes, could also impact TRPV1 and TRPA1 functional activity.

TRPV1 and TRPA1 share similar effector mechanisms at the local level, whereby agonist activation leads to release of sensory neuropeptides such as neurokinins and Substance P release which exert a functional effect via neurokinin receptors and Substance P receptors for example to cause muscle contraction in the bladder. Due to this neuropeptide release and activation of distinct peptidergic receptors, an additional explanation for modulation of function exists and should be considered. For example if the sensory neuropeptides were depleted, then the functional activity of TRPV1 and TRPA1 would be impaired. If the receptor number or pathway altered at the peptidergic level this too would impact on TRPV1/ TRPA1 function. Finally, an alteration in the peptidergic de-activation process i.e. enzymatic breakdown of neuropeptides, would also impact on TRPV1/TRPA1 function.

TRPA1 tool ligands

A standard tool agonist for TRPA1, used extensively in the literature, is the mustard oil derived pungent compound allyl isothiocyanate (AITC). Other tool agonists include garlic-derived compounds (Figure 5.3)

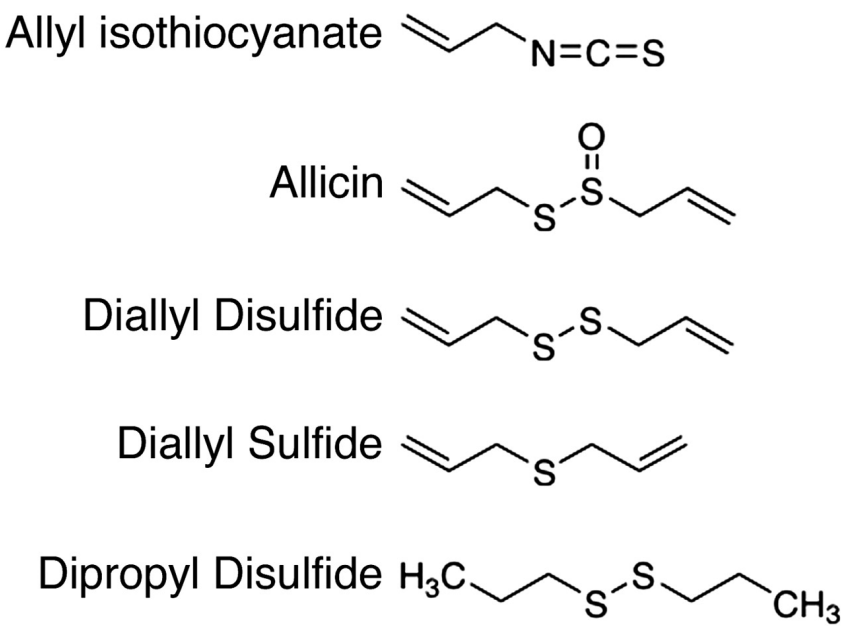

Figure 5.3 Chemical structures of TRPA1 agonist compounds allyl isothiocyanate (mustard oil), and the garlic derivatives, allicin, DADS, DAS, and dipropyl disulfide. Taken from (Bautista et al., 2005).

A potent and selective TRPA1 antagonist is HC-030031 (2-(1,3-Dimethyl-2,6-dioxo-1,2,3,6-tetrahydro-7*H*-purin-7-yl)-*N*-(4-isopropylphenyl)acetamide) Figure 5.4). This has been shown to antagonize AITC calcium influx with an IC50 of 6.2 μM and does not block currents mediated by TRPV1, TRPV3, TRPV4, hERG or Nav1.2 channels. It has also shown to be active *in vivo*, inhibiting AITC-induced flinching (Mcnamara et al., 2007) and blocking AITC effects on COX2 mRNA expression (Moilanen et al., 2012)

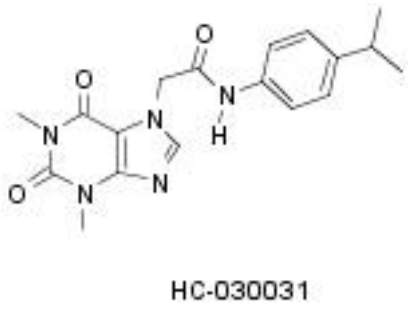

Figure 5.4 Chemical structure of HC-030031

To define the role methylglyoxal plays in modulation of TRPV1 function, the effects of this neuropathy-causing agent were investigated in urinary bladder tissue from control animals and compared to responses seen in the STZ-induced diabetic model. An acute exposure to methylglyoxal was examined on the subsequent responses to capsaicin, carbachol and to electrical field stimulation. The effects of a known TRPA1 agonist AITC were studied to provide comparative responses and a TRPA1 selective antagonist HC-030031 was used to explore the mode of action of methylglyoxal.

Methods

Experiments were performed on 2 weeks post control or STZ-treated rat urinary bladder strips, set-up as previously described. For electrical field stimulation studies bladder strips were suspended between electrodes. STZ-treated animals were only used in these studies if blood glucose levels were > 3 fold higher than control levels.

Direct contractile effects of methylglyoxal and AITC and effects of acute methylglyoxal exposure on subsequent capsaicin responses

In 2 week post control and STZ-treated urinary bladder tissue, single concentrations of methylglyoxal (0.1 mM, 0.3 mM, 1 mM, 3 mM and 10 mM) or cumulative concentrations of AITC (1×10^{-5}M- 3×10^{-3}M) were applied to measure the direct effects of methylglyoxal and AITC as contractile agents. After a 10 minute incubation with no washout which allowed tensions to return to baseline levels, a concentration range of capsaicin was applied cumulatively (1×10^{-9}M- 3×10^{-6}M) to study the effects of methylglyoxal and AITC on TRPV1 responses. Post washout and a 40 minute equilibration, 3 mM methylglyoxal was reapplied to examine whether repeated application would result in contraction.

Monitoring of carbachol responses following acute methylglyoxal exposure

In 2 week post control and STZ-treated urinary bladder tissue, a concentration range of carbachol (1×10^{-8}M- 3 x 10-^{5}M) was applied cumulatively following either vehicle control (water) or methylglyoxal acute exposure.

Effects of a TRPA1 specific antagonist, HC-030031

First a concentration-finding study was performed using 2-week post control urinary bladder tissue. A range of HC-030031 concentrations (10, 30,100 μM) or DMSO control were incubated for 10 minutes prior to application of 0.1 mM

AITC. Following identification of the optimal concentration of 30 μM HC-030031, this concentration was tested against 3 mM methylglyoxal to examine whether methylglyoxal was causing its effects through activation of the TRPA1 receptor.

Effects of acute AITC and methylglyoxal ± TRPA1 antagonist HC-030031 on subsequent capsaicin responses

After exposure to vehicle controls ,0.1 mM AITC or 3 mM methylglyoxal ± 30 μM HC-030031, with no washout, a concentration range of capsaicin was applied cumulatively (1×10^{-9}M- 3×10^{-6}M).

Effect of acute methylglyoxal application on repeated electrically-evoked contractions

In 2 week post control and STZ-treated urinary bladder tissue, the effects of a 5 minute preincubation with 3 mM methylglyoxal were examined on repeated electrically evoked contractions: submaximal voltage, 40 Hz, repeat pulses every minute, 0.1 ms pulse width, rate of 50 Hz, 10 sec duration. Next the effects of 3 mM methylglyoxal were examined during repeat electrically-evoked contractions. Resuts were transformed to percent increases over the pre-methylglyoxal contraction level.

Direct relaxant effects of methylglyoxal and AITC

On the observation that a relaxation was seen on second application of methylglyoxal, an additional study of methylglyoxal's effect on carbachol precontracted tissue was undertaken. Following maximal concentration addition of carbachol (3×10^{-5}M), tissues were allowed to reach the tonic phase of contraction then a cumulative concentration range of methylglyoxal or AITC (1×10^{-5}M- 1×10^{-2}M) was applied. To see if the methylglyoxal relaxant effects were TRPA1 mediated, 10 and 30 μM HC-030031 were incubated for 10 minutes before methylglyoxal additions.

Results

The direct contractile effects of methylglyoxal and AITC

Previous in-house data had demonstrated that application of AITC was able to cause a direct contractile response in urinary bladder (Katisart, 2011). So the first studies were aimed at examining whether methylglyoxal would elicit similar effects and compare these to responses to AITC.

A concentration range of methylglyoxal or AITC was applied and contractile effects measured, a representative trace is shown (Figure 5.5). Following washout, no contractile response to a second application of methylglyoxal was seen, but a small relaxant response from baseline tension was noted.

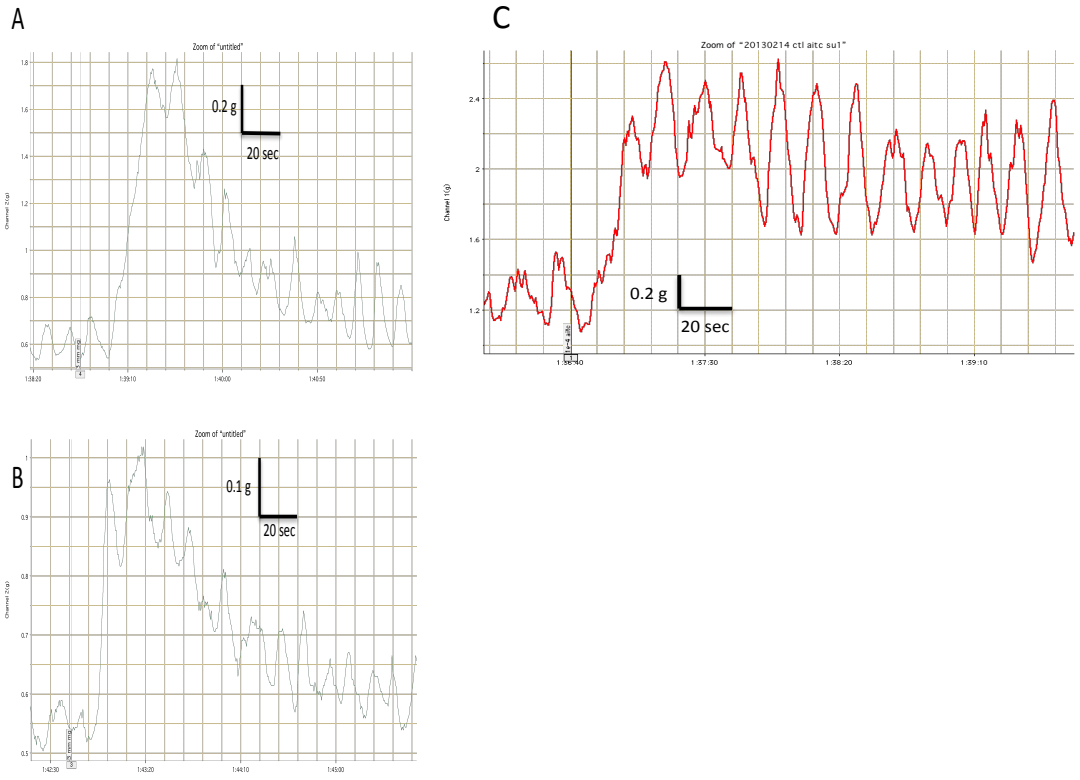

Figure 5.5 Representative trace of urinary bladder responses to methylglyoxal in 2-weeks post control (A) and STZ-treated (B) rats or AITC in 2-weeks post control (C).

The initial response to methylglyoxal was a transient phasic contraction and reduced responses were seen in the STZ-treated animal group. AITC caused a more sustained contraction of similar maximal magnitude and was only tested in control tissues (Figure 5.6). Potency and efficacy estimates were calculated (Table 5.1).

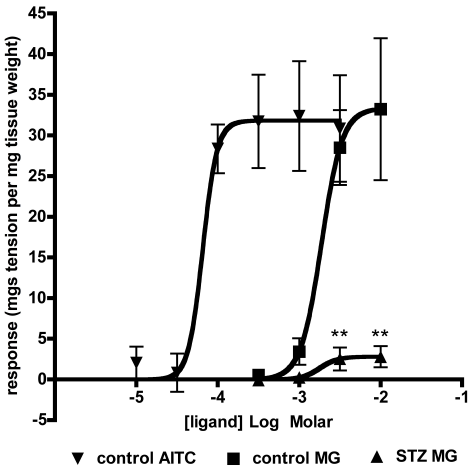

Figure 5.6 Graph showing contractile responses to a concentration range of methylglyoxal or AITC in 2-weeks post control and STZ-treated rat tissue. Data represent mean ± s.e.m. of n >6 urinary bladder strips. Statistical significance was tested by 2-way ANOVA with post-hoc Bonferonni, * represents $p<0.05$, ** $p<0.01$, *** $p<0.001$, comparing responses to methylglyoxal in STZ to control.

Table 5.1 Potency and efficacy estimates for methylglyoxal and AITC in tissue from 2 weeks post control or STZ-treated rats. Data represent mean ± s.e.m for >6 urinary bladder strips.

		pEC50	Emax
AITC	control	4.19 + 0.30	31.82 ± 3.43
MG	control	2.72 ± 0.18	33.35 ± 6.46^{NS}
MG	STZ	2.75 ± 0.41^{NS}	2.79 ± 0.97***

Statistical analysis by Students t-test comparing MG STZ to control NS no significant difference, * $p<0.05$, ** $p<0.01$, *** $p<0.001$, comparing MG control to AITC control *NS* no significant difference.

Effects of methylglyoxal and AITC on TRPV1 responses

The effects of acute methylglyoxal exposure on subsequent responses to capsaicin

Following a 10 minute incubation of a range of concentrations of methylglyoxal with no washout, the responses to a cumulative concentration range of capsacin in 2 weeks control and STZ-treated rat tissue were examined. Capsaicin response in STZ-treated rat tissue compared to control was clearly diminished as seen previously (Figure 5.7).

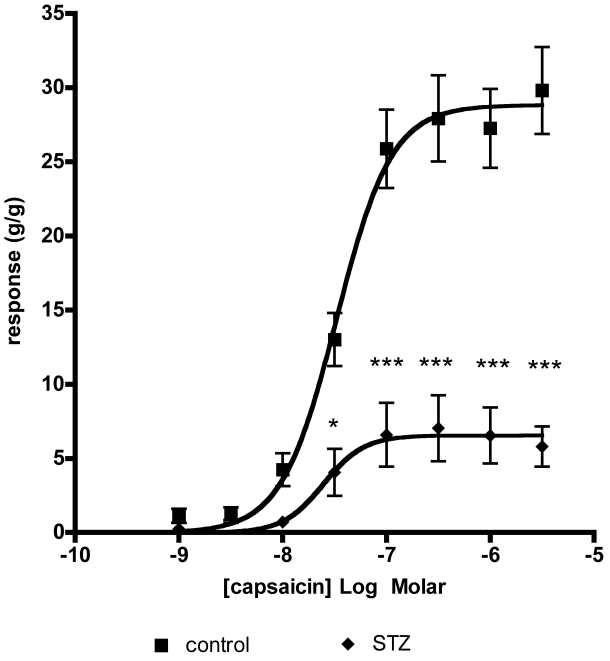

Figure 5.7 Graph showing contractile responses to a concentration range of capsaicin in 2-weeks post control and STZ-treated rat tissue. Data represent mean ± s.e.m. of n >6 urinary bladder strips. Statistical significance was tested by two-way ANOVA with post-hoc Bonferonni, * represents $p<0.05$, ** $p<0.01$, *** $p<0.001$ comparing to control.

In urinary bladder from control animals the capsaicin reponses following 1, 3 and 10 mM methylglyoxal were rightward shifted relating to a decreased potency. The urinary bladder from STZ-treated animals also displayed a rightward shifted response following 3 and 10 mM methylglyoxal exposure (Figure 5.8) (Table 5.2)

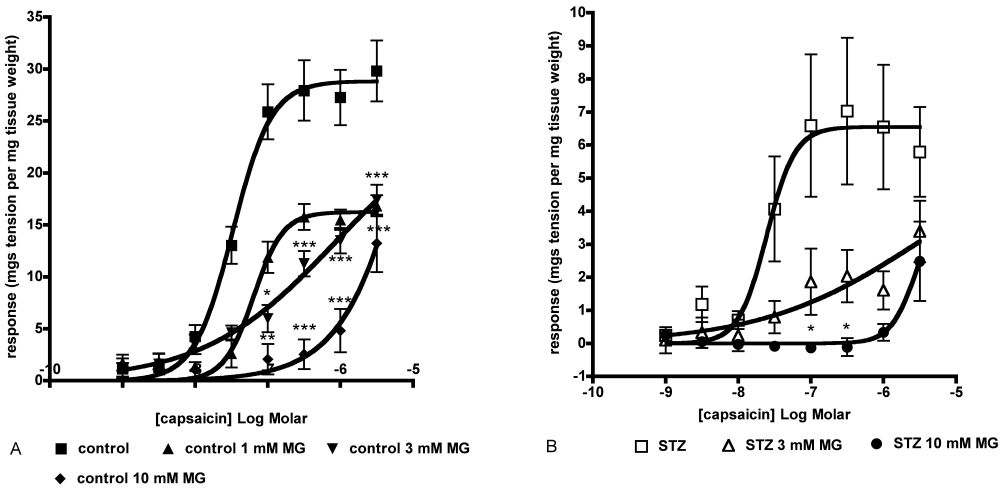

Figure 5.8 Graphs showing contractile responses to a concentration range of capsaicin following acute exposure to a range of concentrations of methylglyoxal in 2-weeks post control (A) and STZ-treated (B) rat tissue. Data represent mean ± s.e.m. of n >6 urinary bladder strips. Statistical significance was tested by two-way ANOVA with post-hoc Bonferonni, * represents $p<0.05$, ** $p<0.01$, *** $p<0.001$ comparing to respective control.

Table 5.2 Potency and efficacy estimates for capsaicin ± acute methylglyoxal in tissue from 2 weeks post control or STZ-treated rats. Data represent mean ± s.e.m for >6 urinary bladder strips.

		pEC50	Emax
control	vehicle	7.48 ± 0.07	28.82 ± 1.34
	1 mM MG	7.20 ± 0.06^{NS}	16.23 ± 0.70^{NS}
	3 mM MG	6.07 ± 0.70^{NS}	26.60 ± 9.43^{NS}
	10 mM MG	5.41 ± 1.64^{NS}	28.82 ± 1.34^{NS}
STZ	vehicle	7.61 ± 0.08	6.55 ± 0.80$^{\$\$\$}$
	3 mM MG	5.48 ± 4.58^{NS}	6.24 ± 13.81^{NS}
	10 mM MG	5.54 ± 7.14^{NS}	4.51 ± 8.29^{NS}

Statistical analysis by one-way ANOVA comparing to control NS no significant difference, * $p<0.05$, $^{**}p<0.01$, $^{***}p<0.001$, or by Students t-test comparing STZ to control, $$$ $p<0.001$.

The effects of acute AITC exposure on subsequent responses to capsaicin

The effect of 0.1 mM AITC on subsequent response to a concentration range of capsaicin in control animal tissue was next examined where it was seen that AITC pre-exposure caused a reduction in capsaicin efficacy (Figure 5.9) (Table 5.3)

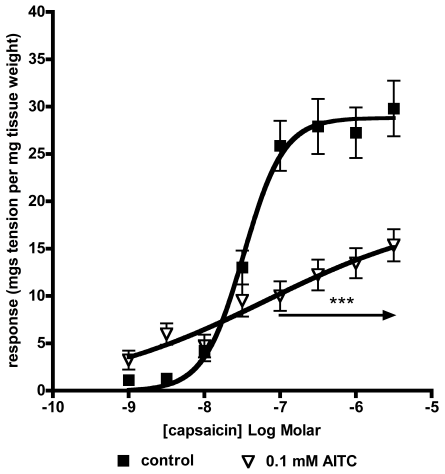

Figure 5.9 Graph showing contractile responses to a concentration range of capsaicin following 0.1 mM AITC exposure in 2-weeks post control rat tissue. Data represent mean ± s.e.m. of n >6 urinary bladder strips. Statistical significance was tested by two-way ANOVA with post-hoc Bonferonni, * represents $p<0.05$, ** $p<0.01$, *** $p<0.001$ comparing to control.

Table 5.3 Potency and efficacy estimates for capsaicin responses ± acute AITC. Data represent mean ± s.e.m n >6 urinary bladder strips.

	pEC50	Emax
vehicle	7.48 ± 0.07	28.82 ± 1.34
0.1 mM AITC	7.19 ± 0.95^{NS}	19.01 ± 6.22*

Statistical analysis by Students t-test comparing to control, NS no significant difference *$p<0.05$.

Monitoring of carbachol responses following acute methylglyoxal exposure

Following methylglyoxal and capsaicin exposure, responses to a cumulative concentration range of carbachol were examined. As seen previously, carbachol efficacy was reduced in the STZ-treated animal group (Figure 5.10)

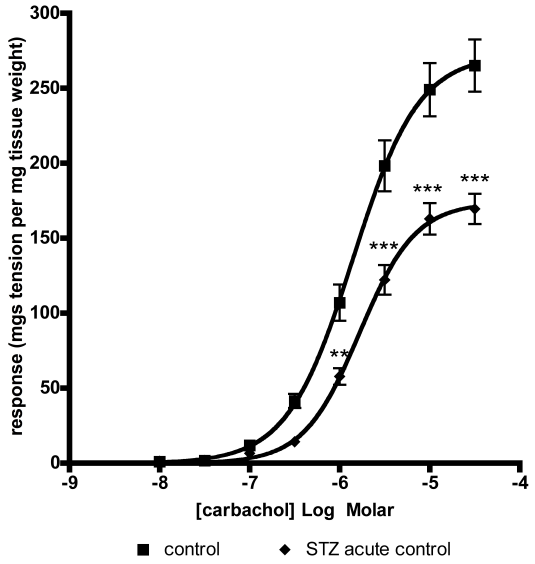

Figure 5.10 Graph showing contractile responses to a concentration range of carbachol in 2-weeks post control and STZ-treated rat tissue. Data represent mean ± s.e.m. of n >6 urinary bladder strips. Statistical significance was tested by two-way ANOVA with post-hoc Bonferonni, * represents $p<0.05$, ** $p<0.01$, *** $p<0.001$, comparing to control.

Responses to carbachol in the control and STZ-treated animal groups were unaltered by the 3 mM methylglyoxal exposure. However 10 mM methylglyoxal exposure caused a depressed maximum efficacy and a slight reduction in potency to carbachol in both control and STZ-treated animal tissue (Figure 5.11) (Table 5.4)

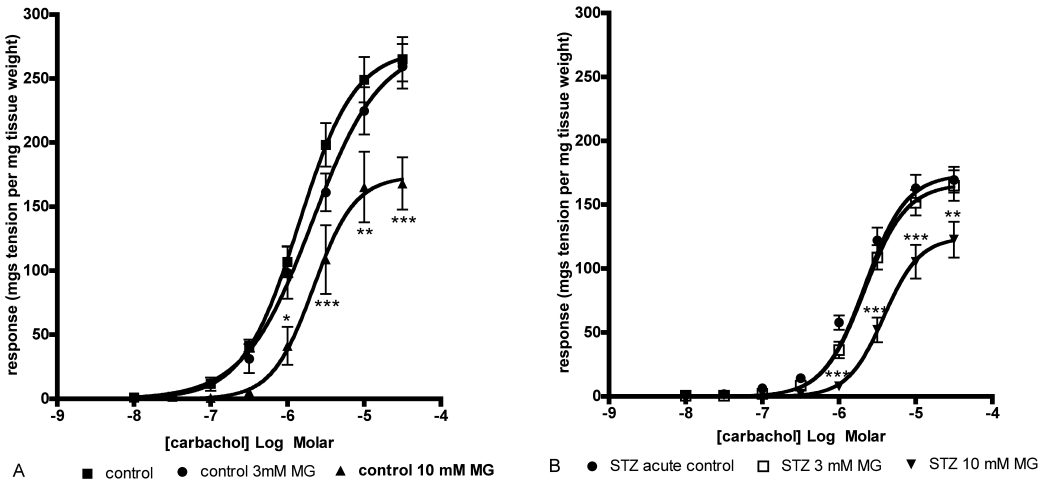

Figure 5.11 Graphs showing contractile responses to a concentration range of carbachol following methylglyoxal exposure in 2-weeks post control (A) and STZ-treated (B) rat tissue. Data represent mean ± s.e.m. of n >6 urinary bladder strips. Statistical significance was tested by two-way ANOVA with post-hoc Bonferonni, * represents $p<0.05$, ** $p<0.01$, *** $p<0.001$ comparing to respective control.

Table 5.4 Potency and efficacy estimates for carbachol ± acute methylglyoxal in tissue from 2 weeks post control or STZ-treated rats. Data represent mean ± s.e.m for >6 urinary bladder strips.

		pEC50	Emax
control	vehicle	5.85 ± 0.07	272.60 ± 13.09
	3 mM MG	5.68 ± 0.11^{NS}	276.00 ± 22.02^{NS}
	10 mM MG	5.66 ± 0.11^{NS}	173.80 ±15.70**
STZ	vehicle	5.78 ± 0.05	173.80 ± 6.78$^{\$\$\$}$
	3 mM MG	5.67 ± 0.05^{NS}	166.30 ± 6.85^{NS}
	10 mM MG	5.42 ± 0.07**	124.50 ± 8.95**

Statistical analysis by one-way ANOVA comparing to control NS no significant difference, * $p<0.05$, $^{**}p<0.01$, $^{***}p<0.001$, or by Students t-test comparing STZ to control, $$$ $p<0.001$.

Monitoring of carbachol responses following acute AITC exposure

Following exposure to 0.1 mM AITC, responses to carbachol in control animal tissue were leftward shifted with no effect on efficacy (Figure 5.12) (Table 5.5).

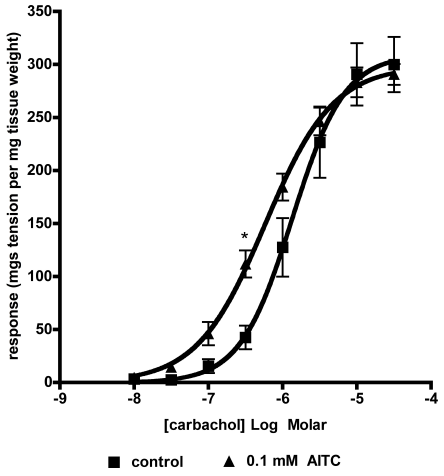

Figure 5.12 Graph showing contractile response to a concentration range of carbachol following 0.1 mM AITC exposure in 2 weeks post control rat tissue. Data represent mean ± s.e.m. of n >6 urinary bladder strips. Statistical significance was tested by two-way ANOVA with post-hoc Bonferonni, * represents $p<0.05$, ** $p<0.01$, *** $p<0.001$ comparing to control.

Table 5.5 Potency and efficacy estimates for carbachol ± acute AITC in tissue from 2 weeks post control rats. Data represent mean ± s.e.m for >6 urinary bladder strips.

	pEC50	Emax
vehicle	5.87 ± 0.10	309.50 ± 21.55
0.1 mM AITC	6.23 ± 0.06*	298.60 ± 10.99NS

Statistical analysis by Students t-test comparing to vehicle, NS no significant difference, * $p<0.05$.

The effects of a TRPA1 antagonist HC-030031

Next the effects of a TRPA1 selective antagonist HC-030031 were examined. First an optimal concentration-finding study was completed by preincubating a concentration range of HC-030031 for 10 minutes prior to application of 0.1 mM TRPA1 agonist AITC (Figure 5.13). Application of 0.1 mM AITC gave a contraction of almost identical magnitude to that seen for 3 mM methylglyoxal, and although 30 μM HC-030031 did not completely inhibit AITC contraction, this was chosen as the optimal antagonist concentration as it showed no adverse effect versus carbachol responses, whereas the 100 μM concentration HC-030031 did cause a depression in carbachol responses. Then 3 mM methylglyoxal direct contractile effects were measured ± preincubation of an optimum HC030031 concentration of 30 μM or vehicle control (Figure 5.13). 30 μM HC-030031 gave a near complete inhibition of 3 mM methyglyoxal direct contractile effects (Figure 5.13).

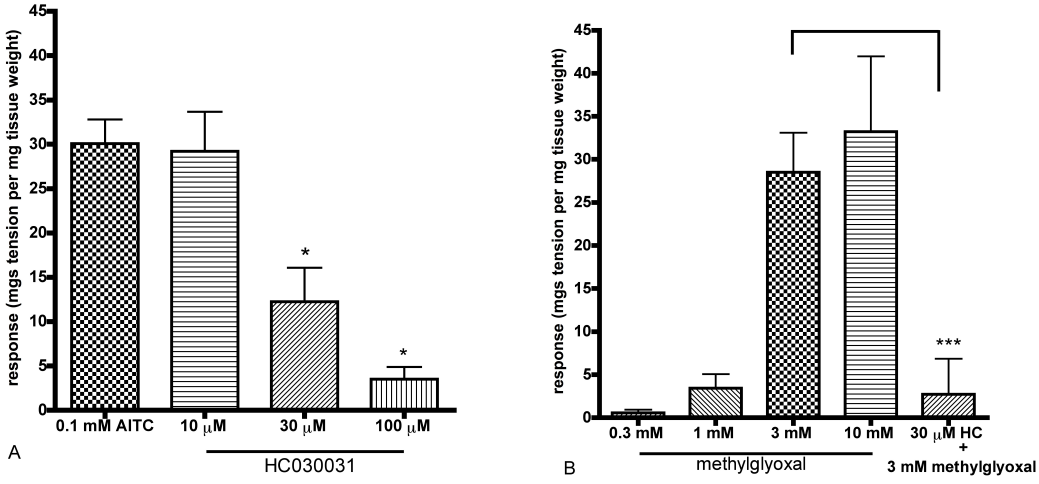

Figure 5.13 Barcharts showing direct contractile effects of AITC ± concentration range of TRPA1 antagonist HC-030031 (A) and methylglyoxal ± single concentration of HC-030031 (B) in urinary bladders from 2 week post control-treated rats. Data represent mean + s.e.m. of n>6 urinary bladder strips. Statistical significance was tested by one-way ANOVA with post-hoc Bonferonni, * represents $p<0.05$, ** $p<0.01$, *** $p<0.001$ comparing to 0.1 mM AITC in A ,or by Students t-test in B comparing to 3 mM methylglyoxal.

The effects of acute AITC and methylglyoxal ± TRPA1 antagonist HC-030031 on subsequent capsaicin responses

Following exposure to 0.1 mM AITC ± 30 μM HC-030031 or 3 mM methylglyoxal ± 30 μM HC-030031, with no washout, the effects of a concentration range of capsaicin were examined in 2 week post control-treated rat tissue. Firstly it was seen that 30 μM HC-030031 alone had no effect on capsaicin responses. Secondly it was seen that 0.1 mM AITC in the presence of 30 μM HC-030031 continued to cause a mild depression of capsaicin efficacy but had increased capsaicin's potency i.e. a leftward shift was seen (Figure 5.14). 3 mM methylglyoxal caused a depressed capsaicin response and this was not altered by preincubation with 30 μM HC-030031 (Figure 5.14)(Table 5.6)

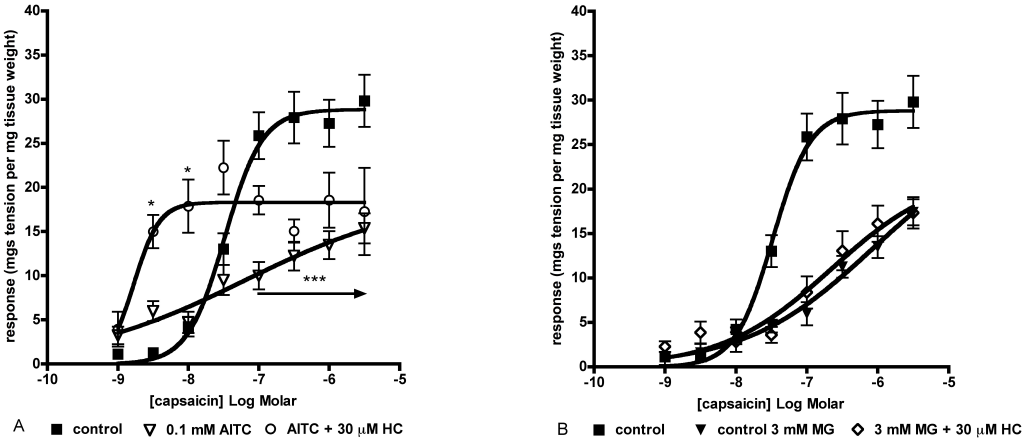

Figure 5.14 Graphs showing contractile responses to a concentration range of capsaicin following 0.1 mM AITC exposure ± 30 μM HC-030031 (A) and following 3 mM methylglyoxal exposure ± 30 μM HC-030031 (B) in 2-weeks post control rat tissue. Data represent mean ± s.e.m. of n >6 urinary bladder strips. Statistical significance was tested by two-way ANOVA with post-hoc Bonferonni, * represents $p<0.05$, ** $p<0.01$, *** $p<0.001$, comparing to control.

Table 5.6 Potency and efficacy estimates for capsaicin responses ± AITC and MG ± HC-030031. Data represent mean ± s.e.m. n>6 urinary bladder strips

	pEC50	Emax
vehicle	7.48 ± 0.07	28.82 ± 1.34
0.1 mM AITC	7.19 ± 0.95^{NS}	19.01 ± 6.22^{NS}
0.1 mM AITC + HC-030031	8.78 ± 0.13^{NS}	18.31 ± 1.17^{NS}
3 mM MG	6.35 ± 0.50*	23.00 ± 5.92^{NS}
3 mM MG + HC-030031	6.66 ± 0.47^{NS}	22.00 ± 5.28^{NS}

Statistical analysis by one-way ANOVA comparing to vehicle NS no significant difference, * $p<0.05$, $^{**}p<0.01$, $^{***}p<0.001$.

Effect of acute methylglyoxal application on repeated electrically-evoked contraction

The acute effects of methylglyoxal on repeated electrically-evoked contraction were studied. A repeated twitch response was instigated using the submaximal voltage, 40 Hz, repeating pulses every minute. Here an initial fade in contractile response was noted which was followed by a reproducible contractile response. A single 3 mM concentration of methylglyoxal was applied to the tissue and incubated for 5 minutes then the repeated electrically-evoked contractions were monitored. Here increased contractile responses were seen (Figure 5.15)

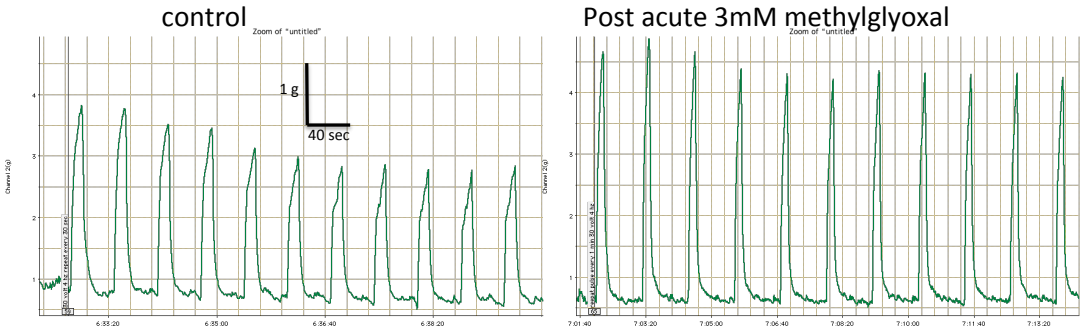

Figure 5.15 Representative trace of raw data for electrically-evoked repeated contractions in control tissue: initial response demonstrates fade followed by reproducible contractions (A), application of 3 mM methylglyoxal induces an increased contraction (B).

Next, repeated electrically-evoked contraction was monitored until sustained contractions were obtained and 3 mM methylglyoxal was then applied. Following methylglyoxal application, the repeated electrically evoked contractions were increased in magnitude and this effect was seen to be maximal by 2 minutes post application. The repeated contractions were bigger in magnitude in the STZ-treated tissue group. However the methylglyoxal induced increases were larger in the control animal tissue, but appeared more variable.

When transformed to percent increase, it could be clearly seen that the methylglyoxal-induced increase was larger in the control group (Figure 5.16)

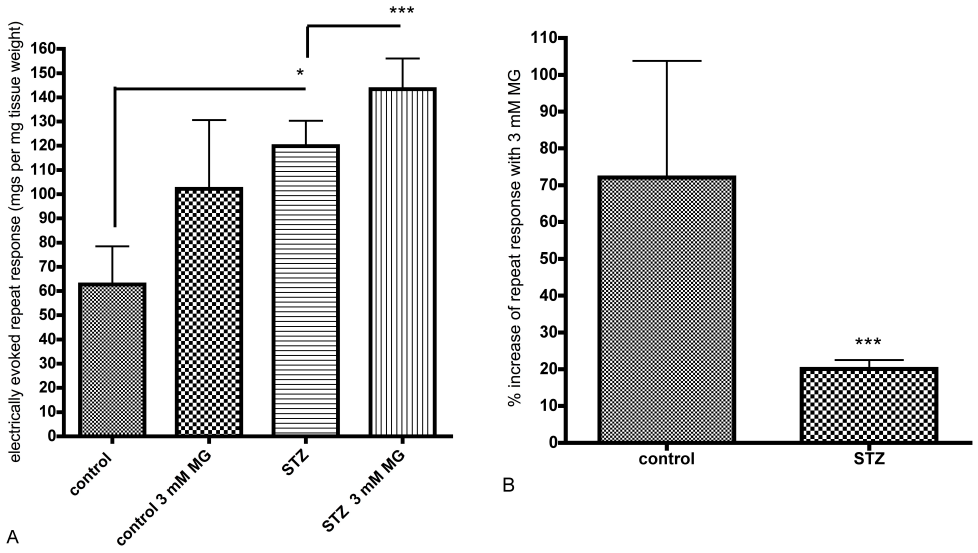

Figure 5.16 Barcharts showing electrically-evoked repeat responses in control and STZ-treated urinary bladder strips before and after 3 mM methylglyoxal application (A) and percent increases induced by 3 mM methylglyoxal (B). Data represent mean ± s.e.m. of n>6 urinary bladder strips. Statistical significance was tested using Students t-test, * represents $p<0.05$, ** $p<0.01$, *** $p<0.001$, comparing to respective control

Direct relaxant effect of methylglyoxal on carbachol pre-contracted urinary bladder

It was seen that a second application of methylglyoxal caused a relaxation from basal tension of the urinary bladder tissue. So this was studied in detail firstly looking at the effect of application of a concentration range of methylglyoxal on carbachol pre-contracted tissue. Following the maximal concentration from the concentration range study of carbachol, tissue was left to reach tonic phase of contraction and then a concentration range of methylglyoxal was applied in a cumulative fashion. A representative trace of raw data is shown (Figure 5.17)

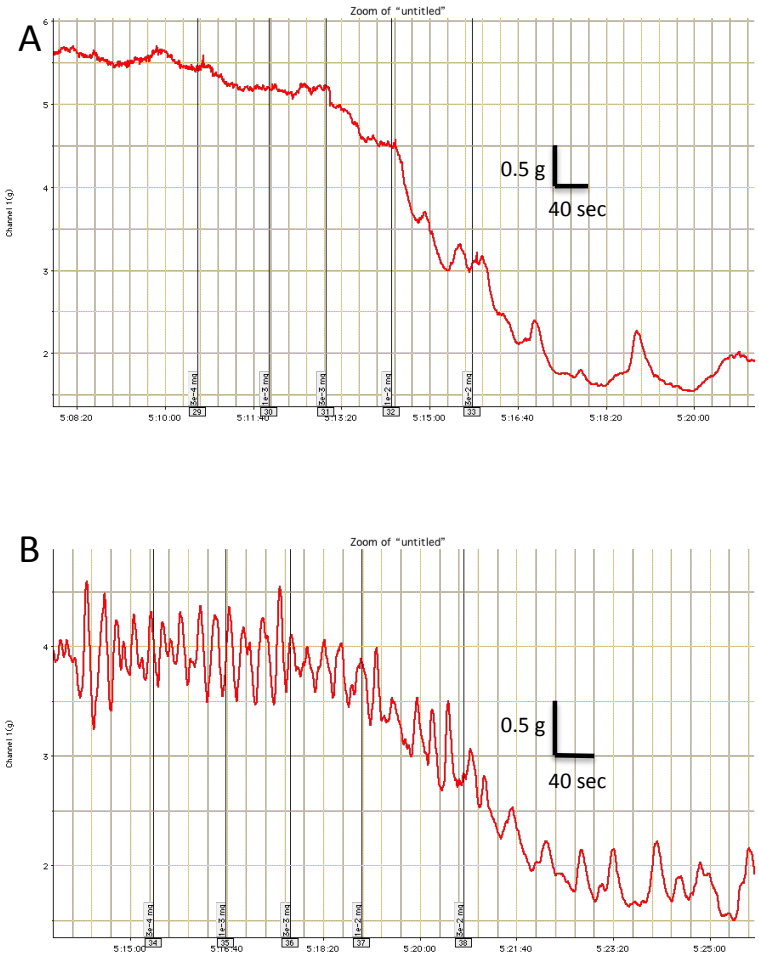

Figure 5.19 Representative trace of raw data responses to carbachol + concentration range of methylglyoxal from 2 weeks post control (A) and STZ-treated (B) urinary bladder.

Responses were normalized to percent relaxation of carbachol contraction and it was seen that relaxant responses to methylglyoxal were concentration related and similar between control and STZ-treated animals (Figure 5.18). Following washout tissues remained viable (data not shown).

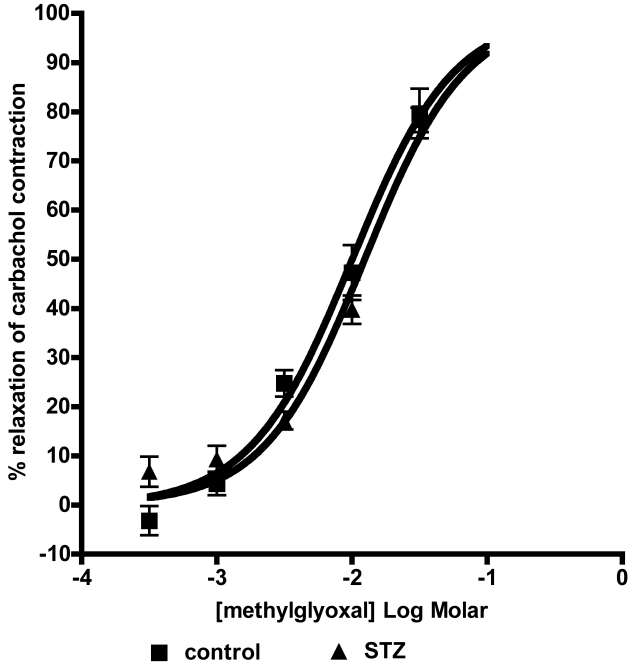

Figure 5.18 Graph showing relaxant response to a concentration range of methylglyoxal in carbachol precontracted 2-weeks post control and STZ-treated rat tissue. Data represent mean ± s.e.m. of n >6 urinary bladder strips. No statistically significant difference was seen between groups when tested by two-way ANOVA.

Next the effect of a TRPA1 selective antagonist on this response was examined on this relaxant effect of methylglyoxal. 10 μM and 30 μM HC030031 did not block the relaxation of carbachol response by methylglyoxal (Figure 5.19)

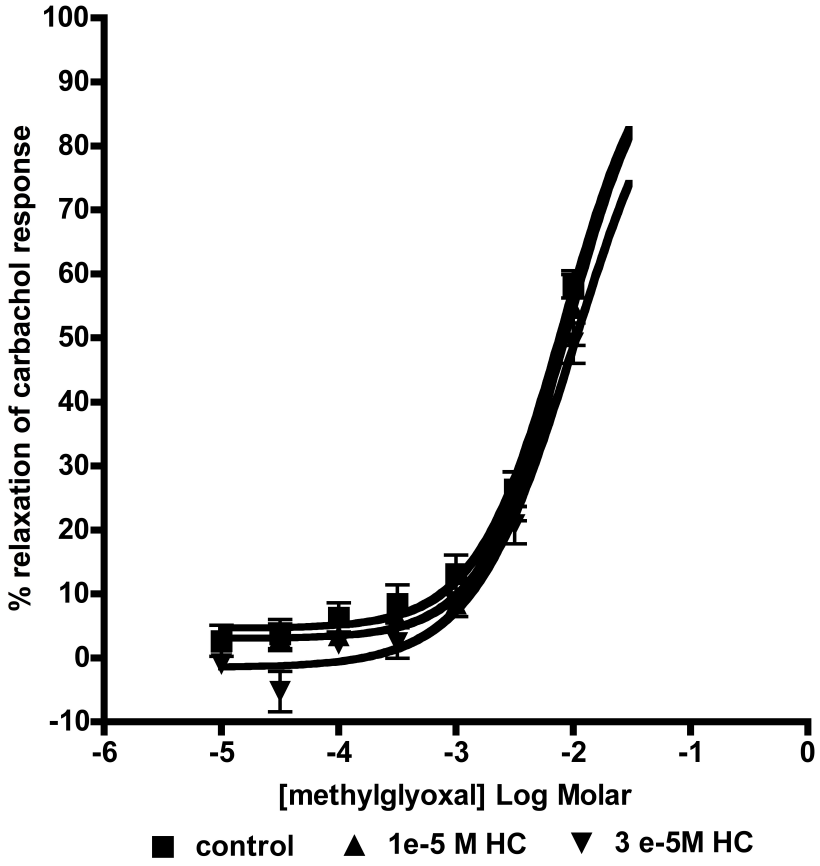

Figure 5.19 Graph showing relaxant response to a concentration range of methylglyoxal ± 10 μM and 30 μM HC030031 in carbachol precontracted 2-weeks post control rat tissue. Data represent mean ± s.e.m. of n >6 urinary bladder strips. No statistically significant difference was seen between groups when tested by two-way ANOVA.

The potential of relaxant responses to a known TRPA1 agonist AITC was next examined, again using carbachol-contracted tissue. Here it was observed that AITC produced a concentration related relaxant response similar to that seen with methylglyoxal (Figure 5.20)

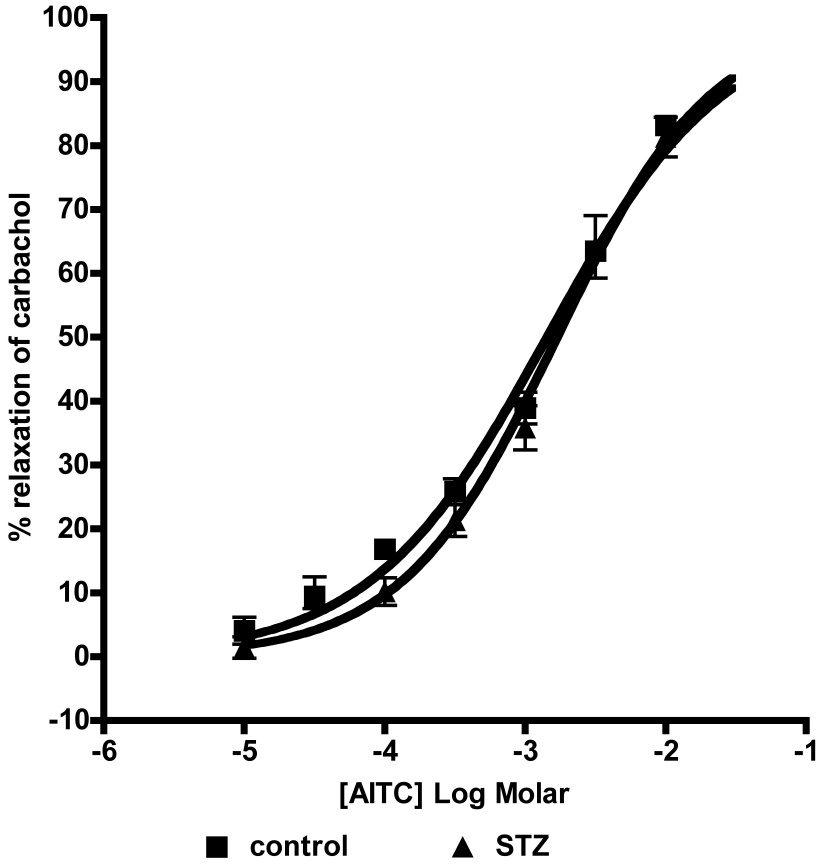

Figure 5.20 Graph showing relaxant response to a concentration range of AITC in carbachol precontracted 2-weeks post control and STZ-treated rat tissue. Data represent mean ± s.e.m. of n >6 urinary bladder strips. No statistically significant difference was seen between groups when tested by two-way ANOVA.

Discussion

To define what role, if any, methylglyoxal plays in sensory neuropathy and the modulation of TRPV1 function during diabetes, these studies were aimed at examining whether an acute exposure to methylglyoxal would affect TRPV1, muscarinic and electrically-evoked responses.

Methylglyoxal causes an immediate direct contractile effect similar in magnitude to the TRPA1 agonist AITC and blocked by a selective TRPA1 antagonist

The first finding was that methylglyoxal application causes an immediate transient contractile response that is concentration-related. AITC was also seen to cause a contractile response but this was a more sustained response, and is believed to be via activation of TRPA1 receptors. The magnitude of responses to methylglyoxal and AITC were very similar; the estimated Emax for methylglyoxal was 33, for AITC 32 mgs tension per mg tissue weight. The use of a TRPA1 selective antagonist HC-030031 at 30 μM, was able to nearly completely block the contractile response seen to AITC and to methylglyoxal suggesting that both compounds were eliciting their contractile activity in this tissue through activation of the TRPA1 receptor. Methylglyoxal responses were seen to be markedly diminished in the tissue from STZ-treated rats. This is suggestive of a down-regulation of TRPA1 function in diabetes. Data was not collected for AITC in STZ-treated tissue, however previous in-house studies have indicated that AITC responses are downregulated by the 2-week timepoint post STZ-administration (Katisart, 2011).

Acute methylglyoxal and AITC caused a diminished TRPV1 response

The next finding was that an acute pre-exposure to methylglyoxal caused a reduced subsequent capsaicin response. The time between methylglyoxal exposure and capsaicin application was long enough to allow the tissue to return

to baseline contractile state. Non-linear regression analysis did provide estimates of efficacy where it appeared that this acute exposure did not affect the efficacy of capsaicin, but had caused a concentration-related reduction in capsaicin potency in both control and in STZ-treated animals. An extension of the concentration range of capsaicin would provide a more definitive answer as to whether efficacy had been reduced; the concentration range used here had been limited to reduce the ethanol load in the system. In the STZ-treated tissue, capsaicin responses were reduced in terms of the efficacy of capsaicin, rather than potency, so although methylglyoxal did reduce capsaicin responses, it was in a different manner to that seen in diabetes. AITC exposure also caused a reduced subsequent response to capsaicin. At the single concentration tested of 0.1 mM, AITC caused a reduced efficacy response to capsaicin with the appearance of a shallow Hillslope (0.35$\pm$ 0.15) that may indicate a multiple affinity component response to capsaicin.

The TRPA1 antagonist was unable to block methylglyoxal effect on TRPV1 responses and revealed a complexity in AITCs effect.

HC-030031 was effective at blocking the direct contractile effect of methylglyoxal on the tissue but was unable to block the diminished responsiveness to capsaicin. This finding is suggestive of an alternate mode of methylglyoxal action in modulation of TRPV1 function and warrants further study. The use of HC-030031 revealed some unexpected results with the AITC/capsaicin combination. Here it appeared that antagonism of TRPA1 together with AITC exposure increased capsaicin potency. This suggests that the interactions between TRPA1 and TRPV1 are complex and multiple mechanisms are likely to be at play. A partial block of TRPA1 activation or compartmental block of TRPA1 may have revealed here a sensitizing role of TRPA1 activation. An alternate explanation is that AITC is acting on additional receptors to TRPA1 such as the P2X /P2Y purinergic receptors (Bartho et al., 2013). A sensitising action of purinergic receptors on TRPV1 has been established in the literature (Wang et al., 2010). So the apparent sensitising activity of AITC on capsaicin response when in the presence of a TRPA1 antagonist HC-030031 could be

explained by a sensitising activity of AITC perhaps via purinoceptor activation, only revealed when the opposing desensitisation via TRPA1 activation is blocked. This could be further explored through the use of purinoceptor antagonists.

High methylglyoxal concentrations caused reduced carbachol responses

Preexposure to methylglyoxal did appear to cause similar effects to carbachol responses as seen with STZ-induced diabetes. The highest concentration of methylglyoxal, 10 mM, caused a reduced efficacy and potency response to carbachol. This however may be indicative of cellular toxicity at this high concentration. In some tissues an abolition of spontaneous contractile activity was noted which might indicate a detrimental effect of the high concentration of methylglyoxal. Carbachol responses following 0.1 mM AITC exposure however appeared to be leftward shifted i.e. increased in potency with no changes in efficacy. The inclusion of the antagonist HC-030031 alone had no effect on carbachol responses and the combination of HC-030031 + AITC gave similar increased potency carbachol responses as seen with AITC alone.

Methylglyoxal potentiated repeated electrically-evoked contractions

Study of repeated electrically evoked contraction with acute exposure to methylglyoxal revealed that methylglyoxal potentiated the electrically-evoked responses. Methylglyoxal has been reported to be a direct $GABA_A$ agonist (Distler et al., 2012) and this might explain the potentiation seen here. This could be examined through the use of HC-030031 and GABA-selective antagonists. Furthermore GABA receptors have been shown to modulate the efferent function of the TRPV1 receptor (Santicioli et al., 1991) which may account for the diminished capsaicin responses seen following methylglyoxal exposure. Comparing the control tissue increases in electrically-evoked contractions with STZ-treated tissue increases, it was seen that methylglyoxal exerts a bigger effect in control tissue. The increase seen could be due to methylglyoxal causing an increased excitability of the membrane. The response to electrical stimuli was

larger in STZ-tissue, therefore one might assume that changes in excitability have already occurred in the diabetic model which would explain the smaller methylglyoxal induced-increases seen in STZ-tissue.

Repeated application of methylglyoxal and AITC caused a relaxant effect not blocked by TRPA1 antagonism

It was noted that a repeat application to methylglyoxal did not cause a second contraction, but it did cause a small relaxation of basal tension. To further explore this, a study of methylglyoxal and AITC was performed on pre-contracted tissue. So a concentration range of methylglyoxal and AITC were applied to carbachol pre-contracted tissue and clear relaxant responses to both compounds were observed. No differences between control and STZ tissue were seen here and no block of the relaxant effect to methylglyoxal was seen using HC-030031. This is suggestive of a common non-TRPA1 mediated effect of AITC and methylglyoxal. Acute methylglyoxal exposure has been shown to activate K_{ATP} channels directly (Yang et al., 2013) and K_{ATP} channel activation in detrusor smooth muscle has been reported to cause relaxation (Gopalakrishnan et al., 1999, Aishima et al., 2006). These channels are also important in maintaining resting membrane potentials so modification by methylglyoxal of the K_{ATP} channel subunits may also lead to changes in membrane excitability.

Methylglyoxal is causing multiple functional alterations which all may play a role in neuropathy

So clearly methylglyoxal is causing alterations in many of the functional parameters tested here in detrusor muscle that may underlie the progression of neuropathy. Methylglyoxal was seen to reduce TRPV1 function, affect muscarinic function and facilitate electrically evoked contractions. Methylglyoxal appeared to be acting in part through activation of the TRPA1 receptor but caused the diminished subsequent TRPV1 function is through an unknown mechanism as the TRPA1 selective antagonist was unable to block this

effect. Methylglyoxal also caused facilitatory changes in other neuronal mechanisms seen through the changes in sensitivity to voltage by electrically-evoked contractions. This facilitation may be through $GABA_A$ agonist activity, K_{ATP} activation or a combination of the two and warrants further study. Methylglyoxal additionally evoked a relaxation of precontracted detrusor muscle, which may be via K_{ATP} activation; this could be further studied using a blocker such as glibenclamide. This relaxant effect may be counterproductive versus detrusor contraction and therefore be important in causing the ineffective bladder emptying seen in diabetics.

Chapter 6

Defining the role that prolonged methylglyoxal exposure may play in TRPV1 modulation

Introduction

In the acute setting, methylglyoxal exposure was seen firstly to induce a diminished subsequent TRPV1 response and secondly to enhance repeated electrically-evoked contractions. Looking at the exposure of methylglyoxal to sensory neurons in the context of diabetes clearly there is a more chronic exposure to this metabolite, and the effects of methylglyoxal may be different in a more chronic paradigm. The diminished TRPV1 responses seen acutely may recover or exacerbate with an increased exposure time and the changes seen in electrically-evoked contractions may also alter. A prolonged exposure setting also allows electrical field stimulation to be studied in more depth, which could provide further insight into how methylglyoxal is affecting neuronal excitability. However the organ bath methodology does have a constraint in how long tissue remains viable and reactive. So working within the constraints of the methodology, a more prolonged four-hour exposure to methylglyoxal was performed to examine the effects of methylglyoxal on subsequent responses to capsaicin, carbachol and electrical field stimulation.

Methods

Effect of prolonged exposure to 3 mM methylglyoxal

3 mM methylglyoxal or vehicle control (water) was applied to equilibrated urinary bladder strips from 2 weeks post control and STZ-treated animals and incubated for 4 hours. Following this time various studies were undertaken to examine the effects of a more chronic exposure to methylglyoxal.

Capsaicin responses were studied using the standard format of application of a concentration range of capsaicin (1×10^{-9}M- 3×10^{-6}M). Carbachol responses were monitored using the standard concentration range ((1×10^{-8}M- 3×10^{-5}M) applied cumulatively. Finally electrical field stimulation was evaluated, firstly by applying a range of voltages (20-90 volts) using 0.1 ms pulse width, rate of 50 Hz, 10 sec duration. Secondly using submaximal voltage, a range of frequencies was next applied (0.25 Hz- 40 Hz). For the 4 Hz dataset, a more in-depth analysis of the data was performed to evaluate the evolution of the electrically-evoked contractile response over time of stimulation. Data points from every 0.5 sec from pre-application of electrical stimulus for a total of 30 seconds were obtained from Labchart and stacked accordingly within excel to allow the generation of a data-rich averaged contractile response plot.

Results

Prolonged incubation of methylglyoxal: effect on capsaicin response

The first studies were to look at the effects of a more chronic 4 hour exposure to 3 mM methylglyoxal on subsequent response to capsaicin in urinary bladder from 2 weeks post control and STZ-treated animals. Control time matched responses gave a less defined, more variable response to capsaicin than seen in acute studies (Figure 6.1). STZ-treated tissue capsaicin responses were significantly diminished when compared to control responses (Figure 6.1) (Table 6.1).

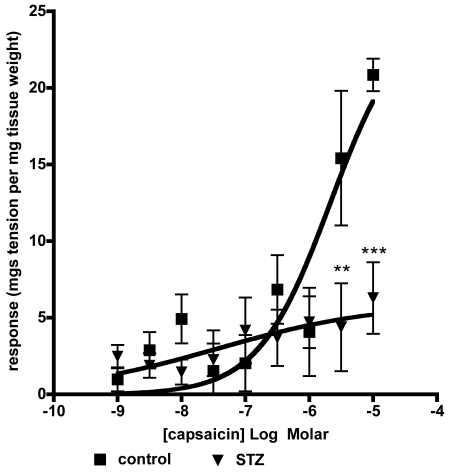

Figure 6.1 Graph showing contractile responses to a concentration range of capsaicin following prolonged incubation (4 hours) in 2-weeks post control and STZ-treated rat tissue. Data represent mean $\pm$ s.e.m. of n >6 urinary bladder strips. Statistical significance was tested by two-way ANOVA with post-hoc Bonferonni, * represents $p<0.05$, ** $p<0.01$, *** $p<0.001$ comparing to control.

Exposure to 3 mM methylglyoxal over 4 hours caused a reduced capsaicin response in control animals and no significant change to the already diminished capsaicin response seen in STZ-treated animal tissue (Figure 6.2) (Table 6.1)

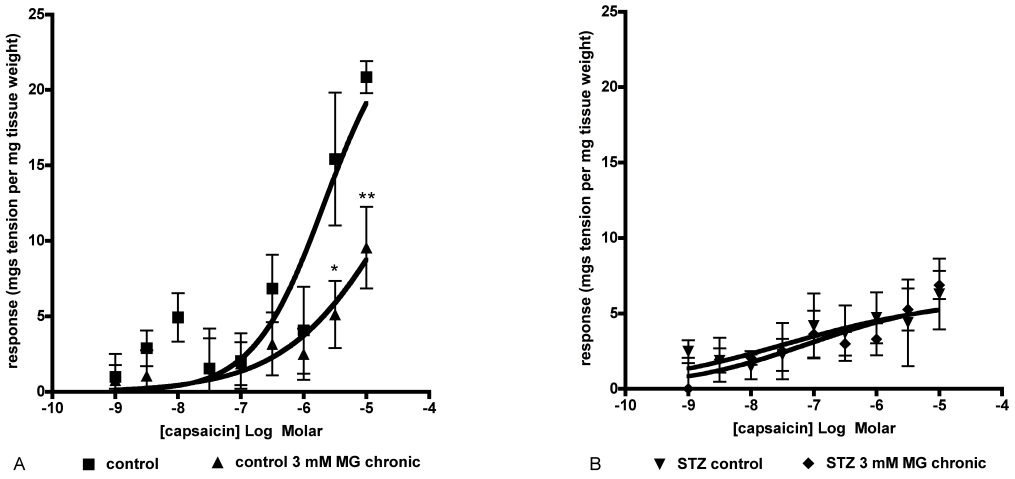

Figure 6.2 Graphs showing contractile responses to a concentration range of capsaicin following prolonged incubation (4 hours) ± 3 mM methylglyoxal in 2-weeks post control (A) and STZ-treated (B) rat tissue. Data represent mean ± s.e.m. of n >6 urinary bladder strips. Statistical significance was tested by two-way ANOVA with post-hoc Bonferonni, * represents $p<0.05$, ** $p<0.01$, *** $p<0.001$ comparing to respective control.

Table 6.1 Potency and efficacy estimates for capsaicin responses ± MG in control and STZ-treated urinary bladder tissue. Data represent mean ± s.e.m. n>6 urinary bladder strips, additional constraint of Hillslope = 1.0 applied.

		pEC50	Emax
control	vehicle	5.65 ± 0.23	25.00 ± 4.64
	3 mM MG	5.51 ± 0.44^{NS}	$11.98 \pm 0.44^{*}$
STZ	vehicle	not determined	$4.85 \pm 0.87^{\$\$}$
	3 mM MG	not determined	4.51 ± 0.70^{NS}

Statistical analysis by Students t-test comparing to control ,NS no significant difference, * $p<0.05$, $^{**}p<0.01$, $^{***}p<0.001$, comparing STZ to control \$\$ $p<0.01$.

Monitoring of carbachol responses following prolonged exposure to methylglyoxal

Following the chronic exposure to methylglyoxal and examination of capsaicin responses, the responses to a concentration range of carbachol were examined. The carbachol responses appeared more robust than capsaicin responses in the prolonged exposure setting. The maximal responses of tissue from STZ-treated rats to carbachol were significantly reduced in comparison to control responses (Figure 6.3). Exposure to 3 mM methylglyoxal over 4 hours caused a slight but non-statistically significant rightward shift in carbachol responses in control animal tissue (Figure 6.4). In tissue from STZ-treated animals, chronic 3 mM methylglyoxal exposure caused a significant enhancement in maximal efficacy of the carbachol response (Figure 6.4) (Table 6.2).

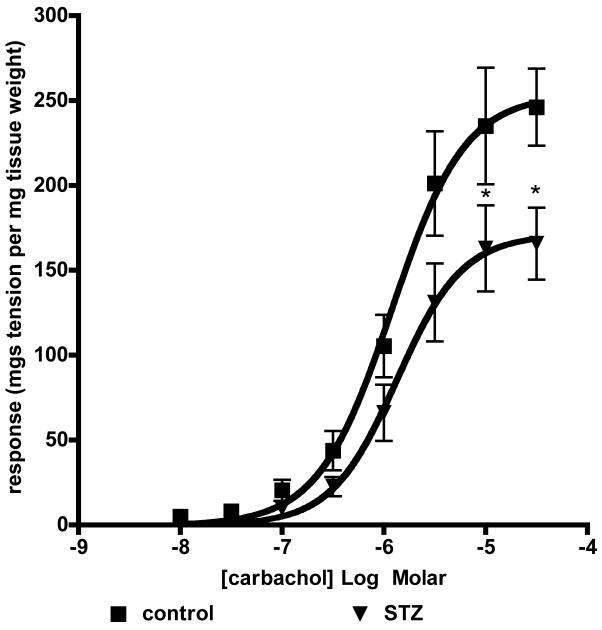

Figure 6.3 Graph showing contractile responses to a concentration range of carbachol following prolonged incubation (4 hours) in 2-weeks post control and STZ-treated rat tissue. Data represent mean ± s.e.m. of n >6 urinary bladder strips. Statistical significance was tested by two-way ANOVA with post-hoc Bonferonni, * represents $p<0.05$, ** $p<0.01$, *** $p<0.001$, comparing to control.

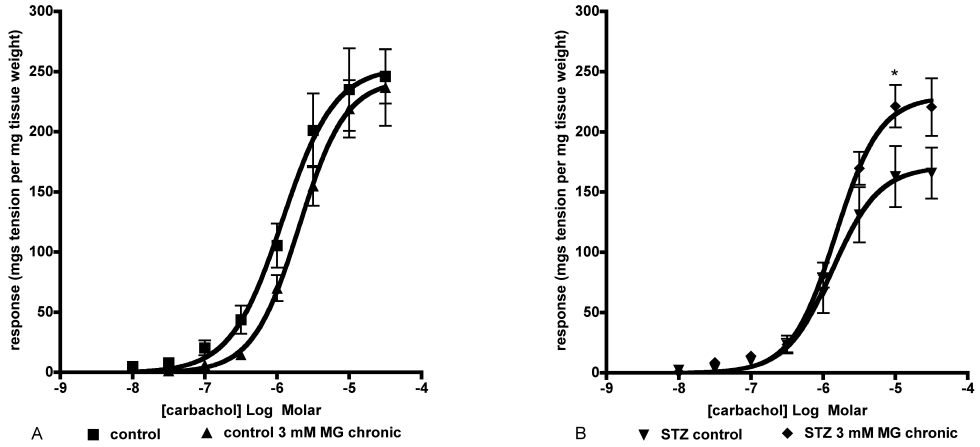

Figure 6.4 Graph showing contractile responses to a concentration range of carbachol following prolonged incubation (4 hours) ± 3 mM methylglyoxal in 2-weeks post control (A) and STZ-treated (B) rat tissue. Data represent mean ± s.e.m. of n >6 urinary bladder strips. Statistical significance was tested by two-way ANOVA with post-hoc Bonferonni, * represents $p<0.05$, ** $p<0.01$, *** $p<0.001$ comparing to respective control.

Table 6.2 Potency and efficacy estimates for carbachol responses ± MG in control and STZ-treated urinary bladder tissue. Data represent mean ± s.e.m. n>6 urinary bladder strips.

		pEC50	Emax
control	vehicle	5.92 ± 0.11	253.60 ± 19.65
	3 mM MG	5.69 ± 0.09^{NS}	243.20 ± 17.33^{NS}
STZ	vehicle	5.87 ± 0.12	$171.00 \pm 14.71^{\$\$}$
	3 mM MG	5.83 ± 0.07^{NS}	$229.30 \pm 11.96^{*}$

Statistical analysis by Students t-test comparing to control ,NS no significant difference, * $p<0.05$, $^{**}p<0.01$, $^{***}p<0.001$, comparing STZ to control \$\$ $p<0.01$.

Electrical field stimulation following chronic exposure to methylglyoxal

A study of electrical field stimulation on control and STZ-treated animal tissue was undertaken to examine neurogenic effects of prolonged exposure to methylglyoxal. First responses to a voltage range at constant 20 Hz were examined. Here following a chronic incubation time of 4 hours, clear differences were seen between tissue from control and STZ-treated animals where STZ-treated tissue was seen to respond at lower voltages so the voltage response curve was leftward shifted and the maximal response was lower than that seen for control tissue. (Figure 6.5). Exposure to 3 mM methylglyoxal caused similar changes in control and STZ-treated animal tissue where in both groups the voltage response curves were leftward shifted (Figure 6.6).

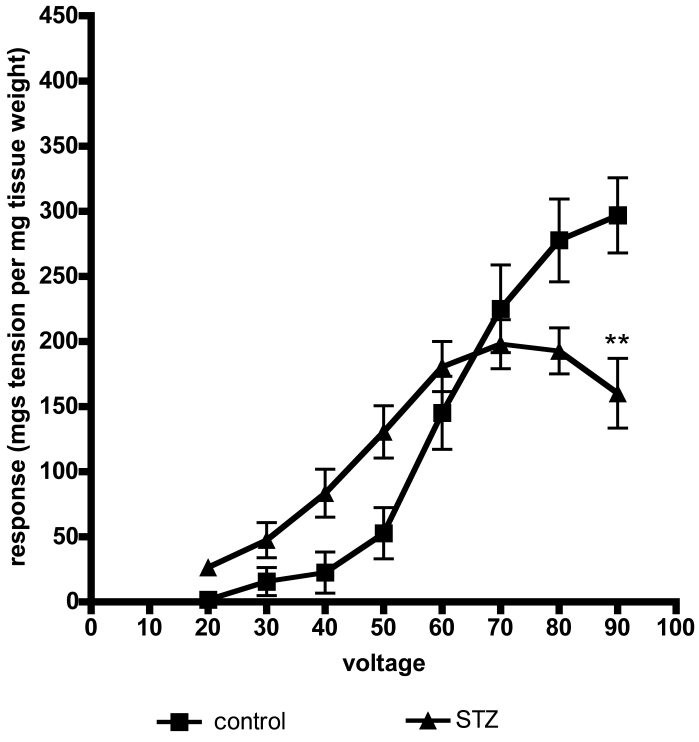

Figure 6.5 Graph showing contractile responses to electrical field stimulation over a range of voltages following prolonged incubation (4 hours) in 2-weeks post control (A) and STZ-treated (B) rat tissue. Data represent mean ± s.e.m. of n >6 urinary bladder strips. Statistical significance was tested by two-way

ANOVA with post-hoc Bonferonni, * represents p<0.05, ** p<0.01, *** p<0.001 comparing to control.

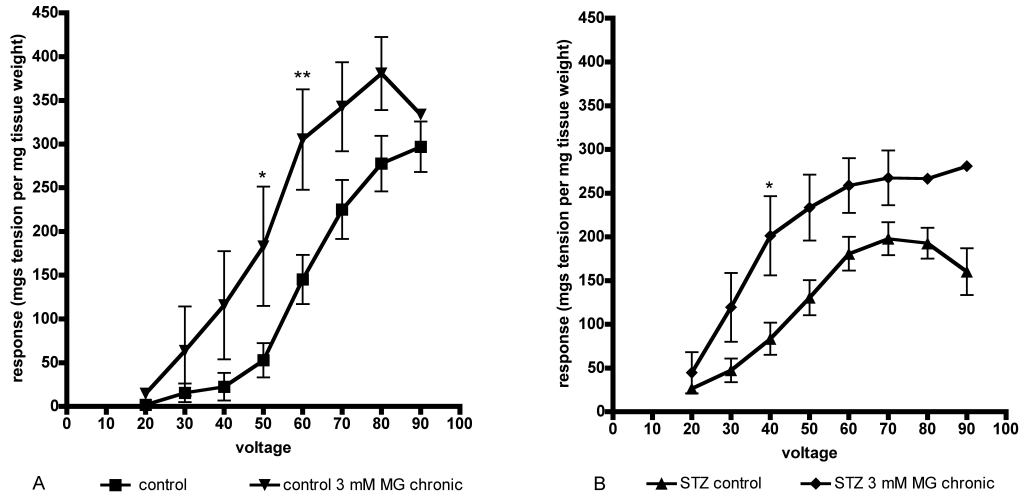

Figure 6.6 Graphs showing contractile responses to electrical field stimulation over a range of voltages following prolonged incubation (4 hours) ± 3 mM methylglyoxal in tissue from 2-weeks post control (A) and STZ-treated (B) rats. Data represent mean ± s.e.m. of n >6 urinary bladder strips. Statistical significance was tested by two-way ANOVA with post-hoc Bonferonni, * represents p<0.05, ** p<0.01, *** p<0.001 comparing to respective control.

Next a frequency response range was studied using maximally effective voltages. Here a comparison of tissue from control and STZ-treated rats showed no difference in responses (Figure 6.7). The prolonged incubation with 3 mM methylglyoxal caused an increase in electrically-evoked contractile responses in tissue from both control and in STZ-treated rats. Greater responses were only seen at the higher frequencies in tissue from control rats whereas in tissue from STZ-treated rats the increased responses were seen over a wider range of frequencies (Figure 6.8)

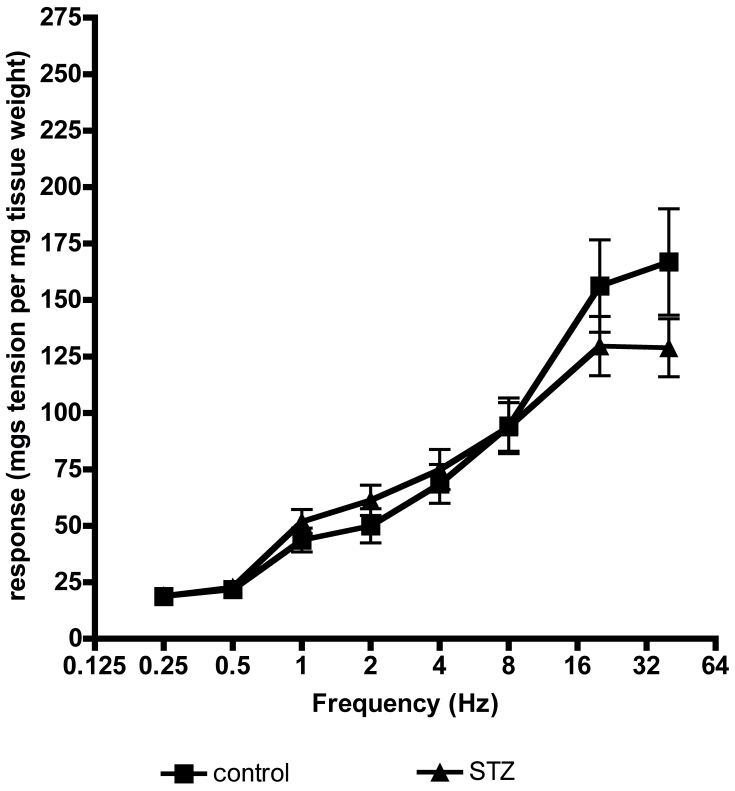

Figure 6.7 Graph showing contractile responses to electrical field stimulation over a range of frequencies following prolonged incubation (4 hours) in tissue from 2-weeks post control (A) and STZ-treated (B) rats. Data represent mean $\pm$ s.e.m. of n >6 urinary bladder strips. No statistically significant differences were seen by two-way ANOVA.

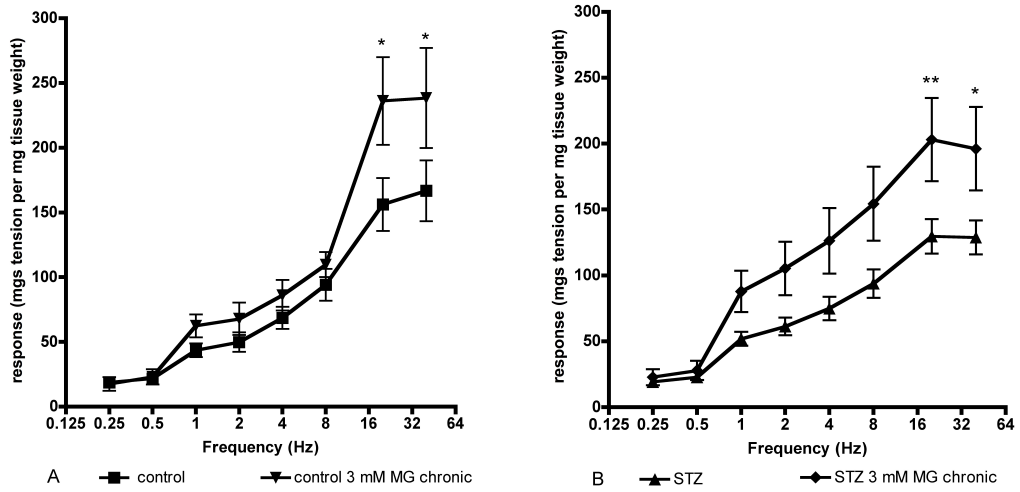

Figure 6.8 Graphs showing contractile responses to electrical field stimulation over a range of frequencies following prolonged incubation (4 hours) ± 3 mM methylglyoxal in tissue from 2-weeks post control (A) and STZ-treated (B) rats. Data represent mean ± s.e.m. of n >6 urinary bladder strips. Statistical significance was tested by two-way ANOVA with post-hoc Bonferonni, * represents $p<0.05$, ** $p<0.01$, *** $p<0.001$ comparing to respective control.

A more in-depth analysis of the data was performed to evaluate the evolution of the electrically-evoked contractile response over time of stimulation. Data points from every 0.5 sec from pre-application of electrical stimulus for a total of 30 seconds were obtained from Labchart and stacked accordingly within excel to allow the generation of a data-rich averaged contractile response plot. Here the 4 Hz data shows differences in contraction between tissue from control and STZ-treated animal groups. Although the magnitude of response is the same, the shape of the contractile event differs subtlety: the STZ response is slower to reach maximum (Figure 6.9).

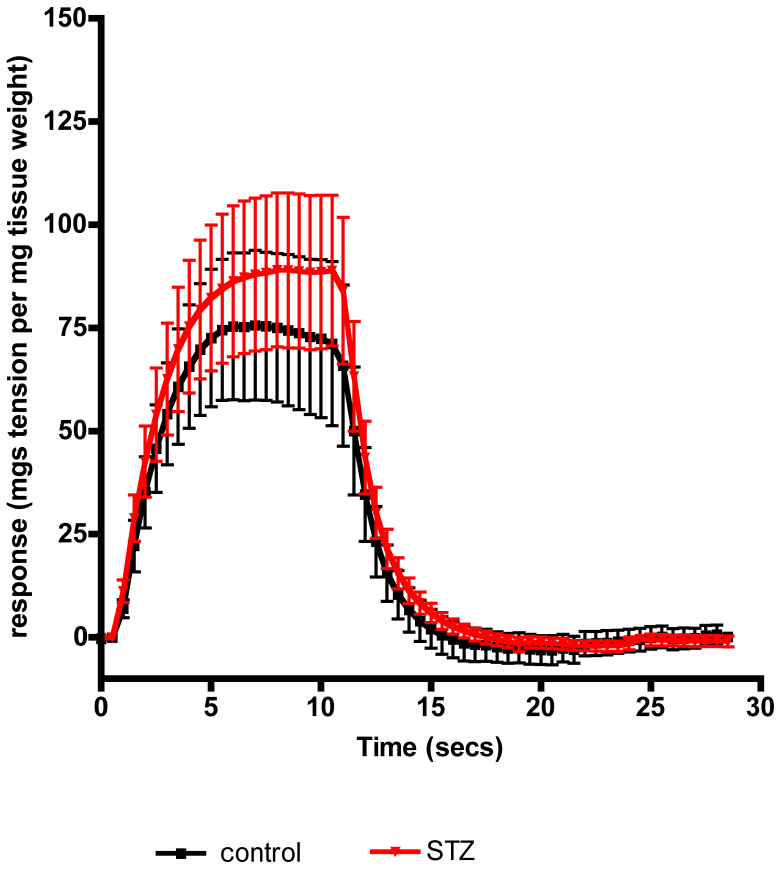

Figure 6.9 Graph showing evolution of 4 Hz electrically-evoked contractile response over time for tissue from control and STZ-treated rats. Data represents mean ± s.e.m. n>6 urinary bladder strips.

Comparison of tissue responses ± chronic exposure to 3 mM methylglyoxal revealed that the methylglyoxal treated control tissue responded to the electrical stimulus to a similar maximum response but took a longer time to reach maximum contraction. Methylglyoxal treated STZ tissue also took a longer time to reach the maximum contraction however the maximum contraction reached was larger in magnitude than untreated STZ tissue (Figure 6.10).

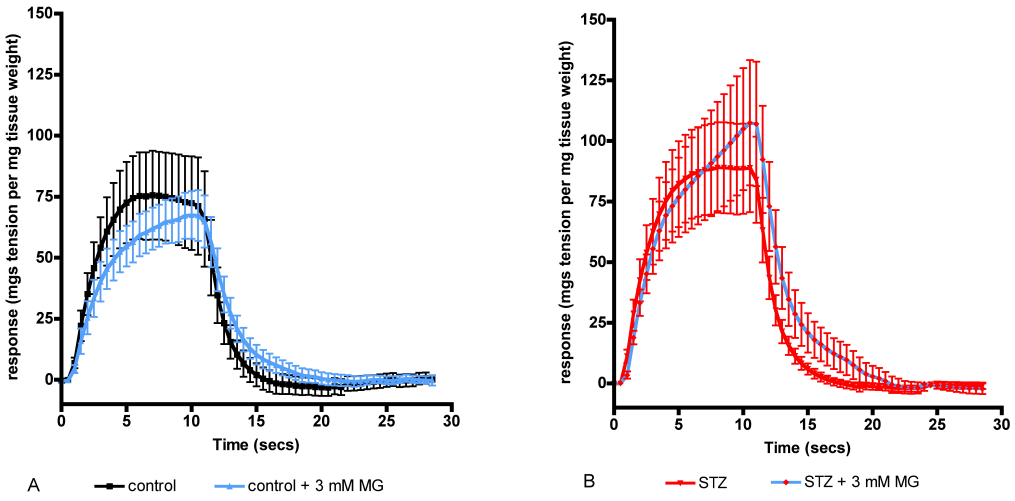

Figure 6.10 Graphs showing evolution of 4 Hz electrically-evoked contractile response over time ± chronic 3 mM methylglyoxal exposure for tissue from control (A) and STZ-treated (B) rats. Data represents mean ± s.e.m. n>6 urinary bladder strips.

These data were analysed to quantify the total contraction using area under the curve (AUC) and time to maximum contraction (Figure 6.11). AUC values were not significantly different between groups, suggesting that the total resultant contractile activity was not altered by methylglyoxal or by STZ-induced diabetes. The time taken to reach maxiumum contraction was seen to be increased in control-methylglyoxal treated and in STZ-induced diabetes, indicative of a kinetic deficit brought about by this metabolite and seen also in the disease.

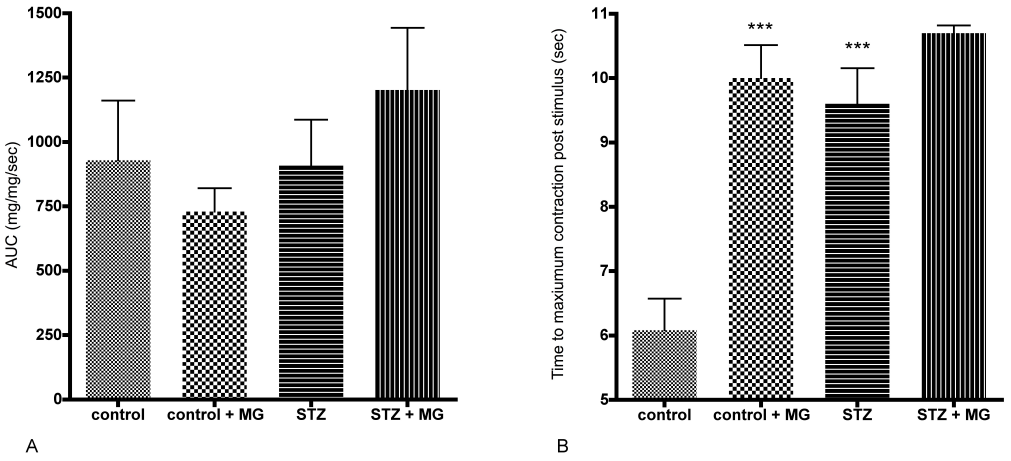

Figure 6.11 Barcharts showing AUC data (A) and time to reach maximum contraction (B) for 4Hz electrically-evoked responses in control and STZ-induced diabetic tissue ± chronic 3 mM methylglyoxal. Data represents mean ± s.e.m. n>6 urinary bladder strips. Statistical significance was tested by one-way ANOVA with post-hoc Bonferonni, ***represents $p<0.001$ comparing to respective control.

Examination of the raw data trace responses to the 20 Hz electrical stimulation, revealed a more similar shaped contractile response over time between the tissue from control and STZ-treated animal groups. The effect of chronic methylglyoxal treatment was to increase the time taken to reach maximum response in both control and STZ-treated animal tissue (Figure 6.12)

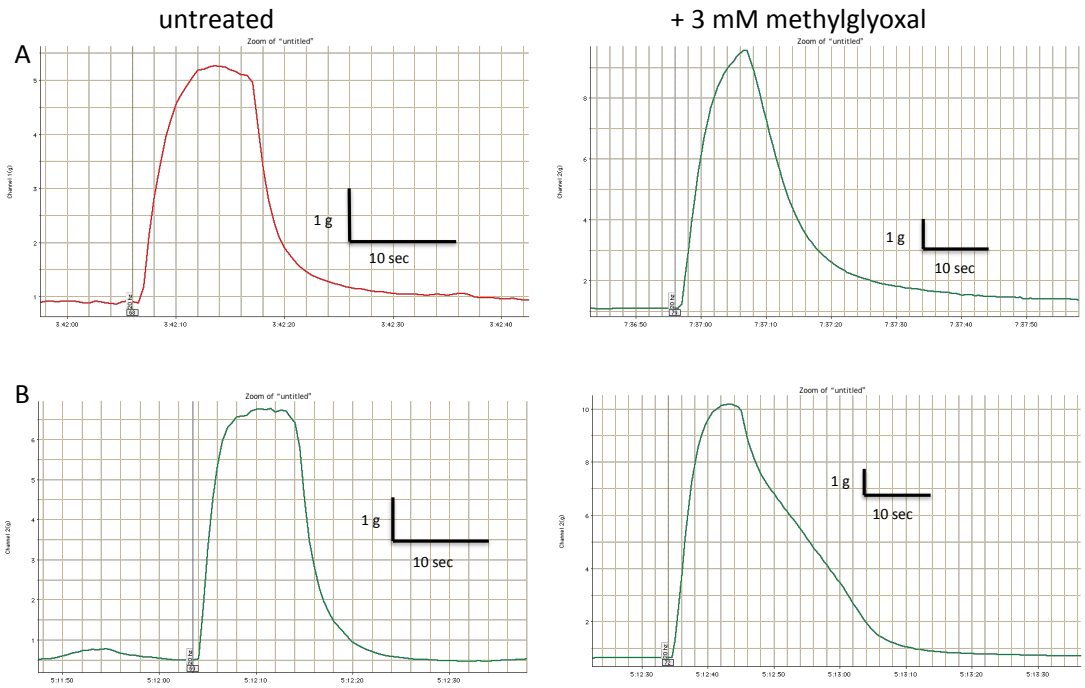

Figure 6.12 Representative raw data traces of 20 Hz electrically evoked contraction in tissue from control (A) and STZ-treated (B) animal groups ± chronic exposure to 3 mM methylglyoxal.

Discussion

Methyglyoxal caused diminished capsaicin responses in tissue from control but responses in general were reduced due to prolonged incubation time

When a more prolonged exposure studies were performed, the first finding was that capsaicin responses in both control and STZ-tissues were diminished, in the control non-methylglyoxal exposed group. This is most likely due to deterioration in the sensory neuron population within the tissue over time. Responses to capsaicin were still present however and it could still be seen that STZ responses were diminished compared to control. 3 mM methylglyoxal caused a reduced efficacy response to capsaicin in control tissue, but responses in STZ-tissue were already virtually nonexistent so no changes could be seen.

Methylglyoxal caused increased efficacy in STZ-carbachol responses

Monitoring of carbachol responses over this longer incubation period revealed that the carbachol response was more robust than the capsaicin response. In controls, methylglyoxal exposure caused a small non-significant rightward shift in carbachol potency with no effect on efficacy. However in the STZ-group, methylglyoxal caused a significant enhancement of carbachol response in terms of efficacy. Perhaps delivery of methylglyoxal to this tissue increased lactate levels through methylglyoxal breakdown, specifically the d-Lactate isoform. Lactate levels have been shown be lower in STZ-induced diabetic smooth muscle (Waring and Wendt, 2000) and it is unknown whether a minor boost in or exposure to d- lactate or another product of methylglyoxal breakdown could result in increased maximal contractile ability. A study of lactate effects in vascular smooth muscle has demonstrated increased KCL induced contractions in the presence of lactate containing buffer (Barron et al., 1997).

Prolonged exposure to methylglyoxal increased the voltage sensitivity in tissue from both control and STZ-treated rats

Finally an examination of electrical field stimulation was undertaken. Here it was seen that in the STZ-group a reduced maximal response to a voltage range was seen, together with a leftward shift in the voltage-response curve i.e. an increased sensitivity to lower voltages. This could be explained by an increased excitability of the cells caused by membrane changes in diabetes. Prolonged exposure to methylglyoxal increased voltage sensitivity in both control and STZ-tissue suggestive of a methylglyoxal-driven alteration in membrane excitability. Methylglyoxal has been reported to modify the NaV1.8 receptor causing an increase in excitability and facilitated firing (Bierhaus et al., 2012) . As the STZ-tissue still displayed increased voltage sensitivity following methylglyoxal, it appears at this early stage of diabetes that the voltage sensitivity increases seen due to the diabetic state are not maximal.

Methylglyoxal caused increased responses to a frequency range of electrically-evoked contractions

No differences between control and STZ tissue were seen using maximal voltages and examining a range of frequencies. However following methylglyoxal exposure, increased responses to the higher frequencies were observed in the control group and to frequencies > 1 Hz in the STZ-group. To try and understand where these differences were occurring a more in-depth analysis of the data was performed. It appeared that the profile of contractile response over time at the 4 Hz level of stimulation was altered following methylglyoxal exposure. In the control methylglyoxal exposed tissue, the electrically-evoked contraction was of the same magnitude as seen in tissue with no methylglyoxal exposure but took longer to reach the maximal contraction. This is suggestive of changes to the slower neurotransmitter release pathways such as the cholinergic system. In STZ tissue, methylglyoxal exposure again caused changes in the profile of contraction: here a higher maximal contraction was obtained and again the

source of this change appeared to be at the slower neurotransmitter responses. At higher frequencies this change in contraction profile persisted.

Chapter 7 Can the diminished TRPV1 response be recovered?

Introduction

Diabetes causes a rapid downregulation of TRPV1 function in the bladder and the final series of studies were to explore the potential of reversing this diminished response. Previous in-house data had shown this was possible with the use of bradykinin (Katisart, 2011). So using this as a starting point I sought to repeat and extend these findings. In addition to this examination of bradykinin, I also chose to explore the potential of other known sensitisers of TRPV1; nerve growth factor (NGF) and insulin.

The TRPV1 receptor can be modulated through dynamic sensitization and desensitisation processes which provide a rapid dial up or dial down control over its physiological function. There are two main ways in which TRPV1 receptor function can be upregulated: firstly through increasing the sensitivity or functionality of the surface expressed receptors and secondly through an increase in surface (plasma membrane) expression of TRPV1 channels.

Phosphorylation of key sites on the TRPV1 receptor may control both processes and site specific mutation studies where small portions of the receptor are modified have allowed identification of the parts of the receptor that are key to this (7.1)(Li et al., Zhang et al., 2005a)

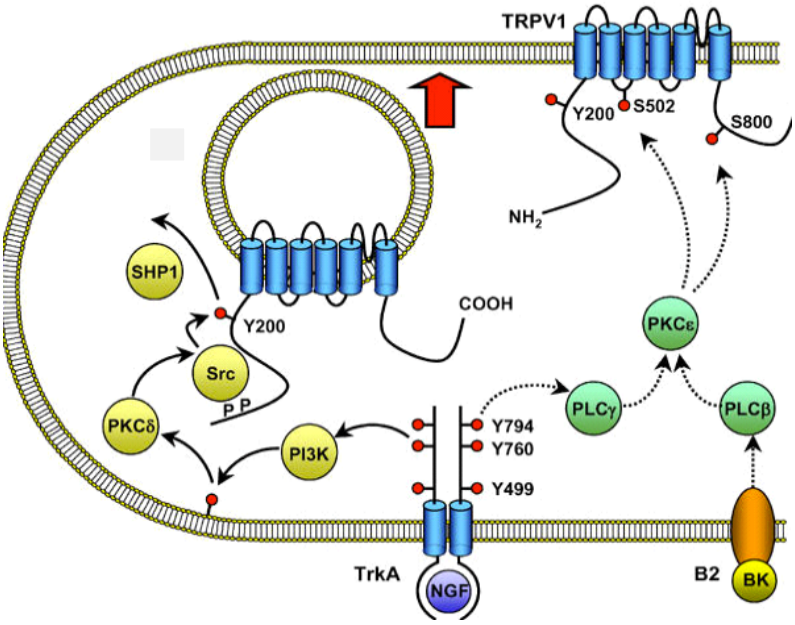

Figure 7.2. Schematic diagram of the signaling pathways important in sensitization of TRPV1 by TrkA. The functionally most significant pathway is shown at the left (yellow, solid arrows). A smaller component of sensitization following exposure to NGF is mediated by phosphorylation of TRPV1 at residues S502 and S801, probably by the PLCγ/PKC pathway (green, dashed arrows). PKC is a crucial intermediate in sensitization of TRPV1 by bradykinin (pathway shown at the lower right of the diagram). From Zhang et al 2005

TRPV1 receptor functionality can be altered by directly increasing the open channel probability as these ion channels exist in different states i.e. closed inactivated, closed and open. TRPV1 receptor state may rely on the presence of intact membrane lipid rafts and has been found to be altered by the manipulation of the raft constituent components such as cholesterol, the phospholipid phosphatidylinositol-4,5-bisphosphate (PIP_2) and ceramide (Liu et al, 2006; Zhang et al, 2004). NGF-mediated sensitization of the excitability of rat sensory neurons is prevented by a blocking antibody to the p75 neurotrophin receptor (Prescott et al., 2003). Phosphorylation of TRPV1 by PIP_2 holds TRPV1 under an inhibited state and sensitization of TRPV1 can be gained by PIP_2 hydrolysis through receptor mediated activation of protein kinase C, A, or

phospholipase A (Prescott et al., 2003). The receptors that can activate protein kinase C/A or phospholipase A include bradykinin, prostaglandin E2 (PGE2), 5HT and nerve growth factor (NGF). Furthermore, reinstatement of active TRPV1 requires PIP_2 phosphorylation and maintenance of active TRPV1 may depend on a continual basal phosphorylation by the PKC isoform, PKC-epsilon (Srinivasan et al., 2008). Cyclin-dependent kinase 5 (Cdk5) can also directly phosphorylate TRPV1 and modulate its function: Cdk5 inhibition has been shown to reduce TRPV1 function (Pareek et al., 2007).

Factors that induce translocation of TRPV1 receptors to the plasma membrane include insulin, insulin growth factor and NGF. Deficiencies in or overexpression of these factors could either impair or sensitise TRPV1 function (Van Buren et al, 2005).
Many of these enzymes, lipids, growth factors and mediators are altered during diabetes:

Bradykinin

Bradykinin is an endogenously produced pro-inflammatory peptide, produced by plasma and tissue kallikrien-kinin systems (Campbell, 2001). Bradykinin acts through two G-protein coupled receptors, bradykinin-1 (BK1) and bradykinin-2 (BK2), and is more selective for BK2 receptors. There may be a third bradykinin receptor, bradykinin-3, proposed on the basis of discrepant ligand affinity, but this has not yet been cloned (Hall, 1997). The BK1 receptor expression is generally low under normal physiological conditions, but is upregulated under stress conditions or after exposure to noxious stimuli such as the cytokines interleukin 1- β or tumor necrosis factor-α (Marceau et al., 1998, Galizzi et al., 1994, Phagoo et al., 2000) and is upregulated in diabetes (Gabra and Sirois, 2003). The BK2 receptors have a constitutively higher level of expression in many tissues and can also be upregulated by cytokine exposure (Schmidlin et al., 1998, Haddad et al., 2000). Bradykinin is a potent mediator of inflammation and causes pain, vasodilation, increased vascular permeability, epithelial fluid secretion and smooth muscle contraction (Bellucci et al., 2007). Bradykinin also

plays an important role in fluid regulation and electrolyte balance. In fibroblasts, bradykinin treatment causes rapid increases in ceramide and sphingosine levels, which are second messanger molecules able to mediate the action of extracellular signals such as cytokines and growth factors (Meacci et al., 1996). Both BK-1 and BK-2 have been shown to contract detrusor smooth muscle in a number of species (Maggi, 1997) and the contraction is believed to be caused through prostaglandin formation (Nakahata et al., 1987)
Selective agonists for BK1 and BK2 are [Lys-des-Arg^{9}]-bradykinin and [Phe^{8}-Y(CH-NH)-Arg^{9}]-bradykinin respectively. The latter peptide is resistant to carboxypeptidase cleavage and exhibits a 5-fold greater potency and a more prolonged duration of action than bradykinin *in vivo* (Drapeau et al., 1988). It is believed that pharmacological block of both receptors may be beneficial in hyperalgesia as bradykinin acts on either receptor to promote hyperalgesia (Levy and Zochodne, 2000). In diabetic models, a BK-1 agonist has been seen to promote thermal hyperalgesia and BK-1 antagonists inhibit this (Gabra and Sirois, 2003). Renal excretion of bradykinin has been seen to be increased by 12 weeks post STZ-induced diabetes (Tschöpe et al., 1996).

Nerve Growth factor (NGF)

Tissues produce neurotrophic factors such as NGF and through retrograde transport along the axon to the dorsal root ganglion for example, maintain the structure and function of the neurons that innervate them (Sofroniew et al., 2001). NGF was originally found to be a survival factor during development for sensory and sympathetic neurons and plays a major a role in pain and hyperalgesia (Hefti et al., 2006). NGF exerts its actions through an interaction with the low-affinity p75 receptor and with Trk, a receptor tyrosine kinase encoded by the *trk* proto-oncogene (Meakin and Shooter, 1992). Disruption of the Trk/NGF receptor system in genetically engineered mice leads to severe sensory neuropathies, highlighting the role NGF plays in the development of an intact and functional sensory system (Smeyne et al., 1994) NGF has been seen to cause an increase in membrane expression of the TRPV1 receptor in cell lines and primary neuronal preparations (Zhang et al., 2005b, Simonetti et al., 2006).

In diabetes it has been hypothesized that the disease impacts on NGF production and/or transport which in turn could deprive neurons of this neurotrophin and thereby be causative to diabetic neuropathy (Hellweg and Hartung, 1990). However increases in bladder NGF followed by increases in DRG NGF levels have been observed acutely in the STZ-diabetic rat model (Steinbacher and Nadelhaft, 1998) . Other studies suggest a later decrease in bladder NGF, and this correlated with their measurement of cystopathy (Sasaki et al., 2002)

Insulin and Insulin like growth factor (IGF)

In the STZ-diabetic model, insulin levels are very low due to the destruction of the pancreatic β-cells. Insulin acts to cause the uptake of glucose and amino acids, but this does not occur in peripheral nerves (Patel et al., 1994). Here , insulin acts together with NGF as neurotrophic factors (Recio-Pinto et al., 1986). There is also evidence that insulin and IGFs activity overlaps with that of NGF as they have been seen to share common signaling pathways (Recio-Pinto et al., 1986). Some evidence also exists that insulin potentiates capsaicin's activity on TRPV1 and directly activates TRPV1, providing an explanation for the burning pain that is associated with hyperinsulinism (Sathianathan et al., 2003)

Methods

Control age-matched and STZ-diabetic rats were setup and monitored as previously described. Urinary bladder tissue was dissected and setup as previously described. STZ-diabetic animal tissues were only included if the blood glucose was >3 fold higher than control blood glucose levels.

Experimental design

Bradykinin

For the investigation of bradykinin effects, firstly a cumulative concentration-response range to bradykinin was examined in urinary bladder strips from control age-matched animals and STZ-induced diabetic animals. Following maximal contraction to bradykinin, tissues were left for 10 minutes (no washout), which allowed tensions to return to baseline, and then a cumulative capsaicin concentration range was applied. Carbachol response curves were also examined for any effects of pretreatment with bradykinin. Bradykinin effects were examined in the acute timecourse studies following STZ-induction of diabetes to pinpoint when bradykinin effects were optimal. Then an exploration of the bradykinin receptor subtype was examined through the use of selective agonists for BK-1 receptor ([Lys-des-Arg9]-BK) and BK-2 receptor ([Phe8-y(Ch-NH)-Arg9]-BK). Again cumulative concentration response curves were constructed for these agonists: following maximal contraction with no washout the tissues were left for 10 minutes after which time a capsaicin concentration range was applied. Further to these studies a combination study was performed using both selective agonists (1 μM ([Lys-des-Arg9]-BK + 1 μM [Phe8-y(Ch-NH)-Arg9]-BK) . Finally a study where the effects of bradykinin were studied on capsaicin response $\pm$ 10 μM indomethacin, an inhibitor of endogenous prostaglandin formation, was completed with the inclusion of an ETOH vehicle control.

NGF

The effects of 20 minute preincubation of 100 and 300 ng/ml of nerve growth factor with no wash out, were investigated on subsequent cumulative concentration range of capsaicin.

Insulin

The effects of a 20 minute preincubation with 1 μM insulin, with no washout, was examined on a cumulatively applied concentration range of capsaicin responses.

Monitoring of effects on carbachol

A cumulative concentration range of carbachol was applied before and after the various treatments to monitor possible effects on muscarinic function.

Results

The effects of bradykinin

First the direct contractile reponses to a cumulative concentration range of bradykinin were examined in urinary bladder tissue from 2 days, 2 weeks and 4 weeks post control or STZ treatment. Bradykinin was seen to directly cause a concentration-related contraction of urinary bladder strips, in control age-matched and STZ-induced diabetic animals, a representative trace from each is shown (Figure 7.2)

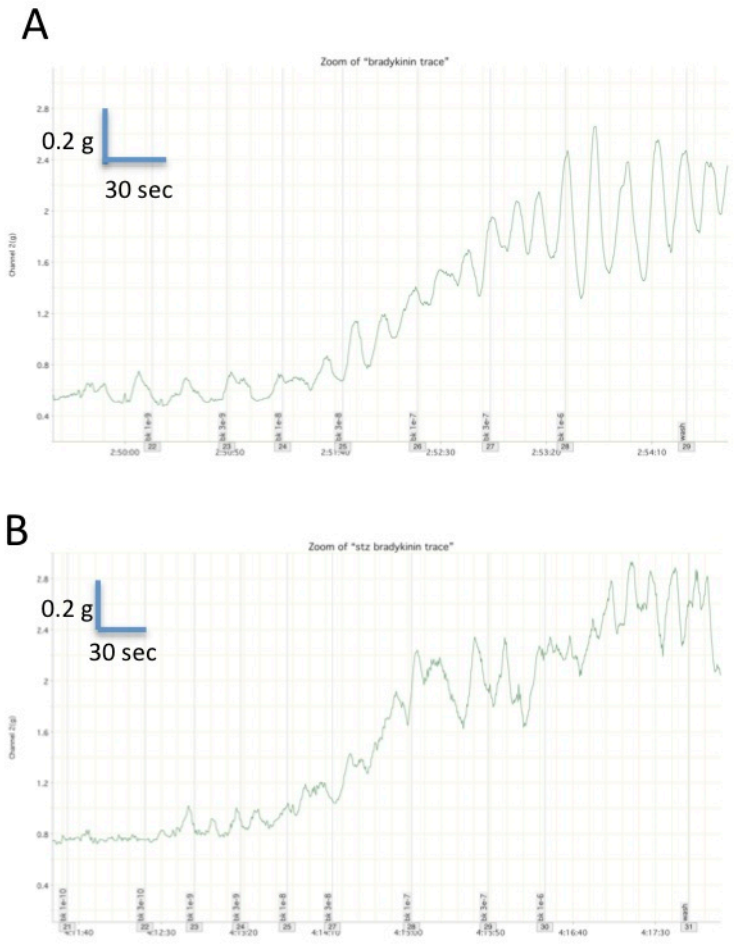

Figure 7.2 Representative raw data traces of the effect of bradykinin on urinary bladder strips from an age-matched control animal (A) and a STZ-induced diabetic animal (B)

The contractile responses to bradykinin remained consistent in control animal tissue at all timepoints studied. Bradykinin responses were enhanced in the 2 days post-STZ group, with responses returning to control levels at 2 weeks and 4-weeks post STZ-administration (Figure 7.3)(Table 7.1).

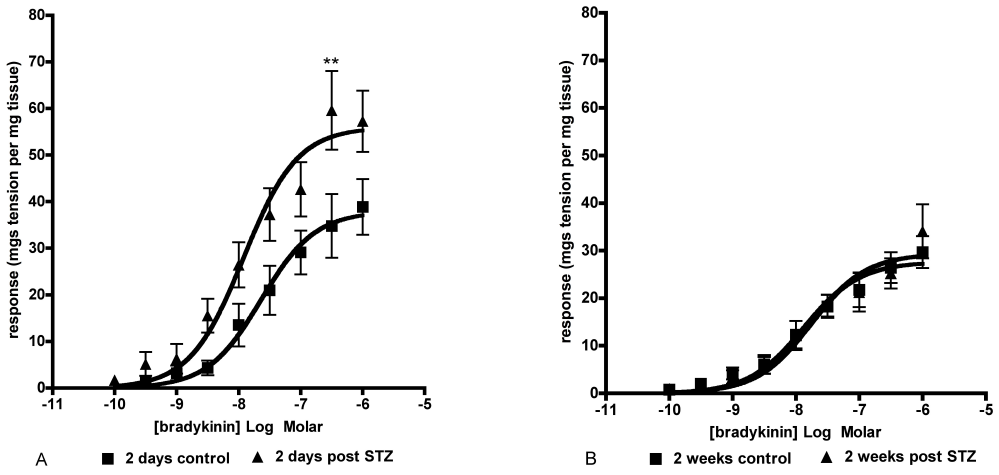

Figure 7.3 Graphs showing direct contractile effect of bradykinin in urinary bladder strips from control and STZ-treated animals at 2 days (A) and 2 weeks (B) post-treatment. Data represent mean + s.e.m. n>6 urinary bladder strips. Statistical significance was tested by two-way ANOVA with post-hoc Bonferonni, * represents $p<0.05$, ** $p<0.01$, *** $p<0.001$ comparing to respective control.

Table 7.1 Direct contractile effects of bradykinin: potency and efficacy in urinary bladder strips from control and STZ-treated rats. Data represent mean $\pm$ s.e.m. of n>6 urinary bladder strips.

Time after treatment	pEC50		Emax	
	control	STZ	control	STZ
2 days	7.64 ± 0.16	7.92 ± 0.13^{NS}	37.93 ± 3.11	55.98 ± 3.39***
2 weeks	7.87 ± 0.13	7.76 ± 0.15^{NS}	27.62 ± 1.67	29.38 ± 2.15^{NS}
4 weeks	8.05 ± 0.17	8.09 ± 0.19^{NS}	24.45 ± 2.03	16.59 ± 1.40*

Statistical analysis by two-way ANOVA comparing to time-matched control, NS non-significant, *p<0.05, **p<0.01, ***p<0.001.

Effects of bradykinin on subsequent responses to capsaicin

Following maximal bradykinin application and a 10-minute equilibration period with no wash-out, responses to a cumulative concentration curve of capsaicin were examined at 2 days and 2 weeks post control or STZ-administration. At the 2 days post treatment group, where no diminishment of capsaicin response was seen between control and STZ-treated rats, no effect of exposure to 1 μM bradykinin for 10 minutes was seen (Figure 7.4).

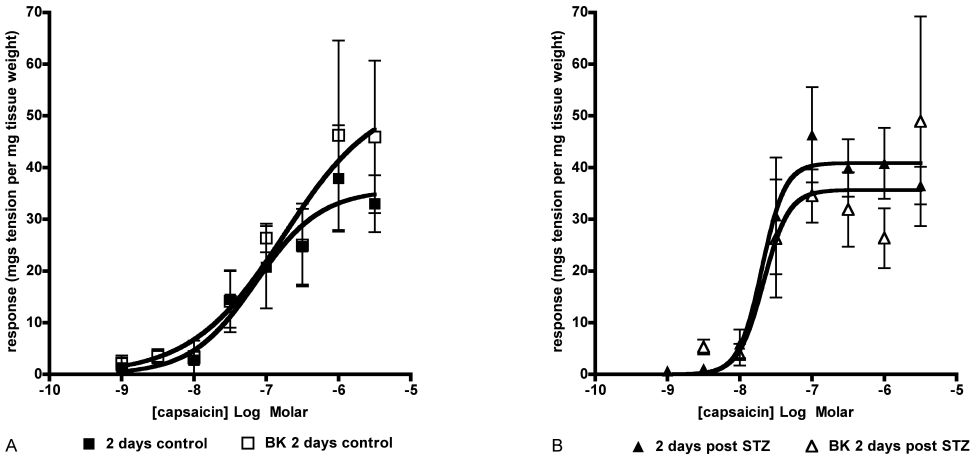

Figure 7.4 Graphs showing responses to capsaicin post-bradykinin exposure in urinary bladder from 2 day post control (A) and STZ-treated rats (B). Data

represent mean ± s.e.m. of >n of 6 urinary bladder strips. No statistical significance was seen by two-way ANOVA.

At the 2 weeks post treatment timepoint, where a clear diminished capsaicin response was seen, no effect of bradykinin pre-exposure was noted in control animal tissue, but a significant enhancement of capsaicin responses back to control values in STZ-treated animal tissue was observed (Figure 7.5).

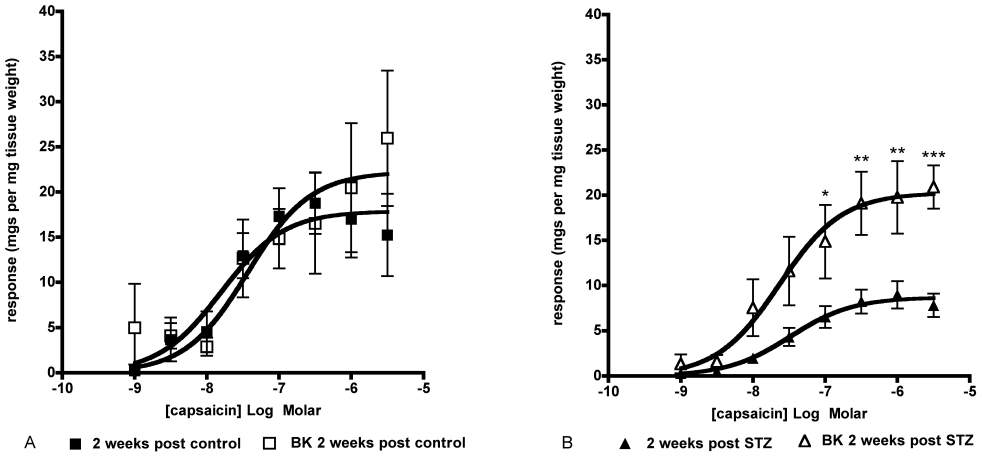

Figure 7.5 Graphs showing responses to capsaicin post-bradykinin exposure in urinary bladder from 2 weeks post control (A) and STZ-treated rats (B). Data represent mean ± s.e.m. of >n of 6 urinary bladder strips. Statistical significance was tested by 2-way ANOVA with post-hoc Bonferonni, * represents $p<0.05$, ** $p<0.01$, *** $p<0.001$ comparing to respective control.

Direct contractile effects of bradykinin receptor subtype selective agonists

Next the direct contractile effects of the BK-1 selective agonist, [Lys-des-Arg9]-BK, and the BK-2 selective agonist, [Phe8-y(Ch-NH)-Arg9]-BK were examined in urinary bladder strips from 2 weeks post control or STZ-treated rats. The BK-1 selective agonist [Lys-des-Arg9]-BK, caused a concentration-related contraction of similar potency in control and in STZ-treated rat tissue (Figure 7.6). There was a significant difference in the magnitude of response, where the STZ-treated

animal tissue had a lower maximum response to this BK-1 selective agonist. The BK-2 selective agonist , [Phe8-y(Ch-NH)-Arg9]-BK also caused a concentration related contractile response, which in control animal tissue was of greater magnitude than seen for BK-1 selctive agonist. The BK-2 selective agonist gave a significantly different profile in STZ-treated animal tissue where a much reduced response was seen (Figure 7.6) (Table 7.2).

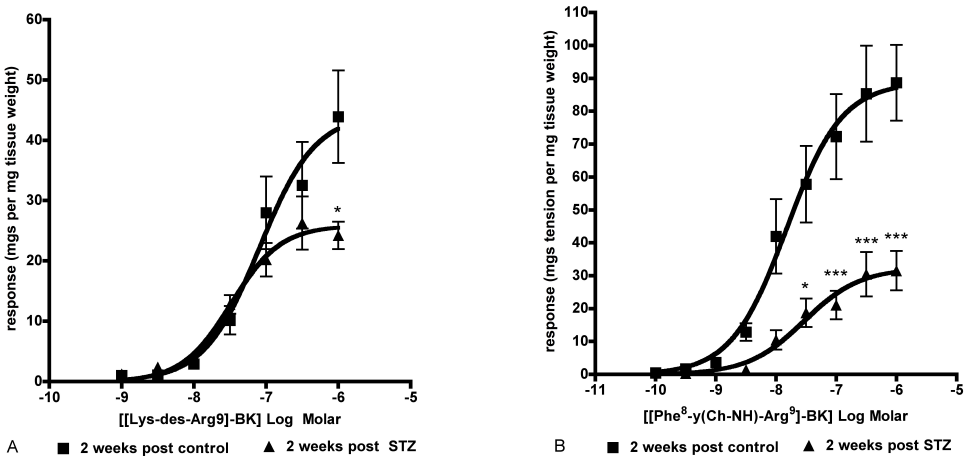

Figure 7.6 Graphs showing responses to BK-1 selective agonist , [Lys-des-Arg9]-BK (A) and BK-2 selective agonist, [Phe8-y(Ch-NH)-Arg9]-BK (B) in urinary bladder from 2 weeks post control and STZ-treated rats. Data represent mean ± s.e.m. of >n of 6 urinary bladder strips. Statistical significance was tested by two-way ANOVA with post-hoc Bonferonni, * represents $p<0.05$, ** $p<0.01$, *** $p<0.001$ comparing to respective control.

Table 7.2: Potency and efficacy estimates for Bradykinin selective agonists on urinary bladder from 2 week post control or STZ administration. Data represent mean ± s.e.m. of n>6 urinary bladder strips.

Agonist	pEC50		Emax	
	control	STZ	control	STZ
[Lys-des-Arg9]-BK	7.09 ± 0.22	7.48 ± 0.12^{NS}	44.46 ± 7.44	25.86 ± 2.10^{NS}
[Phe8-y(Ch-NH)-Arg9]-BK	7.82 ± 0.18	7.54 ± 0.23^{NS}	88.76 ± 8.77	32.30 ± 4.45***

Statistical analysis by two-way ANOVA comparing to control, NS non-significant, *p<0.05, **p<0.01, ***p<0.001.

The effects of bradykinin selective agonists on subsequent response to capsaicin

The effects of 1 μM BK-1 or 1 μM BK-2 selective agonists on the subsequent capsaicin responses were next examined. Neither agonist elicited the same effect as seen for bradykinin, i.e. no reversal of the diminished capsaicin response in STZ-treated animal tissue was seen, although a small leftward shift in capsaicin potency was seen following BK-1 agonist preincubation (Figure 7.7).

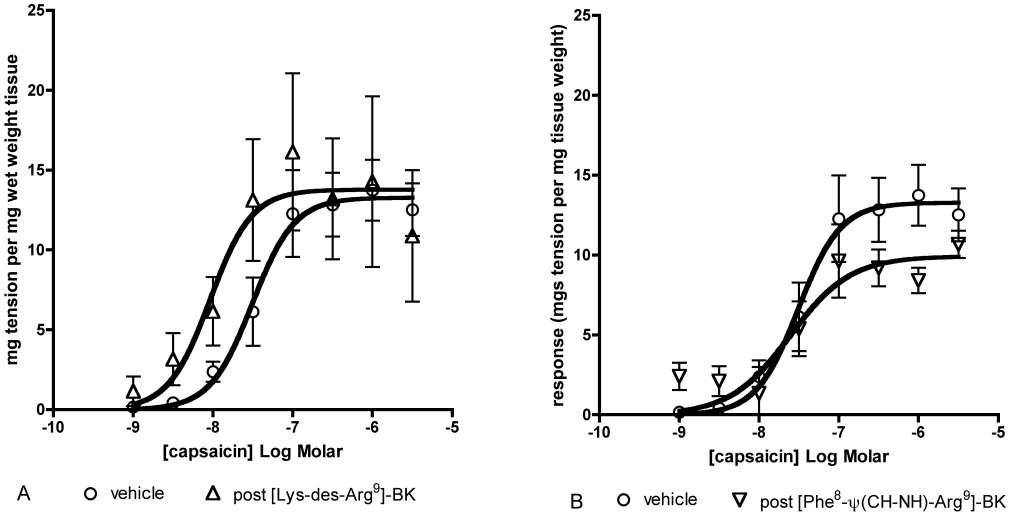

Figure 7.7 Graphs showing responses to capsaicin following pre-exposure to BK-1 selective agonist, [Lys-des-Arg9]-BK (A) and BK-2 selective agonist, [Phe8-y(Ch-NH)-Arg9]-BK (B) in urinary bladder from 2 weeks post STZ-treated rats.

Data represent mean ± s.e.m. of >n of 6 urinary bladder strips. No statistical significance was seen using two-way ANOVA comparing to respective control.

Next the effect of a combination of 1 μM BK-1 and 1 μM BK-2 selective agonist on subsequent response to capsaicin was examined. The combination BK-1/ BK-2 agonist elicited a direct contraction of similar magnitude in control and STZ-treated animal tissue (Figure 7.8) and also enhanced the subsequent response to capsaicin in STZ-treated urinary bladder, to the level seen with bradykinin. In tissue from control-treated animals a slight leftward shift in capsaicin potency was seen, but this was statistically non-significant (Figure 7.9).

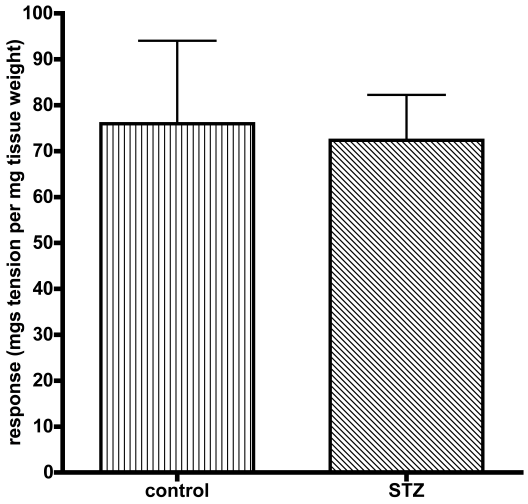

Figure 7.8 Barchart showing direct contractile response to a combination of 1 μM BK-1 selective agonist , [Lys-des-Arg9]-BK and 1 μM BK-2 selective agonist, [Phe8-y(Ch-NH)-Arg9]-BK in urinary bladder from 2 weeks post control and STZ-treated rats. Data represent mean ± s.e.m. of >n of 6 urinary bladder strips. No statistical significance was seen using by Students t-test.

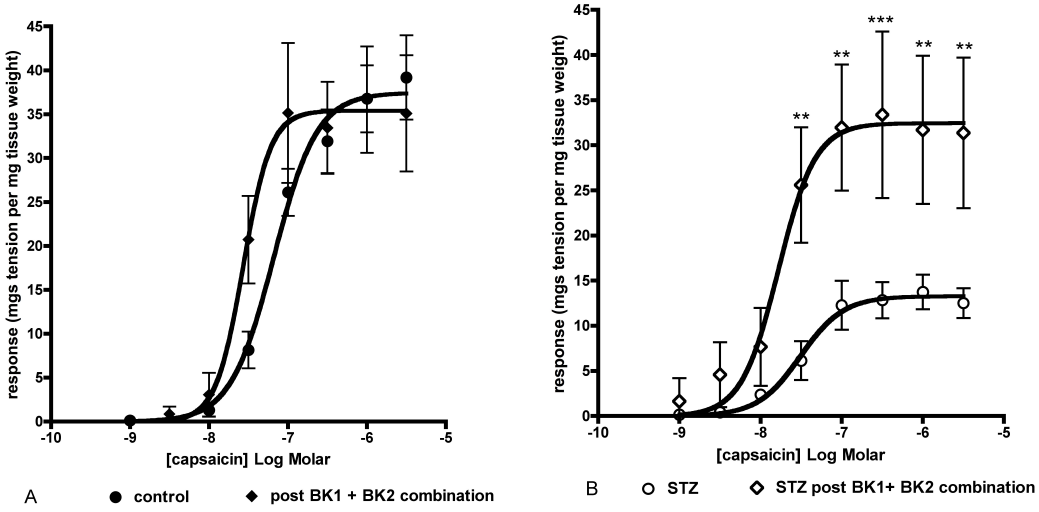

Figure 7.9 Graphs showing responses to capsaicin following pre-exposure to a combination of BK-1 selective agonist , [Lys-des-Arg9]-BK and BK-2 selective agonist, [Phe8-y(Ch-NH)-Arg9]-BK in urinary bladder from 2 weeks post control (A) and STZ-treated (B) rats. Data represent mean ± s.e.m. of >n of 6 urinary bladder strips. Statistical significance was tested by two-way ANOVA with post-hoc Bonferonni, * represents $p<0.05$, ** $p<0.01$, *** $p<0.001$ comparing to respective control.

The effect of indomethacin on bradykinin responses

Finally the effect of 10 μM indomethacin, a cyclooxygenase inhibitor, was examined on the responses to bradykinin in urinary bladder from STZ-treated rats. Firstly direct contractile response to 1μM bradykinin was examined in the presence and absence of indomethacin where it was seen that indomethacin significantly reduced but did not abolish the response (Figure 4.10). Secondly the response to subsequent capsaicin application was examined where it was seen that in the presence of indomethacin, bradykinin pre-exposure was not able to enhance the subsequent capsaicin response to the same degree as seen in the absence of indomethacin (Figure 7.10).

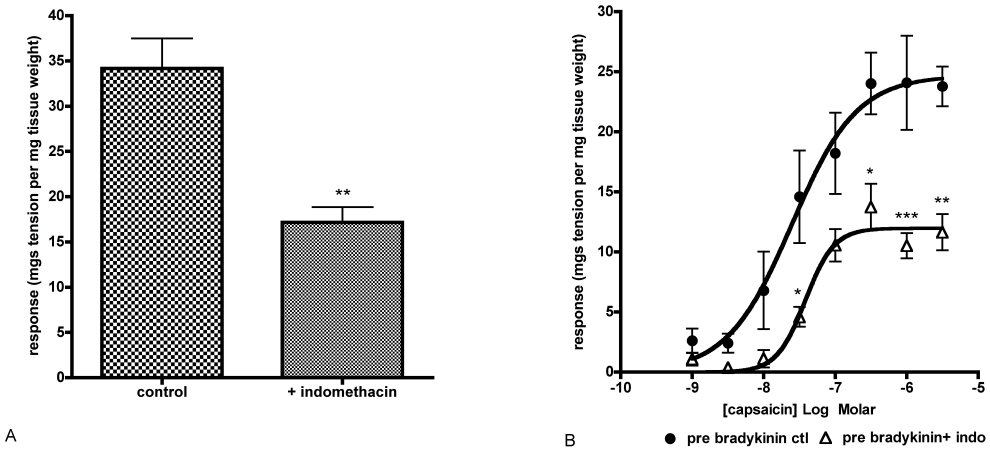

Figure 7.10 Barchart and graph showing direct contractile response to 1 μM bradykinin ± indomethacin (A) and subsequent capsaicin responses (B) in urinary bladder from 2 weeks post STZ-treated rats. Data represent mean ± s.e.m. of n > 6 urinary bladder strips. Statistical significance was tested by Students t-test and by two-way ANOVA with post-hoc Bonferonni, * represents $p<0.05$, ** $p<0.01$, *** $p<0.001$ comparing to control.

The effect of NGF on capsaicin responses

Next the effect of preincubating NGF was examined on the subsequent response to capsaicin in urinary bladder from 2 weeks post control and STZ-treated rats. NGF did not elicit a direct contractile or relaxant response on the urinary bladder strips, and did not enhance subsequent capsaicin responses in tissue from 2 weeks post control or STZ-treated rats (Figure 7.11). At the 300 ng/ml NGF concentration, there did appear to be a mild depression in the control tissue group, whereas no such effect was observed in the STZ-treated group.

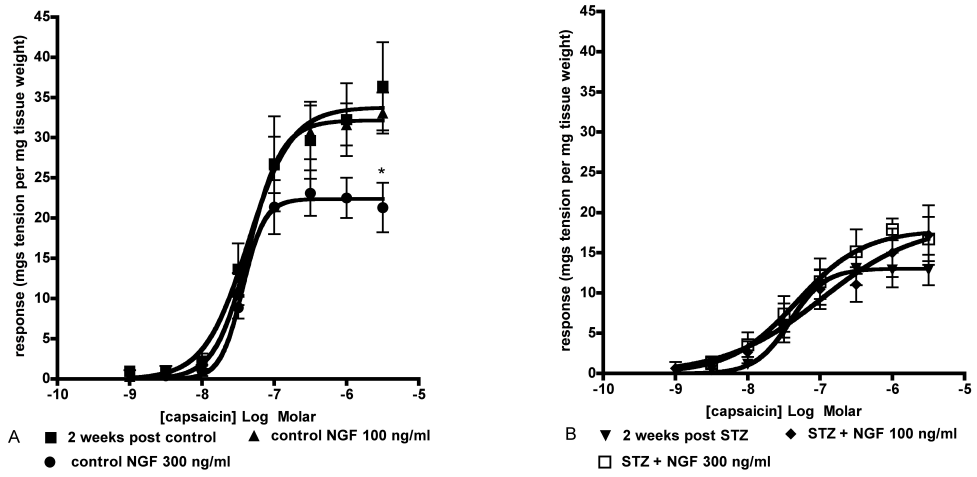

Figure 7.11 Graphs showing effects of NGF preincubation with no washout on subsequent capsaicin responses in urinary bladder from 2 weeks post control (A) and STZ-treated (B) rats. Data represent mean $\pm$ s.e.m. of n > 6 urinary bladder strips. Statistical significance was tested by two-way ANOVA with post-hoc Bonferonni, * represents $p<0.05$, ** $p<0.01$, *** $p<0.001$ comparing to respective control

The effect of insulin on capsaicin and carbachol responses

Finally the effect of 1 μM insulin, incubated for 20 minutes with no washout was studied firstly on capsaicin responses and secondly on carbachol responses of urinary bladder tissue from 2 week post control and STZ-treated rats. The direct application of insulin caused a transient minor relaxation of the urinary bladder strips (control 17.78$\pm$ 4.67, STZ 23.00 $\pm$ 6.35 mgs relaxation per mg tissue

weight) which returned to baseline before capsaicin application. Insulin preincubation had no effect on control or STZ-treated animal tissue responses to capsaicin or carbachol (Figure 7.12)

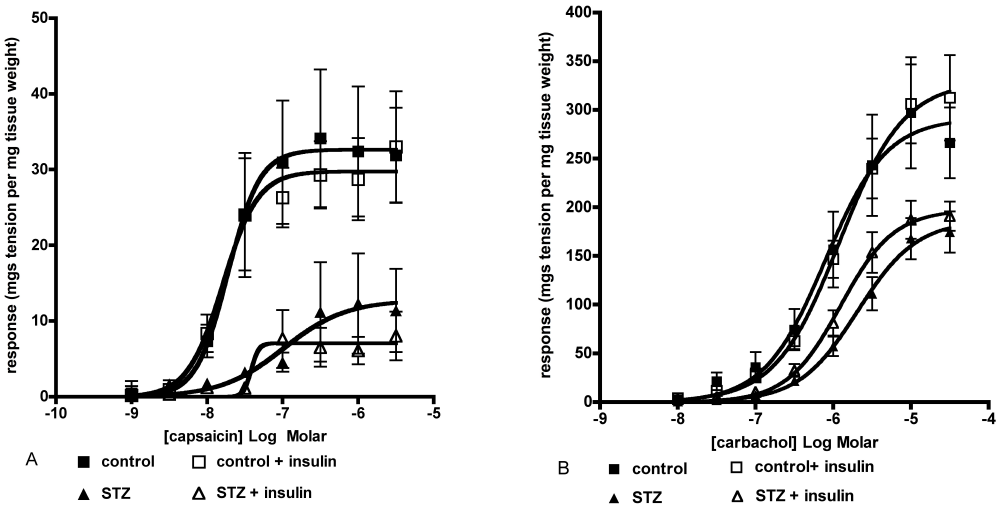

Figure 7.12 Graphs showing effects of insulin preincubation with no washout on subsequent capsaicin responses (A) and carbachol responses (B) in urinary bladder from 2 weeks post control and STZ-treated rats. Data represent mean ± s.e.m. of n > 6 urinary bladder strips. No statistical significance was found for insulin effects by two-way ANOVA.

Monitoring of carbachol responses throughout bradykinin and NGF studies

The response to carbachol was seen to be of lower magnitude in the urinary bladders from 2-week post STZ-treated in agreement with previous data (Table 7.3). No significant alteration of carbachol responses were seen following bradykinin ± indomethacin, indomethacin, BK-1, BK-2 , BK-1 +BK-2 combination or NGF preincubation.

Table 7.3 Potency and efficacy estimates for carbachol responses in urinary bladders from 2 week control and STZ-treated rats. Data represent mean ± s.e.m n>6 urinary bladder strips.

	pEC50		Emax	
	control	STZ	control	STZ
control	5.63 ± 0.03	5.51 ± 0.03^{NS}	339 ± 13	275 ± 9**
BK	5.63± 0.08	5.57± 0.08^{NS}	338± 22	279± 17*
NGF	5.69± 0.07	5.53± 0.06^{NS}	303± 17	250± 12^{NS}

Statistical analysis by two-way ANOVA comparing STZ to control, NS non-significant, *p<0.05, **p<0.01, ***p<0.001. No significant difference was found with two-way ANOVA comparing BK/NGF treatment with respective control.

Discussion

Bradykinin preincubation was able to reverse the diminished TRPV1 response

Bradykinin produced a consistent contractile response in control tissues over the time-phase studied. In the STZ-treated rat tissue, an enhanced efficacy response to bradykinin was seen at the 2-day post STZ-treatment. This could be due to an acute inflammatory response following induction of diabetes by STZ, causing an upregulation of bradykinin receptor activation effector pathways such as prostaglandin release in the bladder. Due to its toxicity, STZ has been shown to cause an acute inflammatory response systemically with vascular leakage and proinflammatory gene upregulation (Kim et al., 2007) . Future work could be to dissect out which bradykinin receptor type was responsible for the enhanced bradykinin response with the use of selective agonist/antagonists. Following bradykinin application, an enhancement of the diminished capsaicin response in 2 weeks post STZ-treated rat urinary bladder tissue was seen with no effect observed on control treated tissue. These data reproduced the findings of Katisart (Katisart, 2011). The bradykinin-capsaicin enhancement was not observed in 2 day post STZ-treated tissue where the capsaicin response had not yet diminished.

Bradykinin reversal required dual BK-1 and BK-2 receptor activation

Next BK-1 and BK-2 selective agonists were used to determine which bradykinin receptor subtype was responsible for the potentiating effect seen. When comparing BK-1 and BK-2 direct contractile effects in STZ-diabetic to control tissue a slight reduction in BK-1 response and a significantly reduced BK-2 response was seen in the STZ-diabetic tissue. Reduced BK-1 and BK-2 responses could imply a reduced receptor expression but published data demonstrates firstly a ubiquitously high expression of BK-2 receptors (Bellucci et al., 2007) and secondly an upregulation of BK-1 receptor expression in the STZ-model of diabetes (Mage et al., 2002). The alteration in responses could be driven by

changes in the effector mechanisms of BK-1 and BK-2 mediated contraction. Bladder bradykinin responses have been reported to increase over time post tissue setup, with larger increases in hypertropic tissue, and these have been attributed to increased prostaglandin production (Sjuve et al., 2000). This finding may offer some explanation as to the data seen here. The studies on BK-1 and BK-2 agonist responses were performed at a similar but not exact time of tissue incubation post setup (4-5 hours), and studies in control and STZ-diabetic were not run in direct parallel as the main aim was to study responses in STZ-diabetic tissue. However, the study of the effects of BK-1 and BK-2 combination was run in direct parallel in control and STZ-diabetic animals. Here the resultant contractile responses were almost identical between control and STZ-diabetic animals. An examination of BK-1 and BK-2 responses at varying times after setup would be a useful addition to this dataset and add confidence to the finding of depressed BK-1 and BK-2 activity seen in STZ-tissue. Furthermore the rate of prostaglandin driven increases in bradykinin responses may very well differ in the STZ-diabetic tissue and provide an explanation for the diminished BK-1 and BK-2 responses seen.

Following BK-1 or BK-2 application, the capsaicin responses were not seen to mirror the potentiated response seen following bradykinin, i.e. no potentiation was seen. However, a combination of BK-1 and BK-2 agonist did produce the potentiated capsaicin response, indicating that the activation of both bradykinin receptor subtypes is essential. This could be further explored through the use of selective BK-1 and BK-2 antagonists which should both inhibit bradykinin activity on the TRPV1 response.

Bradykinin reversal of TRPV1 responses was blocked by cyclooxygenase inhibition

The mechanistic studies with indomethacin revealed that bradykinin direct contractile effect was reduced but not abolished in the presence of indomethacin in STZ-diabetic tissue. This suggests that the mechanism of bradykinin induced bladder muscle contraction is partly through production of prostaglandins. Some

literature evidence has suggested that bradykinin does elicit the contraction of bladder muscle through prostaglandin production in diabetic tissue and removal of the urothelium reduces the contractile effect of bradykinin (Pinna et al., 1994). The potentiating action of bradykinin on capsaicin response was seen to be much reduced in the presence of indomethacin. This finding implies that prostaglandin production is involved in the bradykinin-induced TRPV1 potentiation. The activation of protein kinase C by bradykinin leads to generation of PGE2 from cyclooxygenase 2 (COX2), an inducible enzyme upregulated in inflamed tissue. The use of COX2 specific inhibitors would further strengthen this finding. Additionally it would be useful to study the direct effects of PGE2 and prostanoids receptor agonists/antagonists on TRPV1 function, to gain an understanding of which prostanoid receptor is responsible.

Therapeutic manipulation of TRPV1 dysfunction through ACE inhibition

With the finding that bradykinin has the ability to modulate acute deficits in TRPV1 function, some thought was given to how this information could be applied in the clinic. Therapeutically bradykinin levels can be enhanced through the use of angiotensin converting enzyme (ACE) inhibitors or vasopeptidase inhibitors which inhibit ACE and neutral endopeptidases. ACE not only converts angiotensin but also degrades bradykinin and so inhibiting this enzymes activity should prolong the biological life of bradykinin and increase its concentration. Some clinical evidence was found where a clinical trial of trandolopril, an ACE inhibitor was found to be of some use in diabetic neuropathy (Malik et al., 1998b) but side effects of ACE inhibitors include cough and 'pins and needles'. These effects and side effects could be attributed to TRPV1 modulation (Bessac and Jordt, 2008). No studies on the possible utility of ACE inhibitors in treatment of diabetic cystopathy were found.

Nerve growth factor was unable to reverse diminished TRPV1 responses at this acute stage

The hypothesis that exogenous application of nerve growth factor would potentiate the TRPV1 response either through increased expression of TRPV1 receptor or by sensitizing TRPV1 was next examined. Application of concentrations of NGF reported to elicit TRPV1-sensitising effects (Zhang et al., 2005a) had no effect on capsaicin responses in either control or STZ-diabetic tissue. This raised the question of whether increased TRPV1 expression at the cell surface would result in an increased contractile response to capsaicin bearing in mind that capsaicin is cell penetrant. A study of the effects of NGF on a TRPV1 agonist that is only able to activate exofacial TRPV1 would answer this. In the absence of such a ligand, a more complex study could be performed which examines the antagonist potency of a cell impermeant TRPV1- antagonist such as SB-497794-D. If NGF is able to increase cell surface expression of TRPV1, the antagonist potency versus capsaicin responses should be increased in the presence of NGF. The dataset produced so far implies that exogenously applied NGF is unable to sensitise TRPV1 responses either in control or at the early stage of diabetes. A reduction in NGF levels in the diabetic bladder has been seen by 8 weeks (Li et al.) but NGF mRNA has been reported to be enhanced in the bladder at earlier timepoints (Koo et al., 1993) and therefore this ineffectiveness of NFG exogenously applied may simply be due to timing . NGF is produced and released by smooth muscle cells and urothelial cells of the bladder and transported to the DRG through retrograde axonal transport. If endogenous levels of NGF were already high or unchanged from control levels then exogenous application of NGF would be unlikely to sensitise TRPV1 responses. With this in mind, the importance of NGF to TRPV1 function may become more relevant to TRPV1 dysfunction in this tissue at a later stage of diabetes than has been studied in this project, at a point when NGF levels are reduced.

Insulin application was unable to sensitise TRPV1 responses

Lastly, an acute application of insulin was without effect on either capsaicin responses or carbachol responses. The hypothesis here was that deprivation of insulin may have caused a down regulation of TRPV1 surface expression in the STZ-diabetic tissue and by exposure to insulin a sensitization of TRPV1 response may be afforded. This was not observable in these studies. No direct contractile effect of insulin was observed in urinary bladder from control or STZ-treated rats, but a small relaxant effect was observed. There has been a report that insulin is able to directly activate the TRPV1 receptor in a population of neuronal cells (Sathianathan et al., 2003). If insulin were to directly activate TRPV1 in this system a direct contractile response and a subsequent reduced response to capsaicin would be observed; this was not the case in these studies. Responses to carbachol were monitored in this study, due to the fact that insulin will cause uptake of glucose into the smooth muscle and through this effect may alter muscle responsiveness to the muscarinic receptor activation. Again no significant changes were seen following insulin.

The prominent findings here were that bradykinin was able to reverse the diminished TRPV1 response, whereas NGF and insulin were without effect at this acute stage of diabetes. This implies that at this acute phase in this model system, TRPV1 function retains some level of plasticity and suggests that early therapeutic intervention for e.g. by an ACE inhibitor may be beneficial in the treatment of diabetic cystopathy.

Chapter 8 Overall discussion

Initial validation studies identified the urinary bladder as the most appropriate model for study of TRPV1 modulation in sensory neuropathy

The first studies were aimed at finding the most suitable model to use for exploring how and why TRPV1 function is being modulated during diabetic sensory neuropathy. Native tissue assays such as the urinary bladder in vitro model express numerous receptors endogenously and require minimal manipulation which avoids marked phenotypical changes that could potentially alter TRPV1 responses. Ideally a sensory neuron preparation such as the DRG would have been studied in addition to the bladder. However acutely dissociated DRG preparations require manipulation to enzymatically dissociate the cells, inclusion of NGF to sustain neuronal viability and provision of extracellular matrix protein to cause cellular adherence to a coverslip. All of these steps could potentially alter TRPV1 expression and functional state (Chen et al., 2011, Zhang et al., 2005a, Jeske et al., 2009a), which would be at odds with the experimental aims of examining how this receptor is modulated specifically in sensory neuropathy. To overcome these methodological issues, a functional assay such as intracellular calcium measurement could be studied in an intact DRG preparation. Pilot studies in intact DRG were attempted but insufficient FURA-2AM loading and a subsequent low ratiometric signal hindered progress and therefore efforts were focused on the urinary bladder system.

Rapid onset of TRPV1 dysfunction was seen following induction of diabetes

Next the onset of TRPV1 dysfunction was mapped in urinary bladder using the STZ-induced diabetic rat model. Here diminished responses to capsaicin were seen robustly by 2 weeks, which persisted up to 7-10 weeks following STZ-treatment. There seems to be a slight discrepancy between these data and previous in-house data in this respect(Katisart, 2011), however the STZ-model had been altered to reduce mortality and this may have impacted on the onset of TRPV1 dysfunction.

The source of TRPV1 dysfunction is not entirely through myogenic decline

To try and understand the source of TRPV1 dysfunction which was one of reduced efficacy rather than altered potency, other functional measures were examined. Carbachol responses were measured to monitor myogenic changes and here a gradual progressive decline was seen. The profile of muscarinic decline did not match the acute decline that was seen in TRPV1 function and because of this mismatch, the reduced muscle function could not fully explain the diminished TRPV1 responsiveness. Additionally no difference was seen in the contractile kinetics of carbachol response, which provided additional evidence that muscle contractility was largely unaltered at this acute stage. No differences were seen in frequency of spontaneous activity but a slight significant decrease in amplitude was seen in the urinary bladder from STZ-treated rats, which could be attributed to the minor myogenic decline.

An increase in the mechanisms that terminate the action of the neuropeptides released through TRPV1 activation could explain a diminished TRPV1 function. However, no differences were noted in the rate of recovery of tissue following capsaicin exposure, suggestive of no change to the degradative pathways that terminate the contractile response to the neuropeptides. In terms of neuropeptide content of the tissue, although no measure was made of these in this thesis, there is evidence in the literature that neuropeptides such as Substance P are unaltered in the bladder at up to 9 weeks following diabetic induction (Steers et al., 1994). Therefore it appears that the dysfunction seen in the TRPV1 receptor is due to an alteration in its function.

Diabetes is causing changes in neuroexitability that extend beyond TRPV1 function

Neurally mediated contractile activity was examined through the use of electrical field stimulation and these studies revealed an increased voltage sensitivity in diabetic tissue. This alteration in neurogenically mediated contraction is in agreement with the literature and has been attributed to changes in

neuroexitability (Tammela et al., 1994). Such changes highlight the fact that changes are occurring in the neuronal population and are not just limited to TRPV1 function.

Reduced organ bath temperature changes in muscarinic/ TRPV1 function were deficient in diabetic tissue

TRPV1 is a temperature sensitive ion channel and the effects of organ bath temperature on TRPV1 and muscarinic function were studied. Reduced organ bath temperature caused increased responses to carbachol and capsaicin in control tissue and increased amplitude but decreased frequency of spontaneous activity. In tissue from STZ-diabetic rats, the decreased organ bath temperature had no effect on either carbachol or capsaicin responses but did cause a reduction in frequency and an increase in amplitude of spontaneous activity. These temperature data suggest that the mechanism that drives changes in muscarinic/ TRPV1 responses is deficient in diabetes whereas the mechanism that drives changes in spontaneous activity is not.

Methylglyoxal could be causative to the TRPV1 dysfunction but its actions extend beyond TRPA1 activation

Next to gain an understanding of what could be causing the TRPV1 dysfunction and other neuronal changes in diabetes, the acute exposure to a potential neuropathy causative agent, methylglyoxal was studied. To examine whether methylglyoxal effect was via TRPA1 activation, TRPA1 ligands were used.

Methylglyoxal did cause TRPA1 activation but effects on TRPV1 function were not blocked by TRPA1 antagonism

Methylglyoxal caused a direct contractile response in control tissue of a similar magnitude to that seen with AITC, suggestive of TRPA1 activation. A diminished response was seen to methylglyoxal in STZ-diabetic tissue which implies that a reduced TRPA1 activity accompanies the diminished TRPV1 function in diabetes.

Following acute methylglyoxal and AITC exposure, diminished capsaicin responses were seen, suggestive of a cross-desensitisation of TRPV1. A TRPA1 selective antagonist was seen to block both methylglyoxal and AITCs direct contractile effect in urinary bladder of controls. However the TRPA1 antagonist did not block the effect of methylglyoxal on subsequent capsaicin responses, which implies an alternative mechanism by which methylglyoxal is reducing TRPV1 response. Furthermore TRPA1 antagonism revealed a sensitising action of AITC on capsaicin responses suggestive of a complexity between desensitisation/sensitisation mechanisms between TRPA1 and TRPV1. The highest concentration of methylglyoxal 10 mM was seen to cause a reduced subsequent carbachol response, which may be due to cellular toxicity.

Methylglyoxal demonstrated additional activity

Acute methylglyoxal exposure caused increased responses to repeated electrically-evoked contractions. Increased repeated electrically evoked responses were seen in the presence of acute methylglyoxal and may be via methylglyoxal effect as a GABA A agonist (Distler et al., 2012) as GABA A agonists are known to potentiate neurotransmitter release (Santicioli et al., 1991)

Second application of methylglyoxal was seen to cause a relaxation from basal tension and further study of this revealed that both methylglyoxal and AITC caused relaxation of carbachol precontracted tissue. No differences in this response were seen between control and STZ-tissue and this response was not blocked by TRPA1 antagonism. Although the mechanism for this activity was not defined here, this action of methylglyoxal may have a bearing on bladder function in diabetes.

Prolonged methylglyoxal exposure revealed effects on neuroexcitability

To mimic the exposure to methylglyoxal as would be seen in diabetes, a more prolonged exposure was studied. Here methylglyoxal exposure continued to diminish the subsequent response to capsaicin in control tissue. However the

prolonged exposure protocol had detrimental effects in itself on measurement of TRPV1 function, and capsaicin responses in STZ-treated rat tissue were virtually non-existent. This highlights the fragility of neuronal preparations *in vitro*. Responses to carbachol were seen to be more robust and here prolonged exposure to methylglyoxal caused an enhancement in carbachol efficacy in STZ-treated tissue: the reasons for this are not understood. Pronounced leftward shifts in voltage sensitivity were seen for electrical field stimulation, and these were apparent in both control and STZ-treated groups. Increases were seen in frequency responses for a wide range of frequencies for STZ and a smaller range for control. This increased sensitivity was similar to that seen in STZ-induced diabetes and may suggest that the diabetic-induced changes to membrane excitability are directly due to methylglyoxal. A more detailed examination of the contractile profile data for these responses revealed that methylglyoxal exposure altered the 'slow neurotransmitter' responses and therefore may be affecting cholinergic responses. This could be studied in more depth to gain an understanding of how methylglyoxal is causing changes in membrane excitability.

Diminished TRPV1 responses were reversed by bradykinin, so retained a level of plasticity

The final part of this thesis was to examine the potential of rescuing the diminished TRPV1 response through the use of three known sensitising agents, bradykinin, NGF and insulin. Bradykinin was the only agent seen to reverse the TRPV1 diminished response back up to control equivalent levels. Through the use of bradykinin selective agonists individually and in combination it was seen that the dual activation of BK-1 and BK-2 receptor was necessary to reverse TRPV1 response. The use of indomethacin revealed that the likely mechanism of action of bradykinin was through prostaglandin production as indomethacin blocked diminished TRPV1 reversal. This finding affirms previous data generated in-house (Katisart, 2011), and offers a mechanism of action of bradykinin effect on the diminished TRPV1 responses of prostaglandin

generation. Prostaglandins are known to sensitise TRPV1 responses through activation of protein kinase A/C (Moriyama et al., 2005, Gu et al., 2003), which is thought to release TRPV1 from the inhibitory control of PIP_2. In the urinary bladder a reversal of diminished TRPV1 function would likely be beneficial in treatment of diabetic cystopathy. Increased sensation would aid urinary voiding but a fine balance probably exists regaining normal function and inducing pain. Diabetics are prone to the development of bladder pain/ cystitis following infection (Nicolle, 2005) and are more prone to infections due to the increased glucose levels in their urine (Rayfield et al., 1982, Stapleton, 2002).

Considering the information provided by this thesis a number of potential therapeutic avenues could be explored which may be of benefit in neuropathy

Methylglyoxal interference

An agent that reduces the effects of methylglyoxal either by enhancing its degradation, reducing its production or blocking its effect would be beneficial in the treatment of sensory neuropathy. Metformin, an antidiabetic agent has been shown to bind to methylglyoxal and potentially block methylglyoxal effects (Ruggiero-Lopez et al., 1999), metformin has also been shown to reduce systemic levels of methylglyoxal (Beisswenger et al., 1999). Gliclazide has been shown to act as an antiglycation agent and reduces AGE formation by methylglyoxal (Li et al., 2008). However equimolar concentrations are required which requires large doses of these compounds to be administered. Additionally neither of these compounds are effective at resolution of diabetic complications such as neuropathy and this may be due to efficacy and site of action. In terms of the ideal compound, one designed specifically to interfere with the binding of methylglyoxal to the cysteine residues may be the most effective at blocking the action of methylglyoxal effect on neuropathy.

Enhancement of endogenous bradykinin levels through the use of ACE inhibition

Angiotensin converting enzyme (ACE) inhibitors act to limit the conversion of angiotensin II to angiotensin I and are used as antihypertensives. In addition to its action on angiotensin, ACE also facilitates the breakdown of endogenous bradykinin (Fox et al., 1996) and therefore the early use of an ACE inhibitor may be beneficial in treatment of diabetic cystopathy, through enhancement of endogenous bradykinin levels. As these compounds are in extensive clinical use there is some evidence that ACE inhibitors are of benefit in diabetic neuropathy (Coppey et al., 2006, Reja et al., 1995) but some studies have shown no benefit (Malik et al., 1998a) and none to my knowledge have been designed to specially examine the effectiveness of ACE inhibition on bladder cystopathy.

TRPV1 antagonism

Finally the early use of a TRPV1 antagonist may be beneficial in sensory neuropathy. Not only should the TRPV1 antagonist reduce the pain that is often experienced in neuropathy but may also reduce the detrimental modulation of TRPV1 by interfering with phosphorylation of this receptor. Clinical use of TRPV1 antagonists have been halted by the hyperthermic response to antagonists (Gavva et al., 2008). It is believed that a tonic activation of the TRPV1 receptor is present and when a TRPV1 antagonist is administered, the consequence of this is to cause hyperthermia (Gavva et al., 2007). However given the early peripheral downregulation of TRPV1 function seen in the rat diabetic model, it is unknown how a diabetic would respond to TRPV1 antagonism. The diabetic population may be resistant to such hyperthermic effects and examination of a TRPV1 antagonist on body temperature in control and diabetic rats coupled with effects on pain neuropathic readouts would be a very interesting study. If TRPV1 antagonists caused hyperthermia in the diabetic rat, it would suggest that peripheral TRPV1 function has not been diminished to the same extent as seen in the urinary bladder, as the mechanism of hyperthermia is thought to be via a peripheral vascular thermoregulatory response. If TRPV1

antagonism did not cause hyperthermia in diabetic rats, but were active against neuropathic pain, it potentially opens up a human population in which TRPV1 antagonists could be used therapeutically.

Summary statement

In the acute stage of diabetes, TRPV1 function in the urinary bladder is downregulated. The downregulation at this stage may be caused by exposure to methylglyoxal although methylglyoxal acts via multiple mechanisms and TRPA1 blockade did not prevent TRPV1 downregulation. Bradykinin receptor activation, likely through prostaglandin production, was able to reverse the acute stage STZ-induced TRPV1 downregulation whereas other sensitising agents NGF or insulin were not able to reverse diminished TRPV1 function. These studies have identified that the TRPV1 dysfunction that presents acutely in diabetic sensory neuropathy retains a level of plasticity that could be therapeutically manipulated and thereby be of benefit in treatment of diabetic neuropathy.

Bibliography

AISHIMA, M., TOMODA, T., YUNOKI, T., NAKANO, T., SEKI, N., YONEMITSU, Y., SUEISHI, K., NAITO, S., ITO, Y. & TERAMOTO, N. 2006. Actions of ZD0947, a novel ATP‐sensitive K+ channel opener, on membrane currents in human detrusor myocytes. *British journal of pharmacology,* 149**,** 542-550.

AMADESI, S., COTTRELL, G. S., DIVINO, L., CHAPMAN, K., GRADY, E. F., BAUTISTA, F., KARANJIA, R., BARAJAS‐LOPEZ, C., VANNER, S. & VERGNOLLE, N. 2006. Protease‐activated receptor 2 sensitizes TRPV1 by protein kinase Cε‐and A‐dependent mechanisms in rats and mice. *The Journal of physiology,* 575**,** 555-571.

ANDERSSON, D. A., GENTRY, C., LIGHT, E., VASTANI, N., VALLORTIGARA, J., BIERHAUS, A., FLEMING, T. & BEVAN, S. 2013. Methylglyoxal Evokes Pain by Stimulating TRPA1. *PloS one,* 8**,** e77986.

ANWAR, I. J. & DERBENEV, A. V. 2013. TRPV1-dependent regulation of synaptic activity in the mouse dorsal motor nucleus of the vagus nerve. *Front Neurosci,* 7**,** 238.

ARAKI, I. 2011. TRP channels in urinary bladder mechanosensation. *Transient Receptor Potential Channels.* Springer.

ARONSON, D. 2008. Hyperglycemia and the pathobiology of diabetic complications. *Cardiovascular Diabetology: Clinical, Metabolic and Inflammatory Facets,* 45**,** 1-16.

BARRON, J. T., GU, L. & PARRILLO, J. E. 1997. Cytoplasmic redox potential affects energetics and contractile reactivity of vascular smooth muscle. *Journal of molecular and cellular cardiology,* 29**,** 2225-2232.

BARTHO, L., NORDTVEIT, E., SZOMBATI, V. & BENKO, R. 2013. Purinoceptor-mediated, capsaicin-resistant excitatory effect of allyl isothiocyanate on neurons of the guinea-pig small intestine. *Basic Clin Pharmacol Toxicol,* 113**,** 141-3.

BAUTISTA, D. M., MOVAHED, P., HINMAN, A., AXELSSON, H. E., STERNER, O., HÖGESTÄTT, E. D., JULIUS, D., JORDT, S.-E. & ZYGMUNT, P. M. 2005. Pungent products from garlic activate the sensory ion channel TRPA1. *Proceedings of the National Academy of Sciences of the United States of America,* 102**,** 12248-12252.

BEISSWENGER, P. J., HOWELL, S. K., TOUCHETTE, A. D., LAL, S. & SZWERGOLD, B. S. 1999. Metformin reduces systemic methylglyoxal levels in type 2 diabetes. *Diabetes,* 48**,** 198-202.

BELLUCCI, F., CUCCHI, P., SANTICIOLI, P., LAZZERI, M., TURINI, D. & MEINI, S. 2007. Characterization of kinin receptors in human cultured detrusor smooth muscle cells. *British Journal of Pharmacology,* 150**,** 192-199.

BENHAM, C. D., GUNTHORPE, M. J. & DAVIS, J. B. 2003. TRPV channels as temperature sensors. *Cell calcium,* 33**,** 479-487.

BESSAC, B. F. & JORDT, S.-E. 2008. Breathtaking TRP Channels: TRPA1 and TRPV1 in Airway Chemosensation and Reflex Control. *Physiology,* 23**,** 360-370.

BEVAN, S., HOTHI, S., HUGHES, G., JAMES, I., RANG, H., SHAH, K., WALPOLE, C. & YEATS, J. 1992. Capsazepine: a competitive antagonist of the sensory neurone excitant capsaicin. *British journal of pharmacology,* 107**,** 544-552.

BIERHAUS, A., FLEMING, T., STOYANOV, S., LEFFLER, A., BABES, A., NEACSU, C., SAUER, S. K., EBERHARDT, M., SCHNÖLZER, M. & LASITSCHKA, F. 2012. Methylglyoxal modification of Nav1. 8 facilitates nociceptive neuron firing and causes hyperalgesia in diabetic neuropathy. *Nature medicine,* 18**,** 926-933.

BIRDER, L. A., NAKAMURA, Y., KISS, S., NEALEN, M. L., BARRICK, S., KANAI, A. J., WANG, E., RUIZ, G., DE GROAT, W. C., APODACA, G., WATKINS, S. & CATERINA, M. J. 2002. Altered urinary bladder function in mice lacking the vanilloid receptor TRPV1. *Nature Neuroscience,* 5**,** 856-860.

BLAKE JA, B. C., EPPIG JT, KADIN JA, RICHARDSON JE 2014. The Mouse Genome Database: integration of and access to knowledge about the laboratory mouse. *Nucleic Acids Res.* 2014 ed.

BOULTON, A. J., VILEIKYTE, L., RAGNARSON-TENNVALL, G. & APELQVIST, J. 2005. The global burden of diabetic foot disease. *The Lancet,* 366**,** 1719-1724.

BROWN, W. & FEASBY, T. 1984. Conduction block and denervation in Guillain-Barré polyneuropathy. *Brain,* 107**,** 219-239.

BRUNO, G. & LANDI, A. 2011. Epidemiology and Costs of Diabetes. *Transplantation Proceedings,* 43**,** 327-329.

BURAKGAZI, A. Z., ALSOWAITY, B., BURAKGAZI, Z. A., UNAL, D. & KELLY, J. J. 2012. Bladder dysfunction in peripheral neuropathies. *Muscle & nerve,* 45**,** 2-8.

CAM, M., PEDERSON, R., BROWNSEY, R. & MCNEILL, J. 1993. Long-term effectiveness of oral vanadyl sulphate in streptozotocin-diabetic rats. *Diabetologia,* 36**,** 218-224.

CAMPBELL, D. J. 2001. The kallikrein–kinin system in humans. *Clinical and experimental pharmacology and physiology,* 28**,** 1060-1065.

CATERINA, M. J., LEFFLER, A., MALMBERG, A., MARTIN, W., TRAFTON, J., PETERSEN-ZEITZ, K., KOLTZENBURG, M., BASBAUM, A. & JULIUS, D. 2000. Impaired nociception and pain sensation in mice lacking the capsaicin receptor. *science,* 288**,** 306-313.

CHAPLEN, F. W., FAHL, W. E. & CAMERON, D. C. 1998. Evidence of high levels of methylglyoxal in cultured Chinese hamster ovary cells. *Proceedings of the National Academy of Sciences,* 95**,** 5533-5538.

CHEN, Y., YANG, C. & WANG, Z. 2011. Proteinase-activated receptor 2 sensitizes transient receptor potential vanilloid 1, transient receptor potential vanilloid 4, and transient receptor potential ankyrin 1 in paclitaxel-induced neuropathic pain. *Neuroscience,* 193**,** 440-451.

COOK, L., DAVIES, J., YATES, A., ELLIOTT, A., LOVELL, J., JOULE, J., PEMBERTON, P., THORNALLEY, P. & BEST, L. 1998. Effects of methylglyoxal on rat pancreatic β-cells. *Biochemical pharmacology,* 55**,** 1361-1367.

COOLSAET, B. & BLOK, C. 1986. Detrusor properties related to prostatism. *Neurourology and Urodynamics,* 5**,** 435-447.

COPPEY, L. J., DAVIDSON, E. P., RINEHART, T. W., GELLETT, J. S., OLTMAN, C. L., LUND, D. D. & YOREK, M. A. 2006. ACE inhibitor or angiotensin II receptor antagonist attenuates diabetic neuropathy in streptozotocin-induced diabetic rats. *Diabetes,* 55**,** 341-348.

CULSHAW, A. J., BEVAN, S., CHRISTIANSEN, M., COPP, P., DAVIS, A., DAVIS, C., DYSON, A., DZIADULEWICZ, E. K., EDWARDS, L. & EGGELTE, H. 2006.

Identification and biological characterization of 6-aryl-7-isopropylquinazolinones as novel TRPV1 antagonists that are effective in models of chronic pain. *Journal of medicinal chemistry,* 49**,** 471-474.
DAHLSTRAND, C., DAHLSTROM, A., AHLMAN, H., JONSSON, O., LUNDSTAM, S., NORLEN, L. & PETTERSSON, S. 1992. Effect of substance-P on detrusor muscle in rats with diabetic cystopathyI. *British Journal of Urology,* 70**,** 390-394.
DALY, D., RONG, W., CHESS-WILLIAMS, R., CHAPPLE, C. & GRUNDY, D. 2007. Bladder afferent sensitivity in wild-type and TRPV1 knockout mice. *Journal of Physiology-London,* 583**,** 663-674.
DAVIS, J. B., GRAY, J., GUNTHORPE, M. J., HATCHER, J. P., DAVEY, P. T., OVEREND, P., HARRIES, M. H., LATCHAM, J., CLAPHAM, C. & ATKINSON, K. 2000. Vanilloid receptor-1 is essential for inflammatory thermal hyperalgesia. *Nature,* 405**,** 183-187.
DE JONGHE, P., TIMMERMAN, V., NELIS, E., MARTIN, J. & VAN BROECKHOVEN, C. 1997. Charcot-Marie-Tooth disease and related peripheral neuropathies. *Journal of the peripheral nervous system: JPNS,* 2**,** 370.
DE LA GARZA-RODEA, A. S., KNAÄN-SHANZER, S., DEN HARTIGH, J. D., VERHAEGEN, A. P. & VAN BEKKUM, D. W. 2010. Anomer-equilibrated streptozotocin solution for the induction of experimental diabetes in mice (Mus musculus). *Journal of the American Association for Laboratory Animal Science: JAALAS,* 49**,** 40.
DISTLER, M. G., PLANT, L. D., SOKOLOFF, G., HAWK, A. J., ANEAS, I., WUENSCHELL, G. E., TERMINI, J., MEREDITH, S. C., NOBREGA, M. A. & PALMER, A. A. 2012. Glyoxalase 1 increases anxiety by reducing GABAA receptor agonist methylglyoxal. *The Journal of clinical investigation,* 122**,** 2306.
DONNERER, J. & AMANN, R. 1992. Time course of capsaicin-evoked release of CGRP from rat spinal-cord in vitro- effect of concentration and modulations by ruthenium red. *Calcitonin Gene-Related Peptide,* 657**,** 491-492.
DRAPEAU, G., RHALEB, N.-E., DION, S., JUKIC, D. & REGOLI, D. 1988. [Phe8Ψ (CH2-NH) Arg9] bradykinin, a B2 receptor selective agonist which is not broken down by either kininase I or kininase II. *European journal of pharmacology,* 155**,** 193-195.
DU, J., SUZUKI, H., NAGASE, F., AKHAND, A. A., YOKOYAMA, T., MIYATA, T., KUROKAWA, K. & NAKASHIMA, I. 2000. Methylglyoxal induces apoptosis in Jurkat leukemia T cells by activating c‐Jun N‐Terminal kinase. *Journal of cellular biochemistry,* 77**,** 333-344.
DUX, M., ROSTA, J. & JANCSO, G. Capsaicin-Sensitive Nociceptive Innervation of the Dura Mater: Implications for the Pathomechanism of Headache. *Anti-Inflammatory & Anti-Allergy Agents in Medicinal Chemistry (Formerly Cu,* 10**,** 31-42.
DYCK, P., KRATZ, K., KARNES, J., LITCHY, W., KLEIN, R., PACH, J., WILSON, D., O'BRIEN, P. & MELTON, L. 1993. The prevalence by staged severity of various types of diabetic neuropathy, retinopathy, and nephropathy in a population‐based cohort The Rochester Diabetic Neuropathy Study. *Neurology,* 43**,** 817-817.

EBERHARDT, M. J., FILIPOVIC, M. R., LEFFLER, A., DE LA ROCHE, J., KISTNER, K., FISCHER, M. J., FLEMING, T., ZIMMERMANN, K., IVANOVIC-BURMAZOVIC, I. & NAWROTH, P. P. 2012. Methylglyoxal Activates Nociceptors through Transient Receptor Potential Channel A1 (TRPA1) A POSSIBLE MECHANISM OF METABOLIC NEUROPATHIES. *Journal of Biological Chemistry,* 287**,** 28291-28306.

ESPINOSA-MANSILLA, A., DURÁN-MERÁS, I. & SALINAS, F. 1998. High-performance liquid chromatographic–fluorometric determination of glyoxal, methylglyoxal, and diacetyl in urine by prederivatization to pteridinic rings. *Analytical biochemistry,* 255**,** 263-273.

FINNERUP, N. B., OTTO, M., MCQUAY, H. J., JENSEN, T. S. & SINDRUP, S. H. 2005. Algorithm for neuropathic pain treatment: An evidence based proposal. *Pain,* 118**,** 289-305.

FOX, A. J., LALLOO, U. G., BELVISI, M. G., BERNAREGGI, M., CHUNG, K. F. & BARNES, P. J. 1996. Bradykinin–evoked sensitization of airway sensory nerves: A mechanism for ACE–inhibitor cough. *Nature medicine,* 2**,** 814-817.

FRIMODT-MØLLER, C. 1980. Diabetic cystopathy: epidemiology and related disorders. *Annals of internal medicine,* 92**,** 318-321.

FUKUNAGA, M., MIYATA, S., LIU, B. F., MIYAZAKI, H., HIROTA, Y., HIGO, S., HAMADA, Y., UEYAMA, S. & KASUGA, M. 2004. Methylglyoxal induces apoptosis through activation of p38 MAPK in rat Schwann cells. *Biochemical and biophysical research communications,* 320**,** 689-695.

GABRA, B. H. & SIROIS, P. 2003. Beneficial effect of chronic treatment with the selective bradykinin B< sub> 1</sub> receptor antagonists, R-715 and R-954, in attenuating streptozotocin-diabetic thermal hyperalgesia in mice. *Peptides,* 24**,** 1131-1139.

GALIZZI, J., BODINIER, M., CHAPELAIN, B., LY, S., COUSSY, L., GIRAUD, S., NELIAT, G. & JEAN, T. 1994. Up‐regulation of [3H]‐des‐Arg10‐kallidin binding to the bradykinin B1 receptor by interleukin‐1β in isolated smooth muscle cells: correlation with B1 agonist‐induced PGI2 production. *British journal of pharmacology,* 113**,** 389-394.

GAVVA, N. R., BANNON, A. W., SURAPANENI, S., HOVLAND, D. N., JR., LEHTO, S. G., GORE, A., JUAN, T., DENG, H., HAN, B., KLIONSKY, L., KUANG, R., LE, A., TAMIR, R., WANG, J., YOUNGBLOOD, B., ZHU, D., NORMAN, M. H., MAGAL, E., TREANOR, J. J. S. & LOUIS, J.-C. 2007. The vanilloid receptor TRPV1 is tonically activated in vivo and involved in body temperature regulation. *Journal of Neuroscience,* 27**,** 3366-3374.

GAVVA, N. R., TREANOR, J. J., GARAMI, A., FANG, L., SURAPANENI, S., AKRAMI, A., ALVAREZ, F., BAK, A., DARLING, M. & GORE, A. 2008. Pharmacological blockade of the vanilloid receptor TRPV1 elicits marked hyperthermia in humans. *Pain,* 136**,** 202-210.

GENTILE, S., TURCO, S., OLIVIERO, B. & TORELLA, R. 1998. The role of autonomic neuropathy as a risk factor of Helicobacter pylori infection in dyspeptic patients with Type 2 diabetes mellitus. *Diabetes Research and Clinical Practice,* 42**,** 41-48.

GEVAERT, T., VANDEPITTE, J., HUTCHINGS, G., VRIENS, J., NILIUS, B. & DE RIDDER, D. 2007. TRPV1 is involved in stretch-evoked contractile changes

in the rat autonomous bladder model: A study with piperine, a new TRPV1 agonist. *Neurourology and Urodynamics,* 26**,** 440-450.
GOPALAKRISHNAN, M., WHITEAKER, K. L., MOLINARI, E. J., DAVIS-TABER, R., SCOTT, V. E., SHIEH, C.-C., BUCKNER, S. A., MILICIC, I., CAIN, J. C. & POSTL, S. 1999. Characterization of the ATP-sensitive potassium channels (KATP) expressed in guinea pig bladder smooth muscle cells. *Journal of Pharmacology and Experimental Therapeutics,* 289**,** 551-558.
GU, Q., KWONG, K. & LEE, L.-Y. 2003. Ca2+ transient evoked by chemical stimulation is enhanced by PGE2 in vagal sensory neurons: role of cAMP/PKA signaling pathway. *Journal of neurophysiology,* 89**,** 1985-1993.
GUNTHORPE, M., RAMI, H., JERMAN, J., SMART, D., GILL, C., SOFFIN, E., LUIS HANNAN, S., LAPPIN, S., EGERTON, J. & SMITH, G. 2004. Identification and characterisation of SB-366791, a potent and selective vanilloid receptor (VR1/TRPV1) antagonist. *Neuropharmacology,* 46**,** 133-149.
HADDAD, E.-B., FOX, A. J., ROUSELL, J., BURGESS, G., MCINTYRE, P., BARNES, P. J. & CHUNG, K. F. 2000. Post-transcriptional regulation of bradykinin B1 and B2 receptor gene expression in human lung fibroblasts by tumor necrosis factor-α: modulation by dexamethasone. *Molecular pharmacology,* 57**,** 1123-1131.
HALL, J. M. 1997. Bradykinin receptors. *General Pharmacology: The Vascular System,* 28**,** 1-6.
HALPERIN, J. J., LITTLE, B. W., COYLE, P. K. & DATTWYLER, R. J. 1987. Lyme disease Cause of a treatable peripheral neuropathy. *Neurology,* 37**,** 1700-1700.
HAN, Y., RANDELL, E., VASDEV, S., GILL, V., GADAG, V., NEWHOOK, L. A., GRANT, M. & HAGERTY, D. 2007. Plasma methylglyoxal and glyoxal are elevated and related to early membrane alteration in young, complication-free patients with Type 1 diabetes. *Molecular and cellular biochemistry,* 305**,** 123-131.
HEFTI, F. F., ROSENTHAL, A., WALICKE, P. A., WYATT, S., VERGARA, G., SHELTON, D. L. & DAVIES, A. M. 2006. Novel class of pain drugs based on antagonism of NGF. *Trends in pharmacological sciences,* 27**,** 85-91.
HELLWEG, R. & HARTUNG, H. D. 1990. Endogenous levels of nerve growth factor (NGF) are altered in experiemental diabetes-mellitus- a possible role for NGF in the pathogenesis of diabetic neuropathy. *Journal of Neuroscience Research,* 26**,** 258-267.
HERRERA, G. M. & MEREDITH, A. L. 2010. Diurnal variation in urodynamics of rat. *PloS one,* 5**,** e12298.
HONG, S. S. & WILEY, J. W. 2005. Early painful diabetic neuropathy is associated with differential changes in the expression and function of vanilloid receptor 1. *Journal of Biological Chemistry,* 280**,** 618-627.
HOWARTH, F., JACOBSON, M., NASEER, O. & ADEGHATE, E. 2005. Short-term effects of streptozotocin-induced diabetes on the electrocardiogram, physical activity and body temperature in rats. *Experimental physiology,* 90**,** 237-245.
ISHII, T. & SHIMO, Y. 1985. Cooling-induced supersensitivity to acetylcholine in the isolated airway smooth muscle of the rat. *Naunyn-Schmiedeberg's archives of pharmacology,* 329**,** 167-175.

JESKE, N. A., PATWARDHAN, A. M., HENRY, M. A. & MILAM, S. B. 2009a. Fibronectin stimulates TRPV1 translocation in primary sensory neurons. *Journal of neurochemistry,* 108**,** 591-600.
JESKE, N. A., PATWARDHAN, A. M., RUPAREL, N. B., AKOPIAN, A. N., SHAPIRO, M. S. & HENRY, M. A. 2009b. A-kinase anchoring protein 150 controls protein kinase C-mediated phosphorylation and sensitization of TRPV1. *Pain,* 146**,** 301-307.
JIA, X. 2010. Role of methylglyoxal in the pathogenesis of insulin resistance.
KALRA, S. P., DUBE, M. G., PU, S., XU, B., HORVATH, T. L. & KALRA, P. S. 1999. Interacting appetite-regulating pathways in the hypothalamic regulation of body weight. *Endocrine reviews,* 20**,** 68-99.
KAMKIN, A. G., LOZINSKY, I., JARA-OSEGUERA, A. & ROSENBAUM, T. 2012. *Chapter 3 TRPV1 in Cell Signalling: Molecular Mechanisms of Function and Modulation , Mechanically Gated Channels and Their Regulation*, Springer.
KANAREK, R. B. & HO, L. 1984. Patterns of nutrient selection in rats with streptozotocin-induced diabetes. *Physiology & behavior,* 32**,** 639-645.
KAPLAN, S. A. & BLAIVAS, J. G. 1988. Diabetic cystopathy. *Journal of Diabetic Complications,* 2**,** 133-139.
KARANTH, S., SPRINGALL, D., FRANCAVILLA, S., MIRRLEES, D. & POLAK, J. 1990. Early increase in CGRP-and VIP-immunoreactive nerves in the skin of streptozotocin-induced diabetic rats. *Histochemistry,* 94**,** 659-666.
KATISART, T. 2011. *Transient Receptor Potential Function in Bladder from Control and Streptozotocin Treated Rats.* School of Life Sciences, Faculty of Health and Human Sciences, University of Hertfordshire.
KESWANI, S. C., PARDO, C. A., CHERRY, C. L., HOKE, A. & MCARTHUR, J. C. 2002. HIV-associated sensory neuropathies. *Aids,* 16**,** 2105-2117.
KIEFER, A. S., FLEMING, T., ECKERT, G. J., POINDEXTER, B. B., NAWROTH, P. P. & YODER, M. C. 2013. Methylglyoxal concentrations differ in standard and washed neonatal packed red blood cells. *Pediatric research*.
KIM, Y., CHOI, M., KIM, Y., PARK, C., LEE, J., CHUNG, I., YOO, J., CHOI, W., CHO, G. & KANG, S. 2007. Triamcinolone acetonide protects the rat retina from STZ-induced acute inflammation and early vascular leakage. *Life sciences,* 81**,** 1167-1173.
KITAMURA, A., HOSHINO, T., KON, T. & OGAWA, R. 2000. Patients with diabetic neuropathy are at risk of a greater intraoperative reduction in core temperature. *Anesthesiology,* 92**,** 1311-1318.
KNILL-JONES, R., GOODWILL, C., DAYAN, A. D. & WILLIAMS, R. 1972. Peripheral neuropathy in chronic liver disease: clinical, electrodiagnostic, and nerve biopsy findings. *Journal of Neurology, Neurosurgery & Psychiatry,* 35**,** 22-30.
KOIVISTO, A., HUKKANEN, M., SAARNILEHTO, M., CHAPMAN, H., KUOKKANEN, K., WEI, H., VIISANEN, H., ÅKERMAN, K. E., LINDSTEDT, K. & PERTOVAARA, A. 2012. Inhibiting TRPA1 ion channel reduces loss of cutaneous nerve fiber function in diabetic animals: Sustained activation of the TRPA1 channel contributes to the pathogenesis of peripheral diabetic neuropathy. *Pharmacological Research,* 65**,** 149-158.
KOO, H. P., SANTAROSA, R. P., BUTTYAN, R., SHABSIGH, R., OLSSON, C. A. & KAPLAN, S. A. 1993. EARLY MOLECULAR-CHANGES ASSOCIATED WITH

STREPTOZOTOCIN-INDUCED DIABETIC BLADDER HYPERTROPHY IN THE RAT. *Urological Research,* 21**,** 375-381.
KURIHARA, S., KURIYAMA, H. & MAGARIBUCHI, T. 1974. Effects of rapid cooling on the electrical properties of the smooth muscle of the guinea-pig urinary bladder. *The Journal of physiology,* 238**,** 413-426.
LAZZERI, M., BENEFORTI, P. & TURINI, D. 1997. Urodynamic effects of intravesical resiniferatoxin in humans: preliminary results in stable and unstable detrusor. *The Journal of urology,* 158**,** 2093-2096.
LESSER, H., SHARMA, U., LAMOREAUX, L. & POOLE, R. 2004. Pregabalin relieves symptoms of painful diabetic neuropathy A randomized controlled trial. *Neurology,* 63**,** 2104-2110.
LEVY, D. & ZOCHODNE, D. W. 2000. Increased mRNA expression of the B1 and B2 bradykinin receptors and antinociceptive effects of their antagonists in an animal model of neuropathic pain. *Pain,* 86**,** 265-271.
LI, W., OTA, K., NAKAMURA, J., NARUSE, K., NAKASHIMA, E., OISO, Y. & HAMADA, Y. 2008. A BRIEF COMMUNICATION Antiglycation Effect of Gliclazide on In Vitro AGE Formation from Glucose and Methylglyoxal. *Experimental Biology and Medicine,* 233**,** 176-179.
LI, Y. Z., SHI, B. K., WANG, D., WANG, P., LAUDON, V., ZHANG, J. P. & LIU, Y. L. Nerve growth factor and substance P: expression in a rat model of diabetic bladder. *International Urology and Nephrology,* 43**,** 109-116.
LINCOIN, J., CROCKETT, M., HAVEN, A. & BURNSTOCK, G. 1984. Rat bladder in the early stages of streptozotocin-induced diabetes: adrenergic and cholinergic innervation. *Diabetologia,* 26**,** 81-87.
LIU, G. & DANESHGARI, F. 2005. Alterations in neurogenically mediated contractile responses of urinary bladder in rats with diabetes. *American Journal of Physiology-Renal Physiology,* 288**,** F1220-F1226.
LIU, M., HUANG, W. L., WU, D. S. & PRIESTLEY, J. V. 2006. TRPV1, but not P2X(3), requires cholesterol for its function and membrane expression in rat nociceptors. *European Journal of Neuroscience,* 24**,** 1-6.
LLORENTE, M. D. & MALPHURS, J. E. 2007. *Psychiatric disorders and diabetes mellitus,* London, Informa Healthcare.
LO, T., WESTWOOD, M. E., MCLELLAN, A. C., SELWOOD, T. & THORNALLEY, P. J. 1994. Binding and modification of proteins by methylglyoxal under physiological conditions. A kinetic and mechanistic study with N alpha-acetylarginine, N alpha-acetylcysteine, and N alpha-acetyllysine, and bovine serum albumin. *Journal of Biological Chemistry,* 269**,** 32299-32305.
LONGHURST, P. & BELIS, J. 1986. Abnormalities of rat bladder contractility in streptozotocin-induced diabetes mellitus. *Journal of Pharmacology and Experimental Therapeutics,* 238**,** 773-777.
LONGHURST, P. A., KAUER, J. & LEVIN, R. M. 1991. The ability of insulin treatment to reverse or prevent the changes in urinary bladder function caused by streptozotocin-induced diabetes mellitus. *General Pharmacology: The Vascular System,* 22**,** 305-311.
LUHESHI, G. & ZAR, M. 1991. The effect of streptozotocin‐induced diabetes on cholinergic motor transmission in the rat urinary bladder. *British journal of pharmacology,* 103**,** 1657-1662.
MAGE, M., PÉCHER, C., NEAU, E., CELLIER, E., DOS REISS, M. L., SCHANSTRA, J. P., COUTURE, R., BASCANDS, J.-L. & GIROLAMI, J.-P. 2002. Induction of B1

receptors in streptozotocin diabetic rats: possible involvement in the control of hyperglycemia-induced glomerular Erk 1 and 2 phosphorylation. *Canadian journal of physiology and pharmacology,* 80**,** 328-333.
MAGGI, C. 1997. Bradykinin as an inflammatory mediator in the urinary tract. *The Kinin System. Academic Press: London***,** 235-247.
MALIK, R. A., WILLIAMSON, S., ABBOTT, C., CARRINGTON, A. L., IQBAL, J., SCHADY, W. & BOULTON, A. J. 1998a. Effect of angiotensin-converting-enzyme (ACE) inhibitor trandolapril on human diabetic neuropathy: randomised double-blind controlled trial. *The Lancet,* 352**,** 1978-1981.
MALIK, R. A., WILLIAMSON, S., ABBOTT, C., CARRINGTON, A. L., IQBAL, J., SCHADY, W. & BOULTON, A. J. M. 1998b. Effect of angiotensin-converting-enzyme (ACE) inhibitor trandolapril on human diabetic neuropathy: Randomised doubleblind controlled trial. *Lancet,* 352**,** 1978-1981.
MANZINI, S., PERRETTI, F., TRAMONTANA, M., DELBIANCO, E., SANTICIOLI, P., MAGGI, C. A. & GEPPETTI, P. 1991. Neurochemical evidence of calcitonin gene-related peptide-like immunoreactivity (CGRP-LI) release from capsaicin-sensitive nerves in rat mesenteric-arteries and veins. *General Pharmacology,* 22**,** 275-278.
MARCEAU, F., HESS, J. F. & BACHVAROV, D. R. 1998. The B1 receptors for kinins. *Pharmacological Reviews,* 50**,** 357-386.
MARTYN, C. & HUGHES, R. 1997. Epidemiology of peripheral neuropathy. *Journal of neurology, neurosurgery, and psychiatry,* 62**,** 310.
MASER, R. E., STEENKISTE, A. R., DORMAN, J. S., NIELSEN, V. K., BASS, E. B., MANJOO, Q., DRASH, A. L., BECKER, D. J., KULLER, L. H. & GREENE, D. A. 1989. Epidemiological correlates of diabetic neuropathy: report from Pittsburgh Epidemiology of Diabetes Complications Study. *Diabetes,* 38**,** 1456-1461.
MASON, L., MOORE, R. A., DERRY, S., EDWARDS, J. E. & MCQUAY, H. J. 2004. Systematic review of topical capsaicin for the treatment of chronic pain. *Bmj,* 328**,** 991.
MCCLOSKEY, K. D. 2010. Interstitial cells in the urinary bladder—localization and function. *Neurourology and urodynamics,* 29**,** 82-87.
MCCOMBE, P. & MCLEOD, J. 1984. The peripheral neuropathy of vitamin B< sub> 12</sub> deficiency. *Journal of the neurological sciences,* 66**,** 117-126.
MCLELLAN, A. C., THORNALLEY, P. J., BENN, J. & SONKSEN, P. H. 1994. Glyoxalase system in clinical diabetes mellitus and correlation with diabetic complications. *Clinical Science,* 87**,** 21-29.
MCLEOD, J. 1995. Investigation of peripheral neuropathy. *Journal of neurology, neurosurgery, and psychiatry,* 58**,** 274.
MCNAMARA, C. R., MANDEL-BREHM, J., BAUTISTA, D. M., SIEMENS, J., DERANIAN, K. L., ZHAO, M., HAYWARD, N. J., CHONG, J. A., JULIUS, D. & MORAN, M. M. 2007. TRPA1 mediates formalin-induced pain. *Proceedings of the National Academy of Sciences,* 104**,** 13525-13530.
MEACCI, E., VASTA, V., FARNARARO, M. & BRUNI, P. 1996. Bradykinin increases ceramide and sphingosine content in human fibroblasts: possible involvement of glycosphingolipids. *Biochemical and biophysical research communications,* 221**,** 1-7.

MEAKIN, S. O. & SHOOTER, E. M. 1992. The nerve growth factor family of receptors. *Trends in neurosciences,* 15**,** 323-331.
MENIGOZ, A. & BOUDES, M. 2011. The Expression Pattern of TRPV1 in Brain. *Journal of Neuroscience,* 31**,** 13025-13027.
MINKE, B. 2010. The history of the Drosophila TRP channel: the birth of a new channel superfamily. *J Neurogenet,* 24**,** 216-33.
MOILANEN, L. J., LAAVOLA, M., KUKKONEN, M., KORHONEN, R., LEPPÄNEN, T., HÖGESTÄTT, E. D., ZYGMUNT, P. M., NIEMINEN, R. M. & MOILANEN, E. 2012. TRPA1 contributes to the acute inflammatory response and mediates carrageenan-induced paw edema in the mouse. *Scientific reports,* 2.
MORIYAMA, T., HIGASHI, T., TOGASHI, K., IIDA, T., SEGI, E., SUGIMOTO, Y., TOMINAGA, T., NARUMIYA, S. & TOMINAGA, M. 2005. Sensitization of TRPV1 by EP1 and IP reveals peripheral nociceptive mechanism of prostaglandins. *Molecular pain,* 1**,** 3.
N AKOPIAN, A. 2011. Regulation of nociceptive transmission at the periphery via TRPA1-TRPV1 interactions. *Current pharmaceutical biotechnology,* 12**,** 89-94.
NAKAHATA, N., ONO, T. & NAKANISHI, H. 1987. Contribution of prostaglandin E2 to bradykinin-induced contraction in rabbit urinary detrusor. *Japanese journal of pharmacology,* 43**,** 351.
NICKANDER, K. K., SCHMELZER, J. D., ROHWER, D. A. & LOW, P. A. 1994. Effect of alpha-tocopherol deficiency on indexes of oxidative stress in normal and diabetic peripheral-nerve. *Journal of the Neurological Sciences,* 126**,** 6-14.
NICOLLE, L. E. 2005. Urinary tract infection in diabetes. *Current opinion in infectious diseases,* 18**,** 49-53.
NILIUS, B., OWSIANIK, G., VOETS, T. & PETERS, J. A. 2007. Transient receptor potential cation channels in disease. *Physiological reviews,* 87**,** 165-217.
OHKAWARA, S., TANAKA-KAGAWA, T., FURUKAWA, Y. & JINNO, H. 2012. Methylglyoxal activates the human transient receptor potential ankyrin 1 channel. *Journal of Toxicological Sciences,* 37.
PABBIDI, R. M., CAO, D.-S., PARIHAR, A., PAUZA, M. E. & PREMKUMAR, L. S. 2008a. Direct role of streptozotocin in inducing thermal hyperalgesia by enhanced expression of transient receptor potential vanilloid 1 in sensory neurons. *Molecular pharmacology,* 73**,** 995-1004.
PABBIDI, R. M., YU, S. Q., PENG, S., KHARDORI, R., PAUZA, M. E. & PREMKUMAR, L. S. 2008b. Influence of TRPVI on diabetes-induced alterations in thermal pain sensitivity. *Molecular Pain,* 4.
PARK, Y. S., KOH, Y. H., TAKAHASHI, M., MIYAMOTO, Y., SUZUKI, K., DOHMAE, N., TAKIO, K., HONKE, K. & TANIGUCHI, N. 2003. Identification of the binding site of methylglyoxal on glutathione peroxidase: methylglyoxal inhibits glutathione peroxidase activity via binding to glutathione binding sites Arg 184 and 185. *Free radical research,* 37**,** 205-211.
PATEL, N., LLEWELYN, J., WRIGHT, D. & THOMAS, P. 1994. Glucose and leucine uptake by rat dorsal root ganglia is not insulin sensitive. *Journal of the neurological sciences,* 121**,** 159-162.
PHAGOO, S. B., YAQOOB, M., HERRERA-MARTINEZ, E., MCINTYRE, P., JONES, C. & BURGESS, G. M. 2000. Regulation of bradykinin receptor gene expression

in human lung fibroblasts. *European journal of pharmacology,* 397**,** 237-246.
PINGLE, S. C., MATTA, J. A. & AHERN, G. P. 2007. Capsaicin receptor: TRPV1 a promiscuous TRP channel. *Handb Exp Pharmacol***,** 155-71.
PINNA, C., BOLEGO, C. & PUGLISI, L. 1994. Effect of substance-P and capsaicin on urinary-bladder of diabetic rats and the role of the epithelium. *European Journal of Pharmacology,* 271**,** 151-158.
PREMKUMAR, L. S. & SIKAND, P. 2008. TRPV1: A Target for Next Generation Analgesics. *Current Neuropharmacology,* 6**,** 151-163.
PRESCOTT, E. D. & JULIUS, D. 2003. A modular PIP2 binding site as a determinant of capsaicin receptor sensitivity. *Science,* 300**,** 1284-1288.
PRICE, T. J., JESKE, N. A., FLORES, C. M. & HARGREAVES, K. M. 2005. Pharmacological interactions between calcium/calmodulin-dependent kinase II alpha and TRPV1 receptors in rat trigeminal sensory neurons. *Neuroscience Letters,* 389**,** 94-98.
RAISINGHANI, M., PABBIDI, R. M. & PREMKUMAR, L. S. 2005. Activation of transient receptor potential vanilloid 1 (TRPV1) by resiniferatoxin. *The Journal of physiology,* 567**,** 771-786.
RAMASAMY, R., VANNUCCI, S. J., DU YAN, S. S., HEROLD, K., YAN, S. F. & SCHMIDT, A. M. 2005. Advanced glycation end products and RAGE: a common thread in aging, diabetes, neurodegeneration, and inflammation. *Glycobiology,* 15**,** 16R-28R.
RAYFIELD, E. J., AULT, M. J., KEUSCH, G. T., BROTHERS, M. J., NECHEMIAS, C. & SMITH, H. 1982. Infection and diabetes: the case for glucose control. *The American journal of medicine,* 72**,** 439-450.
RAZAVI, R., CHAN, Y., AFIFIYAN, F. N., LIU, X. J., WAN, X., YANTHA, J., TSUI, H., TANG, L., TSAI, S., SANTAMARIA, P., DRIVERS, J. P., SERREZE, D., SALTER, M. W. & DOSCH, H. M. 2006. TRPV1(+) sensory neurons control beta cell stress and islet inflammation in autoimmune diabetes. *Cell,* 127**,** 1123-1135.
RECIO-PINTO, E., RECHLER, M. M. & ISHII, D. 1986. Effects of insulin, insulin-like growth factor-II, and nerve growth factor on neurite formation and survival in cultured sympathetic and sensory neurons. *The Journal of neuroscience,* 6**,** 1211-1219.
REDDY, V. P. & BEYAZ, A. 2006. Inhibitors of the Maillard reaction and AGE breakers as therapeutics for multiple diseases. *Drug Discovery Today,* 11**,** 646-654.
REES, D. & ALCOLADO, J. 2005. Animal models of diabetes mellitus. *Diabetic medicine,* 22**,** 359-370.
REJA, A., TESFAYE, S., HARRIS, N. & WARD, J. 1995. Is ACE inhibition with lisinopril helpful in diabetic neuropathy? *Diabetic medicine,* 12**,** 307-309.
ROBERTS, L. A. & CONNOR, M. 2006. TRPV1 antagonists as a potential treatment for hyperalgesia. *Recent patents on CNS drug discovery,* 1**,** 65-76.
ROELOFS, R. I., HRUSHESKY, W., ROGIN, J. & ROSENBERG, L. 1984. Peripheral sensory neuropathy and cisplatin chemotherapy. *Neurology,* 34**,** 934-934.
RUGGIERO-LOPEZ, D., LECOMTE, M., MOINET, G., PATEREAU, G., LAGARDE, M. & WIERNSPERGER, N. 1999. Reaction of metformin with dicarbonyl compounds. Possible implication in the inhibition of advanced glycation end product formation. *Biochemical pharmacology,* 58**,** 1765-1773.

SAITO, M., GOTOH, M., KATO, K. & KONDO, A. 1991. Influence of aging on the rat urinary bladder function. *Urologia internationalis,* 47**,** 39-42.
SAITOH, C., KITADA, C., UCHIDA, W., CHANCELLOR, M. B., DE GROAT, W. C. & YOSHIMURA, N. 2007. The differential contractile responses to capsaicin and anandamide in muscle strips isolated from the rat urinary bladder. *European Journal of Pharmacology,* 570**,** 182-187.
SANTICIOLI, P., GAMSE, R., MAGGI, C. A. & MELI, A. 1987a. Cystometric changes in the early phase of streptozotocin-induced diabetes in rats: evidence for sensory changes not correlated to diabetic neuropathy. *Naunyn-Schmiedebergs Archives of Pharmacology,* 335**,** 580-587.
SANTICIOLI, P., PATACCHINI, R., MAGGI, C. A. & MELI, A. 1987b. Exposure to calcium-free medium protects sensory fibers by capsaicin densitization. *Neuroscience Letters,* 80**,** 167-172.
SANTICIOLI, P., TRAMONTANA, M., DELBIANCO, E., MAGGI, C. A. & GEPPETTI, P. 1991. GABA(A) and GABA(B) receptors modulate the K+- evoked release of sensory CGRP from the guinea-pig urinary bladder. *Life Sciences,* 48**,** PL69-PL72.
SASAKI, K., CHANCELLOR, M. B., PHELAN, M. W., YOKOYAMA, T., FRASER, M. O., SEKI, S., KUBO, K., KUMON, H., DE GROAT, W. C. & YOSHIMURA, N. 2002. Diabetic cystopathy correlates with a long-term decrease in nerve growth factor levels in the bladder and lumbosacral dorsal root ganglia. *Journal of Urology,* 168**,** 1259-1264.
SATHIANATHAN, V., AVELINO, A., CHARRUA, A., SANTHA, P., MATESZ, K., CRUZ, F. & NAGY, I. 2003. Insulin induces cobalt uptake in a subpopulation of rat cultured primary sensory neurons. *European Journal of Neuroscience,* 18**,** 2477-2486.
SCHMIDLIN, F., SCHERRER, D., DAEFFLER, L., BERTRAND, C., LANDRY, Y. & GIES, J.-P. 1998. Interleukin-1β induces bradykinin B2 receptor gene expression through a prostanoid cyclic AMP-dependent pathway in human bronchial smooth muscle cells. *Molecular pharmacology,* 53**,** 1009-1015.
SHEADER, E. A., BENSON, R. S. & BEST, L. 2001. Cytotoxic action of methylglyoxal on insulin-secreting cells. *Biochemical pharmacology,* 61**,** 1381-1386.
SILLS, G. J. 2006. The mechanisms of action of gabapentin and pregabalin. *Current opinion in pharmacology,* 6**,** 108-113.
SIMONETTI, M., FABBRO, A., D'ARCO, M., ZWEYER, M., NISTRI, A., GINIATULLIN, R. & FABBRETTI, E. 2006. Comparison of P2X and TRPVI receptors in ganglia or primary culture of trigeminal neurons and their modulation by NGF or serotonin. *Molecular Pain,* 2**,** 15.
SJUVE, R., BOELS, P. J., UVELIUS, B. & ARNER, A. 2000. Up-regulation of bradykinin response in rat and human bladder smooth muscle. *Journal of Urology,* 164**,** 1757-1763.
SKAPARE, E., KONRADE, I., LIEPINSH, E., STRELE, I., MAKRECKA, M., BIERHAUS, A., LEJNIEKS, A., PIRAGS, V. & DAMBROVA, M. 2013. Association of reduced glyoxalase 1 activity and painful peripheral diabetic neuropathy in type 1 and 2 diabetes mellitus patients. *Journal of Diabetes and its Complications,* 27**,** 262-267.
SMEYNE, R. J., KLEIN, R., SCHNAPP, A., LONG, L. K., BRYANT, S., LEWIN, A., LIRA, S. A. & BARBACID, M. 1994. Severe sensory and sympathetic neuropathies in mice carrying a disrupted Trk/NGF receptor gene.

SOFRONIEW, M. V., HOWE, C. L. & MOBLEY, W. C. 2001. Nerve growth factor signaling, neuroprotection, and neural repair. *Annual review of neuroscience,* 24**,** 1217-1281.
SOUHRADA, M. & SOUHRADA, J. 1981. The direct effect of temperature on airway smooth muscle. *Respiration physiology,* 44**,** 311-323.
SOUILEM, O., BIDON, J.-C., GOGNY, M., BLIN, M. & JONDET, A. 1992. Effect of temperature reduction on the reactivity of the mouse vas deferens to adrenergic drugs. *Comparative Biochemistry and Physiology Part C: Comparative Pharmacology,* 103**,** 557-561.
SOUILEM, O., BIDON, J.-C., GOGNY, M., BLIN, M., VU, A. & JONDET, A. 1995. Effect of moderate cooling on contractile responses in mouse vas deferens and its relation to calcium. *Naunyn-Schmiedeberg's archives of pharmacology,* 352**,** 337-345.
SRINIVASAN, R., WOLFE, D., GOSS, J., WATKINS, S., DE GROAT, W. C., SCULPTOREANU, A. & GLORIOSO, J. C. 2008. Protein kinase C epsilon contributes to basal and sensitizing responses of TRPV1 to capsaicin in rat dorsal root ganglion neurons. *European Journal of Neuroscience,* 28**,** 1241-1254.
STANCHEV, D., BLOSA, M., MILIUS, D., GEREVICH, Z., RUBINI, P., SCHMALZING, G., ESCHRICH, K., SCHAEFER, M., WIRKNER, K. & ILLES, P. 2009. Cross-inhibition between native and recombinant TRPV1 and P2X< sub> 3</sub> receptors. *Pain,* 143**,** 26-36.
STÄNDER, S., MOORMANN, C., SCHUMACHER, M., BUDDENKOTTE, J., ARTUC, M., SHPACOVITCH, V., BRZOSKA, T., LIPPERT, U., HENZ, B. M., LUGER, T. A., METZE, D. & STEINHOFF, M. 2004. Expression of vanilloid receptor subtype 1 in cutaneous sensory nerve fibers, mast cells, and epithelial cells of appendage structures. *Experimental Dermatology,* 13**,** 129-139.
STAPLETON, A. 2002. Urinary tract infections in patients with diabetes. *The American journal of medicine,* 113**,** 80-84.
STEERS, W. D., MACKWAY-GERARDI, A. M., CIAMBOTTI, J. & DE GROAT, W. C. 1994. Alterations in neural pathways to the urinary bladder of the rat in response to streptozotocin-induced diabetes. *Journal of the autonomic nervous system,* 47**,** 83-94.
STEINBACHER, B. C. & NADELHAFT, I. 1998. Increased levels of nerve growth factor in the urinary bladder and hypertrophy of dorsal root ganglion neurons in the diabetic rat. *Brain Research,* 782**,** 255-260.
STRENG, T., AXELSSON, H. E., HEDLUND, P., ANDERSSON, D. A., JORDT, S.-E., BEVAN, S., ANDERSSON, K.-E., HÖGESTÄTT, E. D. & ZYGMUNT, P. M. 2008. Distribution and function of the hydrogen sulfide–sensitive TRPA1 ion channel in rat urinary bladder. *European urology,* 53**,** 391-400.
SUGAYA, K. & DE GROAT, W. C. 2000. Influence of temperature on activity of the isolated whole bladder preparation of neonatal and adult rats. *American Journal of Physiology-Regulatory, Integrative and Comparative Physiology,* 278**,** R238-R246.
SUZUKI, H., SAITO, M., KINOSHITA, Y., SATOH, I., KONO, T., SHINBORI, C., ANASTASIOS, S., YAMADA, M. & SATOH, K. 2006. Preventive effects of cyclohexenonic long-chain fatty alcohol on diabetic cystopathy in the rat. *Canadian journal of physiology and pharmacology,* 84**,** 195-201.

SZALLASI, A., CORTRIGHT, D. N., BLUM, C. A. & EID, S. R. 2007. The vanilloid receptor TRPV1: 10 years from channel cloning to antagonist proof-of-concept. *Nature Reviews Drug Discovery,* 6**,** 357-372.

TAKAHASHI, N. & MORI, Y. 2011. TRP channels as sensors and signal integrators of redox status changes. *Frontiers in pharmacology,* 2.

TAMMELA, T. L., BRISCOE, J. A., LEVIN, R. M. & LONGHURST, P. A. 1994. Factors underlying the increased sensitivity to field stimulation of urinary bladder strips from streptozotocin‐induced diabetic rats. *British journal of pharmacology,* 113**,** 195-203.

THOMPSON, G., MACMAHON, M. & CLAES, P. 1970. Precipitation by neomycin compounds of fatty acid and cholesterol from mixed micellar solutions. *European journal of clinical investigation,* 1**,** 40-47.

THORNALLEY, P. 1994. Methylglyoxal, glyoxalases and the development of diabetic complications. *Amino acids,* 6**,** 15-23.

THORNALLEY, P. J. 1988. Modification of the glyoxalase system in human red blood cells by glucose in vitro. *Biochem. J,* 254**,** 751-755.

THULE, P. & LIU, J.-M. 2000. Regulated hepatic insulin gene therapy of STZ-diabetic rats. *Gene therapy,* 7**,** 1744-1752.

TOMINAGA, M. & MORIYAMA, T. 2007. Functional Interaction Between ATP and TRPV1 Receptors. *Molecular Sensors for Cardiovascular Homeostasis.* Springer.

TONG, Y.-C., CHENG, J.-T. & HSU, C.-T. 2006. Alterations of M< sub> 2</sub>-muscarinic receptor protein and mRNA expression in the urothelium and muscle layer of the streptozotocin-induced diabetic rat urinary bladder. *Neuroscience letters,* 406**,** 216-221.

TONG, Y.-C., CHIN, W.-T. & CHENG, J.-T. 1999. Alterations in urinary bladder M< sub> 2</sub>-muscarinic receptor protein and mRNA in 2-week streptozotocin-induced diabetic rats. *Neuroscience letters,* 277**,** 173-176.

TRAUTNER, C., HAASTERT, B., GIANI, G. & BERGER, M. 1996. Incidence of lower limb amputations and diabetes. *Diabetes care,* 19**,** 1006-1009.

TSCHÖPE, C., GAVRILUK, V., REINECKE, A., SEIDL, U., RIESTER, U., HILGENFELDT, U., RITZ, E. & UNGER, T. 1996. Bradykinin excretion is increased in severely hyperglycemic streptozotocin-diabetic rats. *Immunopharmacology,* 33**,** 344-348.

UEDA, T., YOSHIMURA, N. & YOSHIDA, O. 1997. Diabetic cystopathy: relationship to autonomic neuropathy detected by sympathetic skin response. *The Journal of urology,* 157**,** 580-584.

VAN BUREN, J. J., BHAT, S., ROTELLO, R., PAUZA, M. E. & PREMKUMAR, L. S. 2005. Sensitization and translocation of TRPV1 by insulin and IGF-I. *Molecular Pain,* 1.

VARGA, A., NÉMETH, J., SZABÓ, Á., MCDOUGALL, J. J., ZHANG, C., ELEKES, K., PINTÉR, E., SZOLCSÁNYI, J. & HELYES, Z. 2005. Effects of the novel TRPV1 receptor antagonist SB366791 in vitro and in vivo in the rat. *Neuroscience letters,* 385**,** 137-142.

VELLANI, V., MAPPLEBECK, S., MORIONDO, A., DAVIS, J. B. & MCNAUGHTON, P. A. 2001. Protein kinase C activation potentiates gating of the vanilloid receptor VR1 by capsaicin, protons, heat and anandamide. *The Journal of physiology,* 534**,** 813-825.

VETTER, I., WYSE, B. D., ROBERTS-THOMSON, S. J., MONTEITH, G. R. & CABOT, P. J. 2008. Mechanisms involved in potentiation of transient receptor potential vanilloid 1 responses by ethanol. *European Journal of Pain,* 12**,** 441-454.

VON-MERING, J. M., O 1889. Diabetes mellitus nach Pankreas extirpation. *Arch f.exp.Path. u. Pharmakol,* 26**,** 271.

WANG, H., WANG, D. H. & GALLIGAN, J. J. 2010. P2Y2 receptors mediate ATP-induced resensitization of TRPV1 expressed by kidney projecting sensory neurons. *Am J Physiol Regul Integr Comp Physiol,* 298**,** R1634-41.

WARING, J. & WENDT, I. 2000. Effects of anoxia on force, intracellular calcium and lactate production of urinary bladder smooth muscle from control and diabetic rats. *The Journal of urology,* 163**,** 1357-1363.

WHO 1999. Definition, diagnosis and classification of diabetes mellitus and its complications. *Report of a WHO Consultation, Part 1: Diagnosis and Classification of Diabetes Mellitus.* World Health Organisation.

XING, B.-M., YANG, Y.-R., DU, J.-X., CHEN, H.-J., QI, C., HUANG, Z.-H., ZHANG, Y. & WANG, Y. 2012. Cyclin-dependent kinase 5 controls TRPV1 membrane trafficking and the heat sensitivity of nociceptors through KIF13B. *The Journal of Neuroscience,* 32**,** 14709-14721.

YAMADA, T., UGAWA, S., UEDA, T., ISHIDA, Y., KAJITA, K. & SHIMADA, S. 2009. Differential Localizations of the Transient Receptor Potential Channels TRPV4 and TRPV1 in the Mouse Urinary Bladder. *Journal of Histochemistry & Cytochemistry,* 57**,** 277-287.

YANG, Y., KONDURU, A. S., CUI, N., YU, L., TROWER, T. C., SHI, W., SHI, Y. & JIANG, C. 2013. Acute exposure of methylglyoxal leads to activation of KATP channels expressed in HEK293 cells. *Acta Pharmacologica Sinica*.

YAO, J., LIU, B. & QIN, F. 2011. Modular thermal sensors in temperature-gated transient receptor potential (TRP) channels. *Proceedings of the National Academy of Sciences,* 108**,** 11109-11114.

YENILMEZ, A., ÖZÇIFÇI, M., AYDIN, Y., TURGUT, M., UZUNER, K. & ERKUL, A. 2006. Protective effect of high-dose thiamine (B1) on rat detrusor contractility in streptozotocin-induced diabetes mellitus. *Acta Diabetologica,* 43**,** 103-108.

YIM, H.-S., KANG, S.-O., HAH, Y.-C., CHOCK, P. B. & YIM, M. B. 1995. Free radicals generated during the glycation reaction of amino acids by methylglyoxal A model study of protein-cross-linked free radicals. *Journal of Biological Chemistry,* 270**,** 28228-28233.

ZACHAROVA, G. & PALECEK, J. 2009. Parvalbumin and TRPV1 Receptor Expression in Dorsal Root Ganglion Neurons after Acute Peripheral Inflammation. *Physiological Research,* 58**,** 305-309.

ZHANG, X., HUANG, J. & MCNAUGHTON, P. A. 2005a. NGF rapidly increases membrane expression of TRPV1 heat-gated ion channels. *The EMBO journal,* 24**,** 4211.

ZHANG, X. M., HUANG, J. H. & MCNAUGHTON, P. A. 2005b. NGF rapidly increases membrane expression of TRPV1 heat-gated ion channels. *Embo Journal,* 24**,** 4211-4223.

ZHANG, Y. H. & NICOL, G. D. 2004. NGF-mediated sensitization of the excitability of rat sensory neurons is prevented by a blocking antibody to the p75 neurotrophin receptor. *Neuroscience Letters,* 366**,** 187-192.

ZSOMBOK, A., BHASKARAN, M. D., GAO, H., DERBENEV, A. V. & SMITH, B. N. 2011. Functional plasticity of central TRPV1 receptors in brainstem dorsal vagal complex circuits of streptozotocin-treated hyperglycemic mice. *The Journal of Neuroscience,* 31**,** 14024-14031.